

การพัฒนา พี/ซี-ดีเอ็นเอ นาโนไบโอเซนเซอร์สำหรับตรวจวัดโปรตีนที่สามารถจับกับซี-ดีเอ็นเอ



บทคัดย่อและแฟ้มข้อมูลฉบับเต็มของวิทยานิพนธ์ตั้งแต่ปีการศึกษา 2554 ที่ให้บริการในคลังปัญญาจุฬาฯ (CUIR)  
เป็นแฟ้มข้อมูลของนิสิตเจ้าของวิทยานิพนธ์ ที่ส่งผ่านทางบัณฑิตวิทยาลัย

The abstract and full text of theses from the academic year 2011 in Chulalongkorn University Intellectual Repository (CUIR)  
are the thesis authors' files submitted through the University Graduate School.

วิทยานิพนธ์นี้เป็นส่วนหนึ่งของการศึกษาตามหลักสูตรปริญญาเภสัชศาสตรมหาบัณฑิต  
สาขาวิชาเภสัชเคมี ภาควิชาอาหารและเภสัชเคมี  
คณะเภสัชศาสตร์ จุฬาลงกรณ์มหาวิทยาลัย  
ปีการศึกษา 2557  
ลิขสิทธิ์ของจุฬาลงกรณ์มหาวิทยาลัย

DEVELOPMENT OF B/Z-DNA NANOBIOSENSOR FOR DETECTION OF  
Z-DNA BINDING PROTEINS

Miss Kulwadee Sawatpaibontawee



A Thesis Submitted in Partial Fulfillment of the Requirements  
for the Degree of Master of Science in Pharmacy Program in Pharmaceutical

Chemistry

Department of Food and Pharmaceutical Chemistry

Faculty of Pharmaceutical Sciences

Chulalongkorn University

Academic Year 2014

Copyright of Chulalongkorn University

Thesis Title	DEVELOPMENT OF B/Z-DNA NANOBIOSENSOR FOR DETECTION OF Z-DNA BINDING PROTEINS
By	Miss Kulwadee Sawatpaiboontawee
Field of Study	Pharmaceutical Chemistry
Thesis Advisor	Vorait Vongsutilers, Ph.D., R.Ph.
Thesis Co-Advisor	Assistant Professor Bodin Tuesuwan, Ph.D., R.Ph.

---

Accepted by the Faculty of Pharmaceutical Sciences, Chulalongkorn  
University in Partial Fulfillment of the Requirements for the Master's Degree

.....Dean of the Faculty of Pharmaceutical Sciences  
(Assistant Professor Rungpetch Sakulbumrungsil, Ph.D., R.Ph.)

THESIS COMMITTEE

.....Chairman  
(Assistant Professor Nuansri Niwattisaiwong, R.Ph.)

.....Thesis Advisor  
(Vorait Vongsutilers, Ph.D., R.Ph.)

.....Thesis Co-Advisor  
(Assistant Professor Bodin Tuesuwan, Ph.D., R.Ph.)

.....Examiner  
(Associate Professor Wanchai De-eknamkul, Ph.D.)

.....External Examiner  
(Assistant Professor Mitr Pathipvanich, Ph.D., R.Ph.)

กุลวดี สวัสดิ์ไพบูลย์ทวี : การพัฒนา บี/ซี-ดีเอ็นเอ นาโนไบโอเซนเซอร์สำหรับตรวจวัดโปรตีนที่สามารถจับกับซี-ดีเอ็นเอ (DEVELOPMENT OF B/Z-DNA NANOBIOSENSOR FOR DETECTION OF Z-DNA BINDING PROTEINS) อ.ที่ปรึกษาวิทยานิพนธ์หลัก: อ. ภก. ดร. วรสิทธิ์ วงศ์สุทธิเลิศ, อ.ที่ปรึกษาวิทยานิพนธ์ร่วม: ผศ. ภก. ดร. บดินทร์ ทิวสุวรรณ, 135 หน้า.

ซี-ดีเอ็นเอได้ถูกค้นพบและได้รับความสนใจในการค้นหาบทบาทและความสำคัญในระบบชีวภาพ เนื่องจากมีหลักฐานการศึกษาเกี่ยวกับความสัมพันธ์ระหว่างซี-ดีเอ็นเอและพยาธิกำเนิดของโรคต่างๆ อาทิเช่น โรคเอสแอลอี, โรคข้ออักเสบรูมาตอยด์ และโรคอัลไซเมอร์ เป็นต้น กระบวนการทำงานบางอย่างในร่างกายถูกควบคุมจากการเกิดการจับกันระหว่างโปรตีนและดีเอ็นเอ ดังนั้น การศึกษาการเกิดอันตรกิริยากันระหว่างซี-ดีเอ็นเอและโปรตีนที่สามารถจับกับซี-ดีเอ็นเอเป็นหัวใจสำคัญในการเข้าใจถึงบทบาทหน้าที่อันแท้จริงของซี-ดีเอ็นเอในระบบชีวภาพ งานวิจัยนี้ได้ทำการศึกษาออกแบบและพัฒนาบี/ซี-ดีเอ็นเอ นาโนไบโอเซนเซอร์เพื่อตรวจสอบการจับยึดกันระหว่างดีเอ็นเอที่มีความสามารถในการเปลี่ยนรูปร่างเป็นซี-ดีเอ็นเอและโปรตีนที่สามารถจับกับซี-ดีเอ็นเอได้อย่างจำเพาะเจาะจง เช่น ซี-ดีเอ็นเอแอนติบอดี ซึ่งอาศัยหลักการตรวจวัดด้วยเทคนิคคลื่นผิวพลาสมอน โดยสายโพลิโกนิวคลีโอไทด์ถูกออกแบบให้มีการดัดแปลงโครงสร้างของเบสไซโตซีนในส่วนของลำดับเบสที่มีการจัดเรียงเป็นไซโตซีนสลับกับกวานีนเพื่อช่วยส่งเสริมให้เกิดการเปลี่ยนแปลงรูปร่างของดีเอ็นเออย่างขึ้น ซึ่งจากผลการศึกษาพบว่า สายโพลิโกนิวคลีโอไทด์ที่ออกแบบนั้นสามารถในการเปลี่ยนรูปร่างเป็นซี-ดีเอ็นเอและจับกับโปรตีนที่สามารถจับกับซี-ดีเอ็นเอได้อย่างจำเพาะเจาะจงเมื่อนำมาพัฒนาเป็นบี/ซี-ดีเอ็นเอ ไบโอเซนเซอร์พร้อมทั้งศึกษาเกิดการไฮบริดเซชันกับดีเอ็นเอและการจับกันระหว่างดีเอ็นเอและโปรตีนพื้นผิวของไบโอเซนเซอร์ พบว่า ผลการศึกษาแสดงให้เห็นว่า กระบวนการตรึงสายโพลิโกนิวคลีโอไทด์ลงบนพื้นผิวทองของไบโอเซนเซอร์เกิดขึ้นได้อย่างสมบูรณ์ และสายโพลิโกนิวคลีโอไทด์บนพื้นผิวของไบโอเซนเซอร์สามารถเกิดไฮบริดเซชันกับดีเอ็นเอที่มีลำดับเบสคู่สมได้อย่างจำเพาะเจาะจง การศึกษานี้สามารถพัฒนาสถานะที่เหมาะสมในการศึกษาการเกิดไฮบริดเซชัน แต่อย่างไรก็ตามสถานะที่เหมาะสมในขั้นตอนการศึกษาการจับกันระหว่างดีเอ็นเอและโปรตีนพื้นผิวของไบโอเซนเซอร์ยังคงต้องพัฒนาเพื่อให้ได้สถานะที่เหมาะสมต่อไป

ภาควิชา อาหารและเภสัชเคมี

ลายมือชื่อนิสิต .....

สาขาวิชา เภสัชเคมี

ลายมือชื่อ อ.ที่ปรึกษาหลัก .....

ปีการศึกษา 2557

ลายมือชื่อ อ.ที่ปรึกษาร่วม .....

# # 5476201133 : MAJOR PHARMACEUTICAL CHEMISTRY

KEYWORDS: Z-DNA FORMING PROBE, BIOSENSOR, 135 INTERACTION

KULWADEE SAWATPAIBOONTAWEE: DEVELOPMENT OF B/Z-DNA NANOBIOSENSOR FOR DETECTION OF Z-DNA BINDING PROTEINS. ADVISOR: VORASIT VONGSUTILERS, Ph.D., R.Ph., CO-ADVISOR: ASST. PROF. BODIN TUESUWAN, Ph.D., R.Ph.}, pp.

The left-handed Z-DNA has been attempted to elucidate the biological significance since several research studies suggest correlation between the Z-DNA and pathogenesis of many diseases, for example, systemic lupus erythematosus, rheumatoid arthritis, and Alzheimer's disease. Because protein-DNA interaction can control various biological processes, studying of the interaction between Z-DNA and Z-DNA binding proteins is the key to understand biological role of Z-DNA. In this study, B/Z-DNA nanobiosensor was designed and developed to determine the binding of Z-DNA forming probe to specific Z-DNA binding proteins under surface plasmon resonance (SPR) technique detection. Z-DNA forming probe was designed to contain the Z-DNA facilitator, 5-methylcytosine, in an alternating cytosine-guanine tract. The circular dichroism results have demonstrated the designed Z-DNA forming probe could convert to the left-handed conformation and specifically bind to Z-DNA specific binding protein. After B/Z-DNA biosensor development, DNA hybridization study and DNA-protein binding study on surface were investigated. All SPR results have presented the complete of DNA immobilization process and the B/Z-DNA biosensor can hybridized specifically to complementary target. This study provided the optimal SPR condition for DNA hybridization study, nevertheless, the SPR condition for study of DNA- protein binding on biosensor surface needs further optimization.

Department: Food and Pharmaceutical Student's Signature .....

Chemistry Advisor's Signature .....

Field of Study: Pharmaceutical Chemistry Co-Advisor's Signature .....

Academic Year: 2014

## ACKNOWLEDGEMENTS

My sincere gratitude is expressed to my thesis adviser, Dr. Vorasit Vongsutilers, for valuable advice, continual guidance, lightening me how the sequence of study and thought are and encouragement throughout the period of my graduated study.

I am sincerely grateful to my co-adviser, Assistant Professor Dr. Bodin Tuesuwan, for valuable suggestions, kindness during my graduate study.

I am very grateful to all members of thesis committee, Assistant Professor Dr. Mitr Pathipvanich, Associate Professor Dr. Wanchai De-Eknamkul, and Associate Professor Nuansri Niwattisaiwong for providing their valuable suggestions.

I also would like to thank all staffs of the Department of Food and Pharmaceutical Chemistry for their kindness and helpfulness.

Thankful expression is extended to my colleague, Miss Weena Arjhan, for her kindness, helpfulness, encouragement and friendship.

Finally, I would like to express my deeply gratitude to my beloved parents and family for their authentic love, understanding and continued supporting all in my life.

## CONTENTS

	Page
THAI ABSTRACT .....	iv
ENGLISH ABSTRACT .....	v
ACKNOWLEDGEMENTS .....	vi
CONTENTS .....	vii
LIST OF TABLES .....	x
LIST OF FIGURES .....	xi
CHAPTER I INTRODUCTION.....	18
CHAPTER II LITERATURE REVIEW .....	20
Structure and Chemistry of Z-DNA.....	20
Biological significance of Z-DNA.....	22
DNA nanobiosensor .....	23
Circular dichroism (CD) spectroscopy .....	25
Surface plasmon resonance (SPR) spectroscopy .....	27
CHAPTER III MATERIALS AND METHODS .....	29
Apparatus and instrument .....	29
Chemicals and reagents .....	29
Reagent preparation procedures .....	31
Method.....	34
1. Selection of base modification for Z-DNA probe .....	34
1.1 Thermal stress of modified nucleosides .....	36
1.2 Acidic stress of modified nucleosides .....	36
1.3 Alkaline stress of modified nucleosides .....	37

	Page
2. Z-DNA forming probe design and selection.....	37
3. Characterization of Z-DNA prone sequences .....	39
3.1 Purity determination by HPLC method .....	39
3.2 Oligonucleotide quantification .....	40
3.3 Melting temperature measurement.....	40
3.4 B-Z DNA transition study .....	41
3.4.1 Effect of monovalent cations .....	41
3.4.2 Effect of divalent cations.....	41
4. Determination of the interaction between Z-DNA prone sequence and specific Z-DNA binding protein in solution condition .....	43
5. Immobilization of the Z-DNA forming sequence on gold surface DNA immobilization procedure .....	43
6. Detection of DNA hybridization on biosensor surface.....	45
7. Study of Z-DNA forming probe and specific Z-DNA binding protein interaction on biosensor surface.....	45
CHAPTER IV RESULTS AND DISCUSSIONS.....	47
1. Selection of base modification for Z-DNA probe.....	47
1.1 Thermal stress of modified nucleosides .....	48
1.2 Acidic stress of modified nucleosides .....	52
1.3 Alkaline stress of modified nucleosides .....	54
2. Z-DNA forming probe design and selection .....	54
3. Characterization of Z-DNA prone sequences.....	57
3.1 Purity determination of the selected oligonucleotides.....	57
3.2 Oligonucleotide quantification.....	61



	Page
3.3 Melting temperature measurement.....	63
3.4 B-Z DNA transition study .....	64
3.4.1 Effect of monovalent cations.....	64
3.4.2 Effect of divalent cations .....	67
4. Determination of the interaction between Z-DNA prone sequence and specific Z-DNA binding protein in solution condition .....	72
5. Immobilization study of the Z-DNA prone sequence on gold surface .....	75
6. Detection of DNA hybridization on biosensor surface.....	78
7. Study of Z-DNA forming probe and specific Z-DNA binding protein interaction on biosensor surface .....	82
CHAPTER V CONCLUSIONS.....	91
REFERENCES .....	92
APPENDICES.....	98
Appendix A Stability study data of the modified nucleosides.....	99
Appendix B Chromatogram and chromatographic results of the oligonucleotides.....	107
Appendix C UV spectra of the selected oligonucleotides .....	121
Appendix D CD spectra of B-Z transition study and DNA-protein binding study....	126
VITA.....	135

## LIST OF TABLES

<b>Table 3.1</b>	List of the designed oligonucleotides used in this study .....	39
<b>Table 4.1</b>	The first-order kinetic stability data of unmodified and modified nucleosides under thermal stress condition at 80 °C. ....	51
<b>Table 4.2</b>	Estimated $\Delta G$ of dimer and hairpin loops structures of the selected oligonucleotides from OligoAnalyzer software. ....	56
<b>Table 4.3</b>	DNA content of the purchased oligonucleotides. ....	62
<b>Table 4.4</b>	$T_m$ of the oligonucleotide duplexes.....	64



## LIST OF FIGURES

<b>Figure 2.1</b>	The crystal structure of the left-handed Z-DNA compares to the right-handed B-DNA. Z-DNA has only a deep narrow minor groove while B-DNA has major and minor grooves or sugar-phosphate backbone.....	21
<b>Figure 2.2</b>	Examples of modified nucleobases which can stabilize Z-DNA. ....	22
<b>Figure 2.3</b>	Schematic illustration of the principle of biosensor. ....	24
<b>Figure 2.4</b>	Linear polarized light originates from an equal combination of right ( $E_R$ ) and left ( $E_L$ ) circularly polarized light (a). Elliptical polarized light is occurred from unequal absorption of right ( $E_R$ ) and left ( $E_L$ ) circularly polarized light. $\alpha$ represents an angle of rotation.....	26
<b>Figure 2.5</b>	Schematic of principle of surface plasmon resonance based on Kretschmann configuration.....	28
<b>Figure 3.1</b>	Chemical structure of 5-methyl-2'-deoxyguanosine (5-mdC), 8-Bromo-2'-deoxyguanosine (8-BrdG) and 8-carboxyphenyl-2'-deoxyguanosine (8-CpdG). ....	35
<b>Figure 3.2</b>	Structure of the designed oligonucleotide probe containing (1) 5'-alkanethiol modification, (2) non-self-complementary sequences, (3) an alternating cytosine-guanine track and (4) a complementary oligonucleotide sequence. ....	38
<b>Figure 3.3</b>	Immobilization steps of the thiol modified single-stranded oligonucleotides.....	44
<b>Figure 4.1</b>	Mechanism of hydrolysis reaction of unmodified nucleosides, 2'-deoxyguanosine and 2'-deoxycytidine nucleosides.....	48
<b>Figure 4.2</b>	Degradation profile for the first-order kinetics of 2'-deoxyguanosine under thermal stress condition at 80 °C.....	49

<b>Figure 4.3</b>	Degradation profile for the first-order kinetics of 8-bromo-2'-deoxyguanosine under thermal stress condition at 80 °C. ....	49
<b>Figure 4.4</b>	Degradation profile for the first-order kinetics of 8-carboxyphenyl-2'-deoxyguanosine under thermal stress condition at 80 °C. ....	50
<b>Figure 4.5</b>	Degradation profile for the first-order kinetics of 2'-deoxycytidine under thermal stress condition at 80 °C. ....	50
<b>Figure 4.6</b>	Degradation profile for the first-order kinetics of 5-methyl-2'-deoxycytidine under thermal stress condition at 80 °C. ....	51
<b>Figure 4.7</b>	Degradation profile for the first-order kinetics of 2'-deoxyguanosine under acidic stress condition. ....	52
<b>Figure 4.8</b>	Degradation profile for the first-order kinetics of 8-bromo-2'-deoxyguanosine under acidic stress condition. ....	53
<b>Figure 4.9</b>	Degradation profile for the first-order kinetics of 8-carboxyphenyl-2'-deoxyguanosine under acidic stress condition. ....	53
<b>Figure 4.10</b>	Chromatogram of oligo-1 under gradient method from 10% to 40% ACN in 30 minutes (a gradient slope of 1 %ACN/min). The mobile phase was comprised of acetonitrile and 100 mM TEAA, pH 7. The injection volume was set 10 µL. The column temperature was maintained at 40 °C and the UV detection monitored at 260 nm. ....	57
<b>Figure 4.11</b>	Chromatograms of oligo-1 under various gradient conditions. ....	58
<b>Figure 4.12</b>	Chromatogram of the reaction mixture of oligo-2 and DTT under gradient method from 10% to 30% ACN in 30 minutes (a gradient slope of 0.67 %ACN/min) (Bottom) compared to chromatogram of the reaction mixture of oligo-2 and DTT under previous HPLC method (Top). The mobile phase was comprised of acetonitrile and 100 mM TEAA, pH 7. The injection volume was set to 10 µL. The column temperature was maintained at 40 °C and the UV detection monitored at 260 nm. ....	60

- Figure 4.13** Chromatogram of oligo-2 under gradient method from 10% to 30% ACN in 30 minutes (a gradient slope of 0.67 %ACN/min). The mobile phase was comprised of acetonitrile and 100 mM TEAA, pH 7. The injection volume was set 10  $\mu$ L. The column temperature was maintained at 40  $^{\circ}$ C and the UV detection monitored at 260 nm..... 61
- Figure 4.14** CD spectra of the oligo-1, CG decamer, with various concentrations of NaCl. The oligonucleotide sample, approximately 6  $\mu$ M, was prepared in 50 mM phosphate buffer pH 7.4. The CD spectra were monitored at 25  $^{\circ}$ C with a scanning rate of 50 nm/min. Accumulation was set to 5 scans..... 65
- Figure 4.15** CD spectra of the duplex of oligo-4+6 with NaCl range from 100 mM to 4000 mM. The oligonucleotide duplex, approximately 6  $\mu$ M, was prepared in 50 mM phosphate buffer pH 7.4. The CD spectra were monitored at 25  $^{\circ}$ C with a scanning rate of 50 nm/min. Accumulation was set to 5 scans..... 66
- Figure 4.16** CD spectra of the duplex of oligo-5+6 with NaCl range from 100 mM to 4000 mM. The oligonucleotide duplex, approximately 6  $\mu$ M, was prepared in 50 mM phosphate buffer pH 7.4. The CD spectra were monitored at 25  $^{\circ}$ C with a scanning rate of 50 nm/min. Accumulation was set to 5 scans. .... 67
- Figure 4.17** CD spectra of the duplex of oligo-1 in the presence of  $MgCl_2$  300 mM compared to the duplex of oligo-1 in the presence of NaCl 500 mM. The oligonucleotide duplex, approximately 6  $\mu$ M, was prepared in 50 mM phosphate buffer pH 7.4. The CD spectra were monitored at 25  $^{\circ}$ C with a scanning rate of 50 nm/min. Accumulation was set to 5 scans. .... 68
- Figure 4.18** CD spectra of oligo-5+6 in 4 M of NaCl without adding  $MgCl_2$  and with  $MgCl_2$  in range from 10-50 mM. The oligonucleotide duplex, approximately 6  $\mu$ M, was prepared in 50 mM phosphate buffer pH 7.4 and 4 M NaCl. The CD spectra were monitored at 25  $^{\circ}$ C with a scanning rate of 50 nm/min. Accumulation was set to 5 scans. .... 70

- Figure 4.19** CD spectra of oligo-4+6 in 4 M of NaCl without adding MgCl<sub>2</sub> and with MgCl<sub>2</sub> in range from 10-50 mM. The oligonucleotide duplex, approximately 6 μM, was prepared in 50 mM phosphate buffer pH 7.4 and 4 M NaCl. The CD spectra were monitored at 25 °C with a scanning rate of 50 nm/min. Accumulation was set to 5 scans. .... 71
- Figure 4.20** CD spectra of oligo-5+6 in 50 mM Na<sub>2</sub>HPO<sub>4</sub> buffer, pH 7.0 with varied molar ratio of Z-ab. The oligonucleotide concentration was at 3.2 μM. The CD spectra were monitored at 25 °C with a scanning rate of 20 nm/min. Accumulation was set to 10 scans. .... 73
- Figure 4.21** The proposed mechanisms for a complex of oligo-5+6 duplex and Z-ab. .... 74
- Figure 4.22** Thiol-modified oligonucleotide reduction reaction in deprotection step. .... 75
- Figure 4.23** Chromatograms of DTT solution supplied from Sigma Aldrich (Bottom) and DTT solution prepared in 50 mM phosphate buffer, pH 8.4 (freshly prepared) (Top) under gradient method from 10% to 25% ACN in 30 minutes (a gradient slope of 0.25 %ACN/min). The mobile phase was comprised of acetonitrile and 100 mM TEAA, pH 7. The injection volume was set 10 μL. The column temperature was maintained at 40 °C and the UV detection monitored at 260 nm. .... 76
- Figure 4.24** Chromatograms of the reaction mixture of oligo-5 and DTT (Top) and the deprotected oligo-5 (Bottom) under gradient method from 10% to 30% ACN in 30 minutes (a gradient slope of 0.67 %ACN/min). The mobile phase was comprised of acetonitrile and 100 mM TEAA, pH 7. The injection volume was set 10 μL. The column temperature was maintained at 40 °C and the UV detection monitored at 260 nm. .... 77

**Figure 4.25** SPR sensograms of hybridization process of immobilized oligo-2 and oligo-3 under running buffer contained only 50 mM Na<sub>2</sub>HPO<sub>4</sub> buffer, without adding NaCl (a), with adding 50 mM NaCl (b), with adding 100 mM NaCl (c) and with adding 300 mM NaCl (d). The SPR signal of duplex formation of oligo-2+3 were 11.6 mdeg, 23.8 mdeg, 43.1 mdeg, and 23.3 mdeg respectively. The concentration of oligo-3 was prepared of 2 μM in running buffer. The association time and dissociation time were 300 seconds with five-cycle surface regeneration at 25 °C..... 80

**Figure 4.26** SPR sensograms of hybridization study of immobilized oligo-5 with a complementary strand, oligo-6 (a), a non-complementary sequence, oligo-7 (b), and a blank control, 50 mM phosphate buffer solution under running buffer comprising phosphate buffer solution (pH 7.4, 50 mM) and 100 mM NaCl. The oligo-6 gave a relative response of 8.8 mdeg while the oligo-7 and blank control gave only relative response of 0.3 mdeg and -1.4 mdeg, respectively. The association time and dissociation time were 200 seconds with five-cycle surface regeneration at 25 °C..... 81

**Figure 4.27** SPR sensogram of the interaction between immobilized oligo-2 and Z-ab under running buffer comprising phosphate buffer solution (pH 7.4, 50 mM) and 100 mM NaCl. The DNA hybridization step gave a relative response of 46.0 mdeg and the DNA-Z-ab binding step gave a relative response of 112.7 mdeg while the relative response of the post-regeneration phase was 82.5 mdeg. The concentration of oligo-3 solution was 2 μM in running buffer. The concentration of Z-ab solution was 0.250 μM in running buffer. The association time and dissociation time were 300 seconds with five-cycle surface regeneration at 25 °C. .... 82

- Figure 4.28** SPR sensogram of surface regeneration with 2 M NaCl. The relative response of the post-regeneration phase was 0.2 mdeg. The regeneration time was set to 120 seconds with five repeated cycles at 25 °C..... 83
- Figure 4.29** SPR sensogram of surface regeneration with 10 mM NaOH (a) and 100 mM NaOH (b). The relative responses of the post-regeneration phase were -14.4 mdeg and 4.3 mdeg, respectively. The regeneration time was set to 120 seconds with five repeated cycles at 25 °C..... 84
- Figure 4.30** SPR sensogram of the interaction between only immobilized oligo-2 and Z-ab under running buffer comprising phosphate buffer solution (pH 7.4, 50 mM) and 100 mM NaCl. The immobilized DNA-Z-ab binding step gave a relative response of 64.1 mdeg. The concentration of Z-ab solution was 0.125  $\mu$ M in running buffer. The association time and dissociation time were 300 seconds at 25 °C..... 85
- Figure 4.31** SPR sensogram of the interaction between Z-ab and free gold surface under running buffer comprising phosphate buffer solution (pH 7.4, 50 mM) and 100 mM NaCl. The Z-ab binding on surface gave a relative response of 129.5 mdeg. The concentration of Z-ab solution was 0.05  $\mu$ M in running buffer. The association time and dissociation time were 300 seconds at 25 °C..... 86
- Figure 4.32** SPR sensograms of the interaction between immobilized oligo-5 and Z-ab. under running buffer comprising phosphate buffer solution (pH 7.4, 50 mM) and 100 mM NaCl. The DNA hybridization step gave a relative response of 4.3 mdeg and the DNA-Z-ab binding step gave a relative response of 5.6 mdeg. The concentration of oligo-6 solution was 2  $\mu$ M in running buffer. The concentration of Z-ab solution was 0.5 nM in running buffer. The association time and dissociation time were 200 seconds with five-cycle surface regeneration at 25 °C. .... 87



**Figure 4.33** SPR sensograms of the interaction between immobilized oligo-5 and Z-ab. under running buffer comprising phosphate buffer solution (pH 7.4, 50 mM) and 100 mM NaCl. The DNA hybridization step gave a relative response of 4.3 mdeg and the DNA-Z-ab binding step gave a relative response of 4.5 mdeg. The concentration of oligo-6 solution was 2  $\mu$ M in running buffer. The concentration of Z-ab solution was 1.0 nM in running buffer. The association time and dissociation time were 200 seconds with five-cycle surface regeneration at 25 °C. .... 88

**Figure 4.34** CD spectra of oligo-5+6 in 50 mM  $\text{Na}_2\text{HPO}_4$  buffer, pH 7.0 with different production batches of Z-ab at a ratio Z-ab : oligo-5+6 of 0.5. GR 50327 was a new production batches of Z-ab and GR 34943 was a production batches of Z-ab used in the study of DNA-specific Z-DNA binding protein in solution condition. .... 89

**Figure 4.35** CD spectra of oligo-5+6 in 50 mM  $\text{Na}_2\text{HPO}_4$  buffer, pH 7.0 with varied molar ratio of the new production batch of Z-ab (GR 50327). The oligonucleotide concentration was at 3.2  $\mu$ M. The CD spectra were monitored at 25 °C with a scanning rate of 20 nm/min. Accumulation was set to 10 scans. .... 90

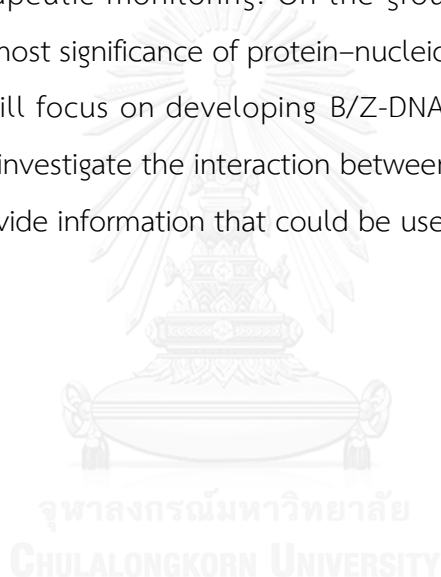
## CHAPTER I

### INTRODUCTION

Deoxyribonucleic acid (DNA) is an essential macromolecule of life which preserves genetic information. The structure and conformation of DNA play important roles in regulation of its function. DNA is usually in right-handed double helix which is known as B-form as demonstrated by Watson and Crick in 1953 (1), nevertheless, DNA has conformational flexibility leading to many polymorphisms. In 1979, Wang et al. (2) discovered an unusual polymorphism of DNA by X-ray crystallography. The X-ray crystal structure of the CG hexamer indicated that the structure was in left-handed helix which the base orientation alternated in *anti*- and *syn*-conformation. The alternated *syn-anti* of bases resulted in a zigzag sugar-phosphate backbone which hints the name Z-DNA (3, 4). After the discovery of Z-DNA, several research groups have attempted to elucidate the significance of Z-DNA in biological system. The evidence from some studies propose that Z-DNA might be associated with expression of gene including, BCL-2, c-MYC and SCL genes (5). The left-handed helix DNA might also be related to autoimmune diseases, such as systemic lupus erythematosus (6), Crohn's disease (7), and rheumatoid arthritis (8), due to the occurrence of Z-DNA antibodies in sera from patients (7, 9). Moreover, the unusual Z-DNA formation was discovered in the hippocampus of Alzheimer's disease patients (10). Although the biological function of Z-DNA is still unclear, these studies suggest correlation between the left-handed DNA and pathogenesis of several diseases.

Z-DNA can bind to Z-DNA binding proteins such as double-stranded RNA adenosine deaminase 1 (ADAR1) (11) which catalyzes the conversion of adenosine to inosine by deamination in RNA editing step (12). Since various biological processes, including DNA transcription, DNA repair, gene expression, and genetic recombination (13, 14), are regulated by protein–nucleic acid interactions, the interaction between Z-DNA binding proteins and Z-DNA may be the key to understand biological role of the left-handed Z-DNA. Thus studying of the interaction between them can bring

about the significance of Z-DNA in biological system and will provide information that can be the foundation of a new drug target discovery. The biosensor is one of the devices to study molecular recognition (15). DNA biosensor is a sensing device, which deoxyribonucleic acid acts as biological recognition element, rely on hybridization between DNA probe on the surface and complementary target sequence according to Watson and Crick base pairs or specific proteins of interest (16). Its advantages include high specificity, easy-to-use, label-free analysis, required small sample volume and the potential for nano-application (17-19) such as a screening of pathogenic proteins or DNA for clinical diagnosis and a quantitative analysis of biomarkers for therapeutic monitoring. On the grounds of the concept of DNA biosensor and the utmost significance of protein–nucleic acid interactions in biological system, this study will focus on developing B/Z-DNA nanobiosensor that will be useful as a model to investigate the interaction between Z-DNA and macromolecules which in turn will provide information that could be useful for drug target discovery.



## CHAPTER II

### LITERATURE REVIEW

#### Structure and Chemistry of Z-DNA

Z-conformation of DNA was revealed by Wang et al. (2). The X-ray crystal structure of the CG hexamer showed that Z-DNA is an anti-parallel double helix containing Watson-Crick hydrogen bond base pairs is similar to B-DNA structure. However, the structure exists in left-handed helical strand with the nucleotide bases orient in alternated *anti*- and *syn*-conformation. It has been shown that purines are more prone to adopt the *syn*-conformation than pyrimidines mainly due to the penalty from Van der Waals crowding. The sugar pucker of purine bases of Z-conformation is C3' endo, while in B-DNA both the purine and pyrimidine bases have the sugar pucker in C2' endo (4). The base conformation and the sugar pucker configuration leads to a zigzag sugar-phosphate backbone (3, 4). Z-DNA structure has only minor groove which is deep and narrow compared to B-DNA (Figure 2.1) (20). The sequences which are likely to form Z-DNA are composed of alternating purines-pyrimidines, especially cytosine-guanine alternating sequences (4, 5).

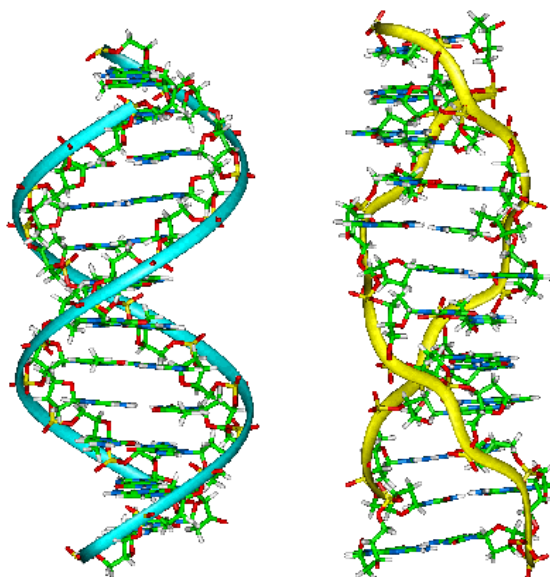


**Figure 2.1** The crystal structure of the left-handed Z-DNA compares to the right-handed B-DNA. Z-DNA has only a deep narrow minor groove while B-DNA has major and minor grooves or sugar-phosphate backbone.

The space of adjacent negatively charged phosphate groups in Z-DNA is much narrower than B-DNA. This structural feature contributes the electrostatic repulsion which destabilizes the Z-DNA structure. Therefore, the Z-conformation is rarely formed without stabilizing factors. Both mono and divalent cations, for example sodium, potassium and magnesium (21), have been shown to stabilize Z-DNA conformation by reducing the repulsion of negative charges. Furthermore, some base modification also increase the stabilization of Z-DNA including methylation at C5 position of cytosine (22, 23), methylation at N7 or C8 position of guanine (24-26), and bromination or arylation at C8 position of guanine (27, 28) (Figure 2.2). The use of cations or base modifications is common in B-Z-DNA conversion study.

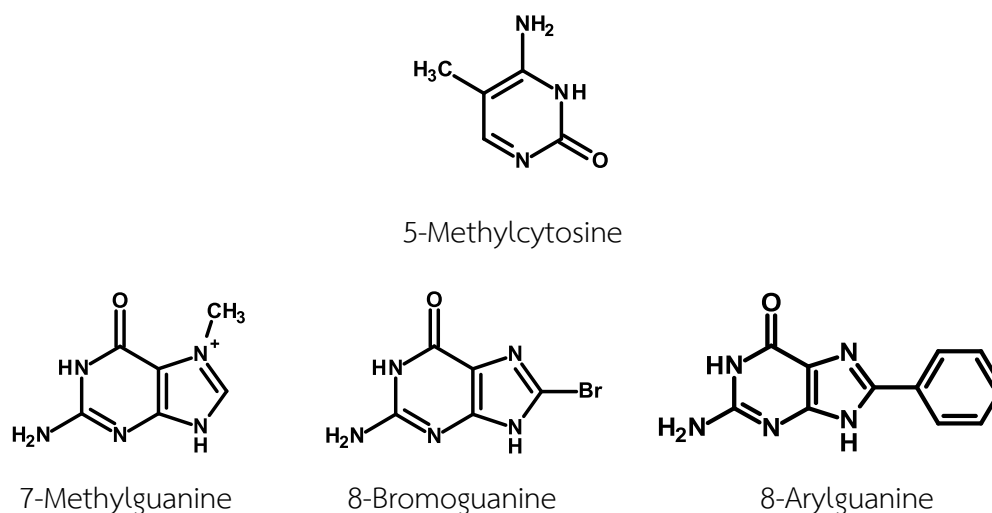


**Figure 2.2** Examples of modified nucleobases which can stabilize Z-DNA.

### Biological significance of Z-DNA

Although several studies have attempted to find the significance of Z-DNA in biological system, the role of Z-DNA is still unclear (3). Lui and Wang (5) explained that Z-DNA was involved in transcription process. Z-DNA formation can be induced by negative supercoiling. Z-DNA has been shown to connect with pathogenesis, such as in blood cancers (29). The translocation in BCL-2, c-MYC and SCL genes can lead to leukemia, lymphoma, and myeloma. There are studies revealed that Z-DNA prone sequences located in these genes. Z-DNA formation contributes to genetic instability and may lead to pathogenesis of blood cancers (20, 30-35). Moreover, Z-DNA has been found at abnormally high level in hippocampus of Alzheimer's disease patients (36). The presence of metal ion ( $Al^{3+}$ ) (37), amyloid beta (38), and polyamines (39) could promote Z-DNA formation in Alzheimer's disease brain. However, Z-DNA that plays role in Alzheimer's disease pathology has still remained unknown (8).

In 1997, Herbert et al. (11) identified and characterized ADAR1, a Z-DNA binding proteins. ADAR1 is an enzyme that has significant role in RNA editing. It can bind Z-DNA through Z-alpha region ( $Z_{\alpha ADAR1}$ ) which results in enhancement of deaminase activity to convert adenine to inosine which is subsequently read as

guanine base. The conversion of adenine to guanine in codon leads to protein diversity and sometimes mutation. Several interesting Z-DNA binding proteins have been discovered including dorsal longitudinal muscle protein (DLM-1) (40), also called Z-DNA binding protein 1 (ZBP1), and vaccinia virus E3L protein (41). Both of them have some homology to ADAR1 and can recognize Z-DNA. Lafer et al. (6) has reported the binding of antibodies which are specific for Z-DNA in human systemic lupus erythematosus sera in 1983. Z-DNA antibodies are also discovered in human sera of autoimmune diseases including rheumatoid arthritis (8) and Crohn's disease (7). From this evidence, association of Z-DNA with gene expression regulation pathogenesis of diseases is hypothesized. However, the functions and roles of left-handed Z-DNA in biological have not been clearly defined. Studying the proteins that can bind to this unusual DNA conformation will help understand the significance of Z-DNA and may be aid the discovery of new drug or target.

#### **DNA nanobiosensor**

As the concept of biosensor, the analytes can be recognized by and interact with biological elements (e.g. enzymes, DNA, antibodies, etc.), then upon their interaction signal is generated which can be measured and interpreted to information of molecular binding (42, 43). Biosensor is composed of two major components which are biological recognition and transducer elements. Biological recognition element can recognize the target analytes. It is attached on electrode or solid substrate that couples with transducer. The examples of the recognition element are enzymes, proteins, DNA, or cells. The second part is a transducer element which is a device that converts the biological signal, from recognition event, to the measurable signal. The signal is proportional to the target analyte concentration. Types of transducer are commonly used including optical, electrochemical, calorimetric, mechanical and magnetic transducers (Figure 2.3) (17, 44, 45).

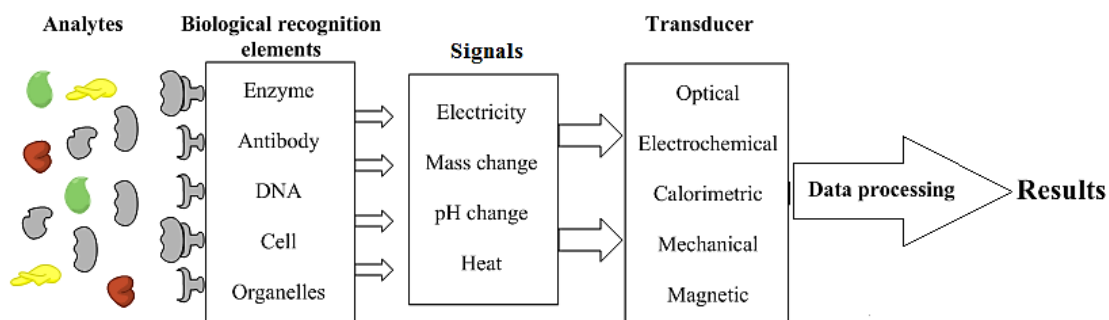


**Figure 2.3** Schematic illustration of the principle of biosensor.

DNA biosensor is constructed by using deoxyribonucleic acids as a biological recognition probe for detection of the analyte of interest including DNA, proteins based on hybridization and DNA-protein interaction. The important step of DNA biosensor development is immobilization of DNA probe onto supporting substrate surface. There are several methods that can be used for immobilization step, such as physical adsorption, covalent attachment and direct immobilization (46). The physical adsorption of DNA probe onto surface is based on electrostatic interaction, hydrogen bond or Van der Waals forces between DNA and surface. The method is quite simple and does not need any modification of the probe or sensor surface but it has some drawbacks on binding specificity and stability (47). The biotin-streptavidin complex, direct immobilization, is also applied to fix the biological recognition element. The principle of method is based on highly specificity and affinity of biotin-avidin binding ( $K_d = 10^{15} \text{ M}^{-1}$ ) (48, 49). The sensor surface is adsorbed by avidin or streptavidin, while DNA probe is labeled with biotin molecule. The immobilization of DNA on the surface is happen via biotin-avidin or streptavidin interaction. This method is often used to immobilize the macromolecule because of their high specificity and reversible, however, it is high cost for preparation (50, 51). In covalent immobilization, the substrate surface or DNA probe need to be chemically modified, for examples, the sensor surface is modified by compounds including carbodiimides, glutaraldehyde, nitrophenemethyl chloride, maleimide (19, 42, 50) which introduce the functional group to form covalent bond with DNA probe. Apart from the sensor surface modification,



DNA probe can also be modified. The modification of DNA probe by thiol group is widely used for attachment onto gold surface substrate. The advantages of this method are stability and strong attachment between DNA probe and substrate surface (48, 50).

Nanotechnology is widely applied in medical applications for example bioanalysis, clinical diagnosis, drug discovery and delivery system. DNA biosensor can also apply with nanotechnology to improve performance of the device. The aim of this project is to develop a reusable B/Z-DNA nanobiosensor for studying the interaction between Z-DNA and its binding proteins. The designed oligonucleotide will be immobilized on gold-coated platform and will be hybridized to complementary strand. The platform will be utilized as model to investigate proteins that can interact with Z-DNA conformation which in turn will provide information that could be useful for drug target discovery.

### **Circular dichroism (CD) spectroscopy**

Circular dichroism is a phenomenon occurred from the difference in absorption between left-handed and right-handed circularly polarized light,  $\Delta\varepsilon = \varepsilon_L - \varepsilon_R$  (52). In fact, linear polarized light is a combination of right and left circularly polarized light which are equal amplitude (Figure 2.4a). When the light passes through an absorbing optically active medium, both of circularly polarized lights are unequally absorbed contributing difference in speed, phase and extent between left and right circularly polarized light. The occurrence of different speed and phase causes a rotation of polarization plane while differently absorbed extents lead to an elliptical polarization of light (Figure 2.4b). If compounds have only chiral elements, they can show optical activity, not circular dichroism. CD spectroscopy is an excellent technique widely used for studying conformation of a chiral molecule, especially nucleic acids and proteins. Since their structures contain chromophore element and chiral element, the nucleic acids and proteins can be determined by CD technique.

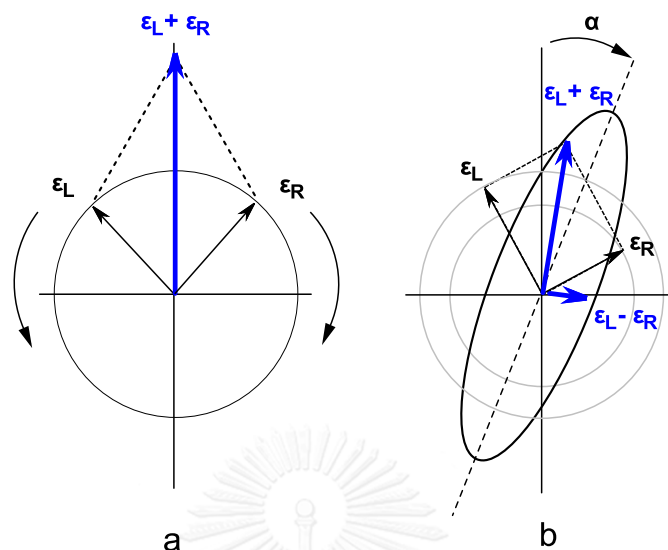


**Figure 2.4** Linear polarized light originates from an equal combination of right ( $E_R$ ) and left ( $E_L$ ) circularly polarized light (a). Elliptical polarized light is occurred from unequal absorption of right ( $E_R$ ) and left ( $E_L$ ) circularly polarized light.  $\alpha$  represents an angle of rotation.

Nucleic acid structure has 3 major components including a deoxyribose sugar, a phosphate residues, and a nitrogenous base. The deoxyribose sugars and phosphate alternating form the backbone of structure which they do not show light absorption in UV region. Unlike sugar and phosphate residues, all nitrogenous bases (A, G, C, and T) which are heterocyclic compounds can strongly absorb UV light due to highly conjugation system. These molecules function as the chromophores of DNA however their symmetrical planar (non-chiral) structures leading to be the optically inactive compounds. Chirality of nucleic acids originates from asymmetrical carbon atoms in 2'-deoxyribose sugars which connect to nitrogenous base therefore the DNA molecule has shown CD activity. The CD spectrum can be used to study and monitor the conformation of DNA because several interactions in three-dimensional structure of DNA and complexity of the higher order structures make the unique CD pattern.

### Surface plasmon resonance (SPR) spectroscopy

Surface plasmons are phenomenon occurs at the interface between a metal and a dielectric medium by exciting the free electrons on metal surface. Based on attenuated total reflection method, Surface plasmon resonance sensors were explained by Kretschmann and Otto (53). In Kretschmann configuration, when the light beam incidents to prism on which a metal film deposited, the generated electromagnetic wave penetrates into the metal film and excites free electrons to oscillate at the outer of metal film. If the frequency of incident light beam matches the frequency of oscillation of free electron, resonance condition is generated (54, 55). The characteristic of the electromagnetic field is an evanescent wave which decays exponentially by increasing in distance from boundary of the metal (Figure 2.5). The angle of incident light causing resonance is called SPR angle where show the minimum intensity of reflected light because of energy transfer of the incident beam to surface plasmons. When the binding occurs at the interface between a dielectric medium and metal surface, the refractive index of the metal surface is changed contributing to SPR angle shift. The shift in SPR angle is linearly proportional to the amount of ligand bound on surface. Therefore, SPR can be applied to investigate the interaction between target protein and DNA probe which is attached on metal surface. Besides the DNA-binding protein detection, SPR can be used for quantitative analysis of DNA-binding protein by constructing a calibration curve.

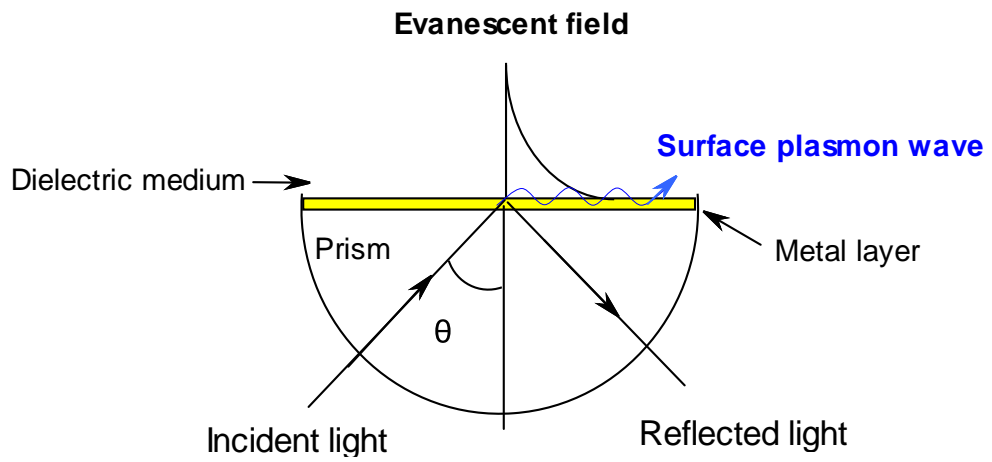


**Figure 2.5** Schematic of principle of surface plasmon resonance based on Kretschmann configuration



## CHAPTER III

### MATERIALS AND METHODS

#### Apparatus and instrument

- HPLC Shimadzu 10A VP DAD HPLC system included two of LC 10ADVP pumps, an autosampler, a column oven, and a photo diode array detector
- C18 column (InertSustain™ 150 x 4.6 mm, packed with 5- $\mu$ m particles) (GL Sciences Inc., Japan)
- Circular dichroism (CD) spectropolarimeter (Jasco J-815 CD spectropolarimeter with CDF-426L/15 temperature controller, Japan)
- AutoLab Esprit SPR (Metrohm, Netherlands)
- Analytical balance (Mettler-Toledo, Switzerland)
- pH meter (Mettler-Toledo, Switzerland)
- Magnetic stirrer/ hot plate (Corning, USA)
- Ultrasonic bath (Elma Schmidbauer, Germany)
- Vortex mixer (Vortex-Genie, Germany)
- Dry bath heat blocks (Witeg Labortechnik, Germany)
- Micropipette (Mettler-Toledo, Switzerland)
- illustra NAP™ 10 columns (GE Healthcare, United Kingdom)
- Nylon membrane filter 0.22  $\mu$ m (Pall Corporation, USA)
- Nylon membrane syringe filters 0.22  $\mu$ m (Filtrex, USA)

#### Chemicals and reagents

- 2'-Deoxyguanosine, hydrate, dG (Tokyo Chemical Industry Co., Ltd., Japan)

- 8-Bromo-2'-deoxyguanosine, 8-BrdG (Synthesized and characterized in laboratory)
- 8-Carboxyphenyl-2'-deoxyguanosine, 8-CpdG (Synthesized and characterized in laboratory)
- 2'-Deoxycytidine, dC (Tokyo Chemical Industry Co., Ltd., Japan)
- 5-Methyl-2' -deoxycytidine, 5-mdC (Tokyo Chemical Industry Co., Ltd., Japan)
- Oligonucleotides (Sigma-Aldrich, USA)
- Sheep polyclonal anti-Z-DNA antibody, Z-ab (Abcam Ltd., United Kingdom)
- Bovine serum albumin, BSA (PAA Laboratories GmbH., USA)
- Disodium hydrogen phosphate (anhydrous),  $\text{Na}_2\text{HPO}_4$  (Merck, Germany)
- Sodium chloride, NaCl (Merck, Germany)
- Magnesium chloride hexahydrate,  $\text{MgCl}_2 \cdot 6\text{H}_2\text{O}$  (Merck, Germany)
- Orthophosphoric acid (Merck, Germany)
- Sulfuric acid,  $\text{H}_2\text{SO}_4$  (Merck, Germany)
- Hydrochloric acid fuming, HCl (Emsure, Germany)
- Ammonium acetate,  $\text{CH}_3\text{COONH}_4$  (Merck, Germany)
- Ammonia solution (Lobachemie, India)
- 30% Hydrogen peroxide,  $\text{H}_2\text{O}_2$  (Merck, Germany)
- Triethanolamine (Merck, Germany)
- Glacial acetic acid (Baker, USA)
- Mercaptohexanol, MCH (Sigma-Aldrich, USA)
- Dithiothreitol, DTT (OmniPur Merck, Germany)
- Acetonitrile (HPLC grade) (Burdick and Jackson, USA)
- Ultrapure Milli-Q water (Millipore, Germany)

- Deionized water (ELGA, France)
- Nitrogen gas 99.9 % (Praxair, Thailand)

### Reagent preparation procedures

#### 50 mM of phosphate buffer preparation (pH 7.4)

0.71 g of anhydrous  $\text{Na}_2\text{HPO}_4$  was dissolved in 80 mL of water. After adjusting the pH to 7.4 with 3 N of phosphoric acid, the volume was adjusted to make a final volume of 100 mL with water.

#### Nucleoside stock solutions (100 $\mu\text{g}/\text{mL}$ )

25 mg of dG, 8-BrdG, 8-CpdG, dC and 5-mdC were accurately weighed into 250-mL volumetric flasks and added 150 mL of mobile phase, individually. All solutions were sonicated with an ultrasonic bath to help dissolution. The volume was adjusted to make a final volume of 250 mL with mobile phase.

#### 90 mM of ammonium acetate buffer preparation (pH 6.0)

6.552 g of  $\text{CH}_3\text{COONH}_4$  was dissolved in 800 mL of water. 0.27 mL of glacial acetic acid was added then the final volume was adjusted with water to 1000 mL. After adjusting the final volume, the pH was adjusted to 6.0 with glacial acetic acid or ammonia solution.

#### 250 mM of hydrochloric acid solution preparation

An amount of 2.07 mL of 37% fuming HCl was transferred into 80 mL of water and mixed with stirrer. The final volume was adjusted with water to 100 mL.

### **1 M of ammonium hydroxide solution preparation**

An amount of 1.87 mL of 25% ammonia solution was transferred into 80 mL of water and mixed with stirrer. The final volume was adjusted with water to 100 mL.

### **100 mM of triethylammonium acetate buffer preparation (TEAA, pH 7.0)**

An amount of 14.0 mL of triethylamine was transferred into 900 mL of water, and mixed with stirrer. Then the pH of solution was adjusted to 7.0 with glacial acetic acid, slowly added. The final volume was adjusted with water to 1000 mL. The buffer solution was filtered through 0.22  $\mu\text{m}$  nylon membrane filter and degassed by ultrasonic bath for 15 min before use.

### **250 mM of phosphate buffer preparation (pH 7.4)**

1.775 g of anhydrous  $\text{Na}_2\text{HPO}_4$  was dissolved in 40 mL of water. After adjusting the pH to 7.4 with 3 N of phosphoric acid, the volume was adjusted to make a final volume of 50 mL with water.

### **4 M of NaCl solution preparation**

11.7 g of NaCl was dissolved in 40 mL of water until completely clear. The final volume was adjusted with water to 50 mL.

### **2 M of magnesium chloride solution preparation**

20.33 g of magnesium chloride was dissolved in 10 mL of water. The volume was adjusted to give a final volume of 20 mL with water.



**50 mM of phosphate buffer for DTT solution preparation (pH 8.4)**

0.177 g of anhydrous  $\text{Na}_2\text{HPO}_4$  was dissolved in 20 mL of water. After adjusting the pH to 7.4 with 3 N of phosphoric acid, the volume was adjusted to make a final volume of 25 mL with water.

**100 mM of DTT solution preparation**

15.4 mg of DTT was dissolved in 1 mL of 50 mM phosphate buffer pH 8.4 then the solution was mixed on a vortex mixer (prepared fresh).

**1 mM of MCH solution preparation**

14 mg of MCH was weighed and dissolved in 10 mL of ethanol to make a 100 mM MCH stock solution. A 50  $\mu\text{L}$  of MCH stock solution was transferred into 4.95 mL of water and mixed well.

**Phosphate buffer for immobilization preparation**

1.17 g of NaCl was weighed and dissolved in 5 mL of 50 mM phosphate buffer pH 7.4. The volume was adjusted to give a final volume of 10 mL with 50 mM phosphate buffer pH 7.4 and mixed well.

**Piranha solution preparation**

2.5 mL of 30%  $\text{H}_2\text{O}_2$  was added into 7.5 mL of concentrated  $\text{H}_2\text{SO}_4$  slowly and gently mixed, under the fume hood. The solution was allowed to cool before use.

### **100 mM of phosphate buffer preparation (pH 7.4)**

14.2 g of anhydrous  $\text{Na}_2\text{HPO}_4$  was dissolved in 900 mL of water. After adjusting the pH to 7.4 with 3 N of phosphoric acid, the volume was adjusted to make a final volume of 1000 mL with water.

### **2 M of NaCl solution preparation**

11.7 g of NaCl was dissolved in 80 mL of water until completely clear. The volume was adjusted to give a final volume of 100 mL with water.

### **Running buffer preparation (50 mM phosphate buffer pH 7.4 with various NaCl concentrations)**

500 mL of 100 mM  $\text{Na}_2\text{HPO}_4$  buffer, pH 7.4 and an amount of 2 M of NaCl (depending on the salt concentration, 0-300 mM) were added to a 1000-mL volumetric flask. The solution was diluted with water to volume and mixed. Running buffer was filtered through 0.22  $\mu\text{m}$  nylon membrane filter and degassed by ultrasonic bath for 15 min before use.

## **Method**

### **1. Selection of base modification for Z-DNA probe**

Base modification can facilitate the stabilization of Z-DNA conformation, thus modified nucleobases were designed to incorporate in the oligonucleotide probe including 5-methylcytosine, 8-bromoguanine and 8-carboxyphenylguanine. Prior to Z-DNA forming probe design and selection, the base-modified nucleosides (Figure 3.1) are needed to be evaluated the stability of nucleoside structure since modification on nucleobase may lead to increasing of deglycosylation rates. Decreasing in stability of N-glycosyl bonds impacts the quality and the binding capability of oligonucleotide probe. The reversed phase high-performance liquid chromatography (RP-HPLC) condition was developed and used to determine

the stability study of modified nucleosides. The HPLC experiments were performed on a Shimadzu LC-10AD VP and a C18 column (InertSustain™ 150 x 4.6 mm, packed with 5- $\mu$ m particles). The mobile phase was comprised of 90 mM ammonium acetate buffer, pH 6.0, and acetonitrile in ratio of 92:8 v/v and flow rate was set at 1 mL/min. The UV detection monitored at 253 nm for 2'-deoxyguanosine (dG) and its derivatives (8-BrdG, 8-CpdG) and at 270 nm for 2'-deoxycytidine (dC) and its derivatives (5-mdC) with setting the column temperature at 30 °C. The injection volume was set to 20  $\mu$ L.

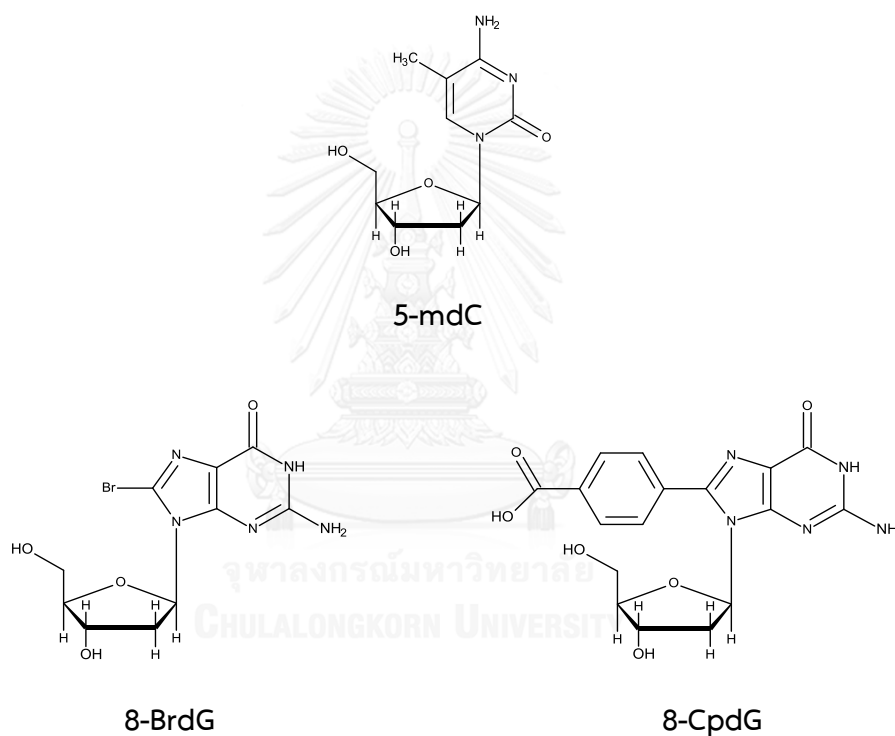


**Figure 3.1** Chemical structure of 5-methyl-2'-deoxyguanosine (5-mdC), 8-Bromo-2'-deoxyguanosine (8-BrdG) and 8-carboxyphenyl-2'-deoxyguanosine (8-CpdG).

Stability studies of modified nucleosides were evaluated the hydrolysis of N-glycosidic bond under acidic, alkaline and thermal stress conditions which are primary factors catalyzing hydrolysis reaction. Procedures of stability studies were described as follows,

### 1.1 Thermal stress of modified nucleosides

All thermal stress samples were prepared to 10 µg/mL by diluting nucleoside stock solutions with diluent (mobile phase) and exposed to heat at 80±0.5 °C with a temperature controlled water bath. After incubation, the thermal stress samples were collected at various time points until the significant degradation of modified nucleosides were observed. When samples were collected, the reaction was stopped by immediately immersing in an ice bath, then the samples were filtered through 0.22 µm nylon membrane syringe filters before HPLC measurement.

The experiments were controlled by using a negative control sample and a blank control sample. The negative control sample was prepared by allowing the nucleoside samples at ambient room temperature for 72 hours for dG sample, 10 hours for 8-BrdG and 8-CpdG samples while 115 hours for dC and 5-mdC samples. The blank control sample was prepared by heating diluent at 80±0.5 °C for 72 hours.

### 1.2 Acidic stress of modified nucleosides

All acidic stress samples were prepared by mixing 1.5 mL of nucleoside stock solution with 0.5 mL of 250 mM HCl into 50-mL volumetric flasks and storing in the dark at room temperature. After incubation, the acidic stress samples were collected at various time points until the significant degradation of modified nucleosides were observed. When the samples were collected, the reaction was stopped by immediately adding diluent to adjust the final volume of 50 mL, then they were measured the pH (pH 6.0 ±0.3) and filtered through 0.22 µm nylon membrane syringe filters before HPLC measurement. The final concentration of nucleoside acidic stress samples was approximate 3 µg/mL.

The experiments were controlled by using a blank control sample which was prepared by mixing 1.5 mL of diluent with 0.5 mL of 250 mM HCl into 50-mL volumetric flask and storing in the dark at room temperature for 114 hours.

### 1.3 Alkaline stress of modified nucleosides

All nucleoside alkaline stress samples were prepared by mixing 1.5 mL of nucleoside stock solution with 0.75 mL of 1 N  $\text{NH}_4\text{OH}$  into 50-mL volumetric flasks and storing in the dark at room temperature. After incubation, the alkaline stress samples were collected at various time points until the significant degradation of modified nucleosides were observed. When the samples were collected, the reaction was stopped by immediately adding diluent to adjust the final volume of 50 mL, then they were measured the pH (pH  $6.0 \pm 0.3$ ) and filtered through 0.22  $\mu\text{m}$  nylon membrane syringe filters before HPLC measurement. The final concentration of nucleoside acidic stress samples was approximate 3  $\mu\text{g}/\text{mL}$ .

The experiments were controlled by using a blank control sample which was prepared by mixing 1.5 mL of diluent with 0.75 mL of 1 N  $\text{NH}_4\text{OH}$  into 50-mL volumetric flask and storing in the dark at room temperature for 48 hours.

All base-modified nucleosides were potent facilitator of the B-Z-DNA transition, however, stability of structure of modified nucleosides was an important key to select for insertion in the oligonucleotide probe. The base-modified nucleoside with a lower rate constant of hydrolysis reaction was considered to be suitable for selection.

## 2. Z-DNA forming probe design and selection

The oligonucleotide probes were designed to comprise four major parts, including 5'-alkanethiol modification, which formed disulfide bond with protecting group, for attachment onto gold chip surface. The second part was an alternating cytosine-guanine track that can convert to Z-conformation. The third part was two non-self-complementary sequences at both ends of an oligonucleotide to reduce incomplete hybridization, and the fourth part was a complementary sequence to form DNA duplex. The negative control of Z-DNA forming probe has also been designed by

substitution alternating purines-pyrimidines track with random sequence, which cannot form Z-DNA conformation.

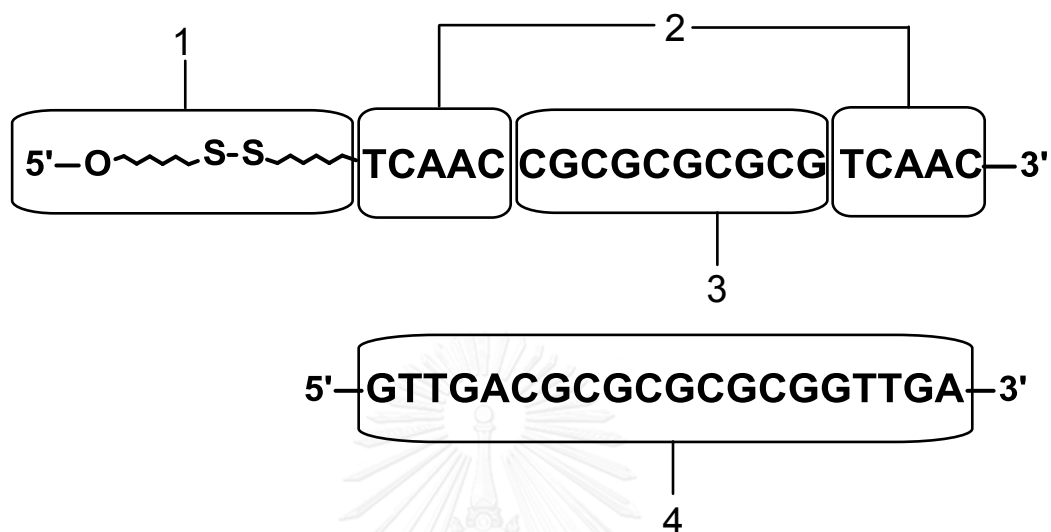


**Figure 3.2** Structure of the designed oligonucleotide probe containing (1) 5'-alkanethiol modification, (2) non-self-complementary sequences, (3) an alternating cytosine-guanine track and (4) a complementary oligonucleotide sequence.

OligoCalc (56) and OligoAnalyzer Tool (Integrated DNA Technologies, Inc.) were used to estimate the properties of oligonucleotides, such as hybridization potential, self-complementarity and hairpin loop formation in order to avoid unfavorable secondary structure of oligonucleotide probe selection. All oligonucleotide sequences used in this study were selected as listed in Table 3.1. Oligo-1, CG decamer, was used as a positive control due to its known capability to form Z conformation. Oligo-2 and Oligo-3 are complementary which were used as a negative control owing to lack of B-Z transition potential. The duplexes of oligo-4+6 and oligo-5+6 were Z-DNA prone sequences because of containing an alternating cytosine-guanine track. Particularly, oligo-5+6 were designed to have modified nucleobase in CG track therefore they would have more potential to stabilize Z-form

than the former. Oligo-7 is a non-complimentary sequence of all oligonucleotides in order to use as a negative control in hybridization step.

**Table 3.1** List of the designed oligonucleotides used in this study

Oligonucleotides	Base sequences	No. of base
Oligo-1	5' -CGC GCG CGC G -3'	10
Oligo-2	5' -(CH <sub>2</sub> ) <sub>6</sub> -S-S-(CH <sub>2</sub> ) <sub>6</sub> - TCA ACC TAA CCA GTA TCA AC -3'	20
Oligo-3	5' -GTT GAT ACT GGT TAG GTT GA -3'	20
Oligo-4	5' -(CH <sub>2</sub> ) <sub>6</sub> -S-S-(CH <sub>2</sub> ) <sub>6</sub> - TCA ACC GCG CGC GCG TCA AC -3'	20
Oligo-5	5' -(CH <sub>2</sub> ) <sub>6</sub> -S-S-(CH <sub>2</sub> ) <sub>6</sub> - TCA ACC* G*C*G* C*G*C* G*C*G* TCA AC -3'	20
Oligo-6	5' -GTT GAC GCG CGC GCG GTT GA -3'	20
Oligo-7	5' -TAA TCA AGA GTA TTT AGC AT -3'	20

Note : C\* and G\* represent modified base that can replace normal base in CG track.

### 3. Characterization of Z-DNA prone sequences

#### 3.1 Purity determination by HPLC method

Prior to characterization, immobilization study and protein-DNA binding study of the selected oligonucleotides, purity of DNA is needed to be evaluated. Because the impurities of the synthesized oligonucleotides can interfere the experiments, the reversed phase high-performance liquid chromatography (RP-HPLC) condition was developed and used to determine the purity of oligonucleotides. The HPLC experiments were performed on a Shimadzu LC-10AD VP and a C18 column (InertSustain<sup>TM</sup> 150 x 4.6 mm, packed with 5- $\mu$ m particles). The mobile phase was comprised of acetonitrile and 100 mM TEAA,

pH 7 in various ratio of organic phase. TEAA buffer was used as an ion-pairing agent to allow the use of RP-HPLC for DNA analysis because of the negatively charges on phosphates of DNA backbone. The UV detection monitored at 260 nm with setting the column temperature at 40 °C. The injection volume was set 10 µL.

### **Oligonucleotide sample preparations**

The oligonucleotide samples were prepared to 3 µM by diluting DNA stock solution with diluent, 50 mM phosphate buffer pH 7.4. The experiments were controlled by using diluent as a blank control sample.

### **3.2 Oligonucleotide quantification**

The oligonucleotide samples were prepared from DNA stock solution by diluting with 50 mM phosphate buffer pH 7.4. The final concentration of DNA sample was about 10 µM. The baseline measurement was determined from 50 mM phosphate buffer pH 7.4. The spectra of all oligonucleotides were recorded from 230 nm to 280 nm with accumulation of 5 scans and 50 nm/min scanning speed corrected with baseline subtracting. The measurement was performed at 25 °C by using 1 mm path length quartz cuvette, and calculated DNA content from the UV absorbance at 260 nm according to Beer-Lambert law.

### **3.3 Melting temperature measurement**

The mixture of complimentary oligonucleotides (6 µM) was prepared in 50 mM phosphate buffer pH 7.4. The oligonucleotide sample solutions were annealed by heating at 90 °C in dry bath heat blocks for 30 minutes and slowly cooling down to room temperature. Thermal analysis of the oligonucleotides was measured UV absorbance at 260 nm with variable temperatures that started from 10 °C to 90 °C at fix rate of 1 °C/min. Data pitch and delay time were set up 5 °C and 60 seconds, respectively. The negative control samples were prepared from



only the oligonucleotides without the presence of their complementary sequences.

### **3.4 B-Z DNA transition study**

The conformational conversion of selected oligonucleotides was evaluated by CD spectroscopic technique. CD pattern of B-DNA shows positive band at approximately 280 nm and 220 nm and a negative band at approximately 250 nm while Z-DNA has a unique CD pattern which a positive band shows at approximately 250 nm and negative band at approximately 295 nm. Cations can stabilize the structure of left-handed Z-DNA so they were used to determine a B-Z DNA transition capability of selected oligonucleotides.

#### **3.4.1 Effect of monovalent cations**

The oligonucleotide duplexes, approximately 6  $\mu\text{M}$ , were prepared individually in 50 mM phosphate buffer pH 7.4 with variable of NaCl concentrations (100 mM to 4000 mM of sodium salt). All oligonucleotide sample solutions were annealed prior to measurement by heating at 90 °C for 15 minutes and slowly cooling down to room temperature. DNA sample solutions in sodium salt from 100 mM to 2000 mM were prepared by adding with 4M of NaCl. The DNA sample solution in 4000 mM of salt was prepared by addition of solid NaCl. Each blank control sample was prepared from 50 mM phosphate buffer pH 7.4 in varying salt concentrations without the presence of oligonucleotide to provide a baseline. All CD spectra were recorded in a range of 200–340 nm at 25 °C with a scanning rate of 50 nm/min and were corrected with baseline subtracting. Data integration time was fixed of 1 second. Accumulation was set to 5 scans.

#### **3.4.2 Effect of divalent cations**

The oligonucleotide duplexes of oligo-1 and oligo-4+6, approximately 6  $\mu\text{M}$ , were prepared in 50 mM phosphate buffer pH 7.4 with variable of  $\text{MgCl}_2$

concentrations (10 mM to 1000 mM of magnesium salt). Each DNA sample was prepared by adding 2M of  $MgCl_2$  to make a final magnesium concentration. All oligonucleotide sample solutions were annealed prior to measurement by heating at 90 °C for 15 minutes and slowly cooling down to room temperature. Each blank control sample was prepared from 50 mM phosphate buffer pH 7.4 in varying salt concentrations without adding oligonucleotide to provide a baseline. The CD spectra were recorded in a range of 200–340 nm at 25 °C with a scanning rate of 50 nm/min and were corrected with baseline subtracting. Data integration time was fixed of 1 second. Accumulation was set to 5 scans.

Moreover, the duplexes of oligo-4+6 and oligo-5+6 were determined potential of B-Z DNA transition with variable of  $MgCl_2$  in high salt condition. Each DNA sample was prepared by adding 2M of  $MgCl_2$  into oligonucleotide solution in the presence of 4 M NaCl. The CD spectra were recorded in a range of 200–340 nm at 25 °C with a scanning rate of 50 nm/min and were corrected with baseline subtracting. Data integration time was fixed of 1 second. Accumulation was set to 5 scans.



#### 4. Determination of the interaction between Z-DNA prone sequence and specific Z-DNA binding protein in solution condition

The duplex of the oligonucleotides (approximately 3  $\mu\text{M}$ ) was prepared and annealed in 50 mM phosphate buffer pH 7.4. A Z-ab stock solution (approximately 16  $\mu\text{M}$ ), specific Z-DNA binding protein, was prepared in phosphate buffer saline. While BSA (40  $\mu\text{M}$ ) was prepared in 50 mM phosphate buffer pH 7.4 and used as a negative control protein. Each stock protein solution was gradually added into the annealed oligonucleotide solution. Interaction between oligonucleotides and protein was determined by CD spectropolarimeter. The CD measurement parameters were set to monitor in a range of 220–320 nm at 25 °C with a scanning rate of 20 nm/min. Data integration time was fixed of 1 sec. Accumulation was set to 10 scans.

The dilution test was performed by adding 50 mM phosphate buffer pH 7.4 instead of Z-ab stock solution into the oligonucleotides duplex solution while the blank control sample was prepared by adding Z-ab stock solution into 50 mM phosphate buffer pH 7.4 without the presence of oligonucleotides.

#### 5. Immobilization of the Z-DNA forming sequence on gold surface DNA immobilization procedure

Thiol modified Z-DNA prone oligonucleotide was immobilized on gold-coated glass chip, which made of BK-7 glass with 48 nm of gold deposited on a thin layer of titanium, through Au-S chemistry. Procedure of DNA immobilization was demonstrated in Figure 3.2.

1. Organic residue was cleaned from bare gold disk. Its surface was directly applied and stayed in Piranha solution for 30 minutes. Then it was rinsed five times with 20 mL of water and dried with blowing nitrogen gas.

2. The protecting group of thiol modified oligonucleotide on the 5' end (20 nmole) was removed by incubating with 1 mL of 100 mM DTT for 1 hour at ambient temperature.

3. A desalted column, NAP-10, was equilibrated with 5 mL of 50 mM phosphate buffer pH 7.4 for three times prior to use. After removal, the deprotected oligonucleotide was purified by adding the mixture onto NAP-10 column and allowing to completely enter the gel bed.

4. The deprotected oligonucleotide was eluted by loading 1.5 mL of 50 mM phosphate buffer pH 7.4 and collected by gravity flow. Purity of the deprotected oligonucleotide was determined prior to use by HPLC method.

5. 1.4 mL of the eluate was transferred to 3.6 mL of phosphate buffer for immobilization, mixed well, to make an oligonucleotide sample solution (approximately 2  $\mu$ M).

6. A cleaned bare gold disk was immersed into oligonucleotide sample solution under nitrogen gas over 24 hours to form self-assembled monolayer. After DNA immobilization, the gold disk was rinsed three times with 15 mL of 50 mM phosphate buffer pH 7.4 thoroughly.

7. The immobilized chip was transferred into 5 mL of 1 mM of MCH solution, 1 hour, to minimize non-specific adsorption on surface then rinsed three times with 15 mL of water and dried with blowing nitrogen gas.

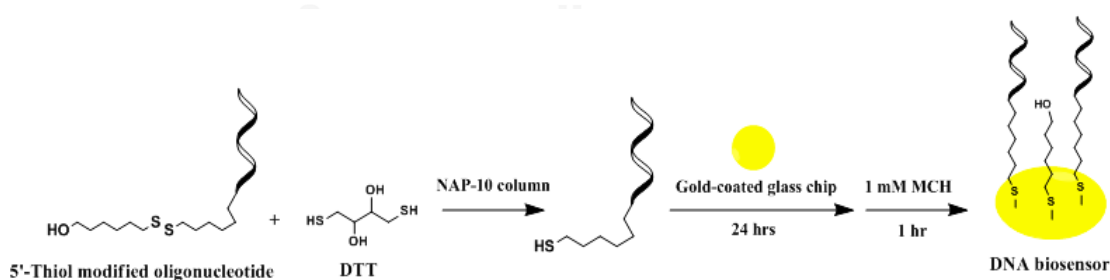


**Figure 3.3** Immobilization steps of the thiol modified single-stranded oligonucleotides.

## **6. Detection of DNA hybridization on biosensor surface**

Surface plasmon resonance (SPR) was performed to investigate the hybridization process of DNA and the interaction between Z-DNA forming probe and proteins. All SPR experiments were conducted using an AutoLab Esprit SPR.

Prior to study of DNA hybridization and DNA-protein interaction, the DNA probe on gold chip was stabilized with running buffer. Oligonucleotide samples were injected onto surface of gold chip to monitor the shift of SPR angle. The positive SPR response occurred when the DNA probe hybridized to complementary strand or bound to protein resulting from the alteration of refractive index at interface. In hybridization study, the ionic strength is a factor effecting on the hybridization efficiency therefore the running buffer for hybridization study has been developed by varying NaCl concentration (0-300 mM) in 50 mM phosphate buffer pH 7.4. Moreover, hybridization study of the immobilized DNA probe was confirmed by negative control test which used oligo-7 as a non-complement strand. All hybridization experiments used oligonucleotide samples with the concentration of 2  $\mu\text{M}$  in running buffer. The blank control sample was prepared from running buffer and was performed prior to hybridization study. The SPR measurement was set association time and dissociation time of 300 seconds with surface regeneration time of 50 seconds for five cycles. Temperature was monitored at 25  $^{\circ}\text{C}$  and sample volume was injected of 50  $\mu\text{L}$ .

## **7. Study of Z-DNA forming probe and specific Z-DNA binding protein interaction on biosensor surface**

The study of binding between DNA probe on gold chip and protein was performed on running buffer contained 50 mM phosphate buffer pH 7.4 with 100 mM NaCl. Prior to study of DNA-protein interaction, the DNA probe on gold chip was stabilized with running buffer. The sheep polyclonal anti-Z-DNA antibody, Z-ab, was used as a specific Z-DNA binding protein to investigate Z-DNA forming probe-protein interaction. The DNA-Z-DNA binding protein interaction experiments used Z-ab samples with the concentration in range of 0.5-5 nM in running buffer.

The blank control sample was prepared from running buffer and was performed prior to DNA-protein binding study. The SPR measurement was set association time and dissociation time of 300 seconds with surface regeneration time of 50 seconds for five cycles. Temperature was monitored at 25 °C and sample volume was injected of 50  $\mu$ L.



## CHAPTER IV

### RESULTS AND DISCUSSIONS

#### 1. Selection of base modification for Z-DNA probe

The dG, dC and 5-mdC were purchased from Tokyo Chemical Industry Co., Ltd. while 8-BrdG and 8-CpdG were synthesized in our laboratory according to previously reported protocol (57). Stability studies of unmodified and modified nucleosides was conducted on HPLC method which the mobile phase was comprised of 90 mM ammonium acetate buffer pH 6.0 and acetonitrile in the ratio of 92:8, %v/v. The chromatograms of the nucleosides showed isolated peak with peak purity index more than 0.99 which indicates there is no peak co-eluted with the peak of the analytes. When the nucleosides were performed on forced degradation study under acid and thermal stress conditions, the chromatograms showed the peaks of the degradation products could be separated from the major peak of nucleosides.

In thermal stress condition at 80 °C and acidic stress condition, the chromatograms of unmodified nucleosides showed the peak of degraded dG product was eluted at the same retention time as the peak of guanine nucleobase while the peak of degraded dC product was eluted at the same retention time as the peak of cytosine nucleobase which indicates the hydrolysis reaction of nucleosides cleaves N-glycosidic bond and gives a nucleobase and a deoxyribose sugar as the hydrolytic products (Figure 4.1) (58). Because of similar chemistry of core structure of nucleoside, the hydrolytic pathway of modified nucleosides was proposed to occur through the N-glycosidic linkage.

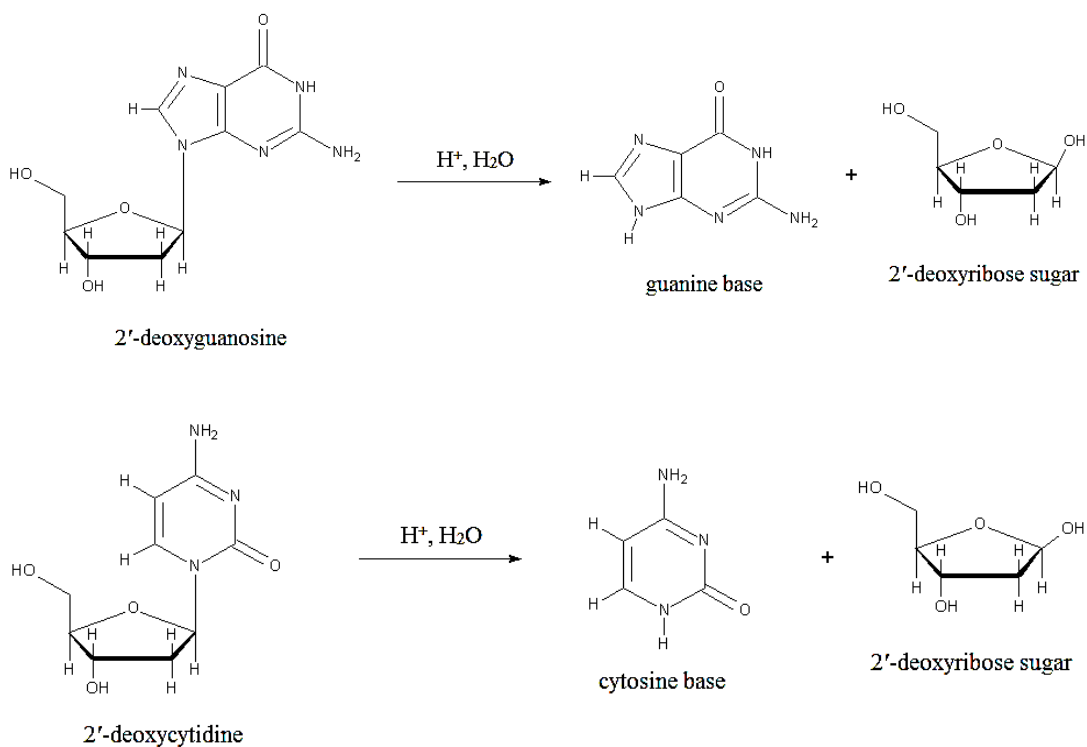


**Figure 4.1** Mechanism of hydrolysis reaction of unmodified nucleosides, 2'-deoxyguanosine and 2'-deoxycytidine nucleosides.

### 1.1 Thermal stress of modified nucleosides

In kinetic study of thermal hydrolysis of nucleosides, the degradation profiles of nucleosides were constructed from the nucleoside concentrations as a function of time. The linear relationship between the natural logarithm of a nucleoside concentration and time indicates all nucleoside degradations under thermal stress condition were observed (Figure 4.2-4.6). The rate constants ( $k$ ) and half-lives ( $t_{1/2}$ ) were presented in Table 4.1.



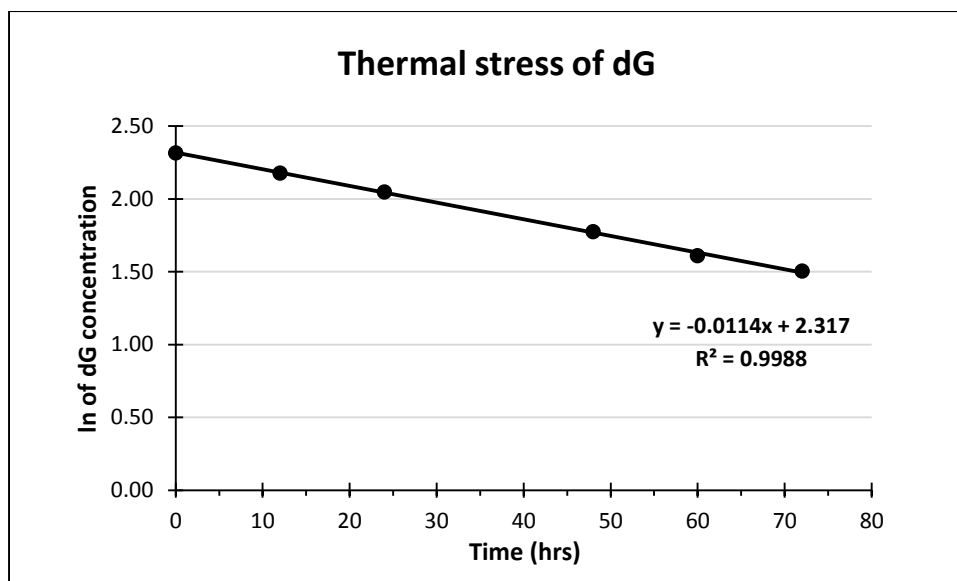


**Figure 4.2** Degradation profile for the first-order kinetics of 2'-deoxyguanosine under thermal stress condition at 80 °C.

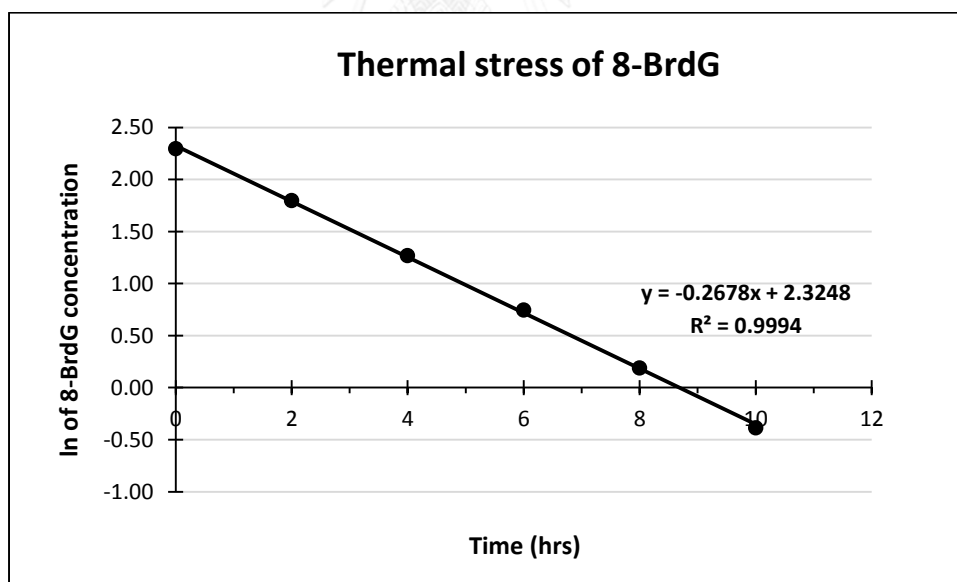


**Figure 4.3** Degradation profile for the first-order kinetics of 8-bromo-2'-deoxyguanosine under thermal stress condition at 80 °C.

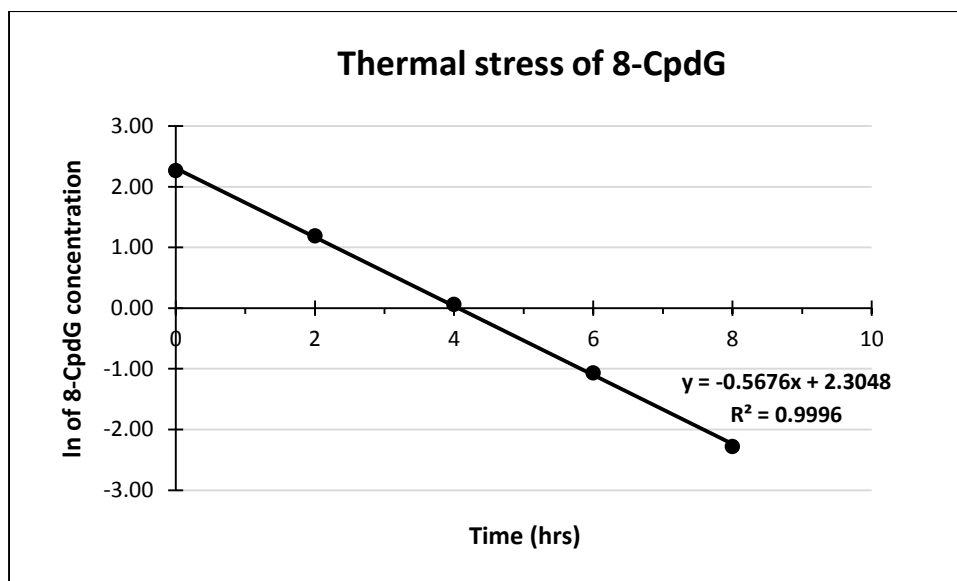


**Figure 4.4** Degradation profile for the first-order kinetics of 8-carboxyphenyl-2'-deoxyguanosine under thermal stress condition at 80 °C.

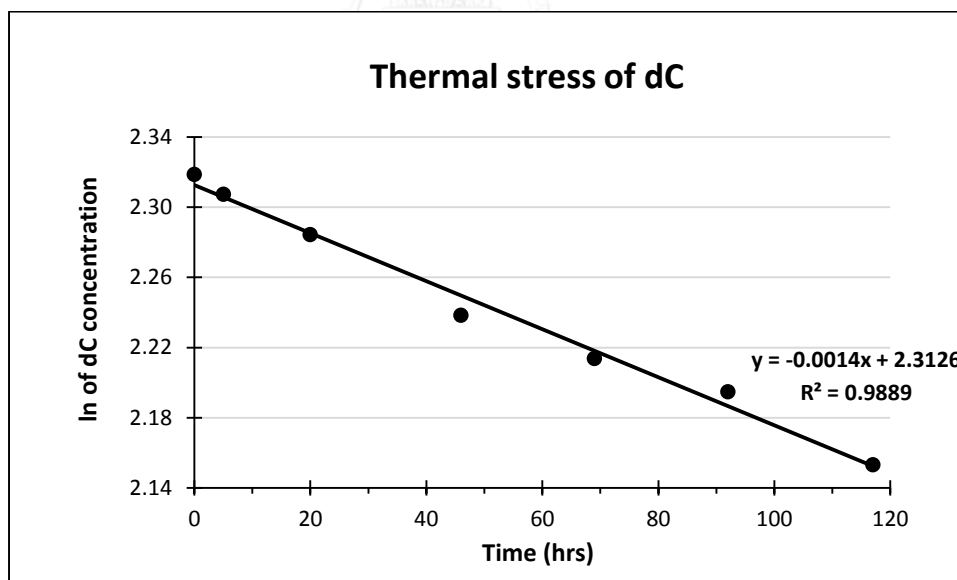


**Figure 4.5** Degradation profile for the first-order kinetics of 2'-deoxycytidine under thermal stress condition at 80 °C.

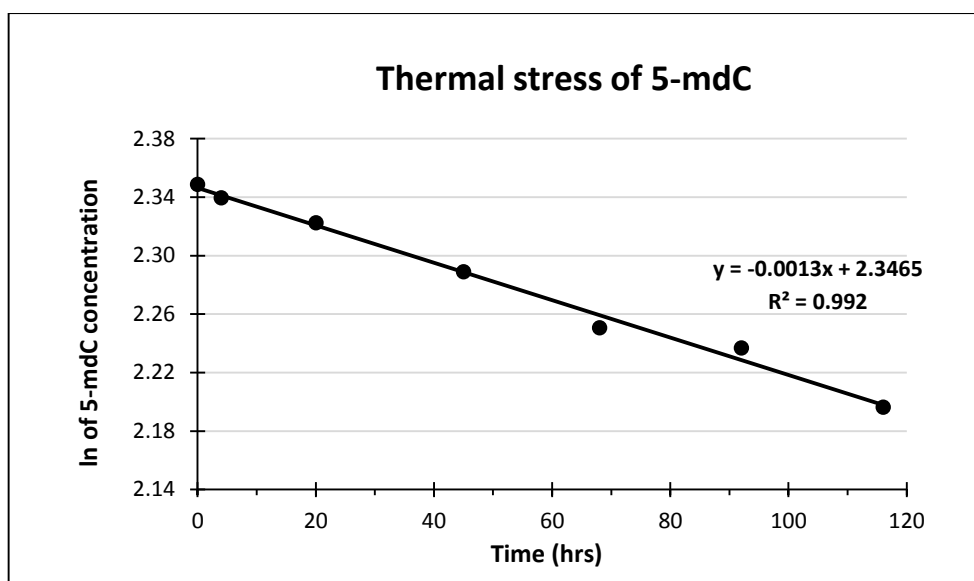


**Figure 4.6** Degradation profile for the first-order kinetics of 5-methyl-2'-deoxycytidine under thermal stress condition at 80 °C.

**Table 4.1** The first-order kinetic stability data of unmodified and modified nucleosides under thermal stress condition at 80 °C.

Nucleosides	k (hour <sup>-1</sup> )	t <sub>1/2</sub> (hours)
dG	1.1 × 10 <sup>-2</sup>	60.8
8-BrdG	2.7 × 10 <sup>-1</sup>	2.6
8-CphdG	5.7 × 10 <sup>-1</sup>	1.3
dC	1.4 × 10 <sup>-3</sup>	495.0
5-mdC	1.3 × 10 <sup>-3</sup>	533.1

## 1.2 Acidic stress of modified nucleosides

In kinetic study of acidic hydrolysis of nucleosides, the degradation profiles of nucleosides were constructed from the nucleoside concentrations as a function of time. The linear relationships between the natural logarithm of a nucleoside concentration and time of dG and modified dG (8-BrdG, 8-CpdG) indicate the degradation profiles of dG and its derivatives under acidic stress condition were the first-order kinetics (Figure 4.7-4.9). The first-order rate constants were  $1.5 \times 10^{-2} \text{ hour}^{-1}$  ( $t_{1/2} \approx 47.5$  hours) for dG,  $8.1 \times 10^{-2} \text{ hour}^{-1}$  ( $t_{1/2} \approx 8.6$  hours) for 8-BrdG, and  $7.4 \times 10^{-1} \text{ hour}^{-1}$  ( $t_{1/2} \approx 0.9$  hours) for 8-CphdG. The degradations of dC and 5-mdC under acidic stress condition were rarely observed even if the samples were incubated for more than 4 days which indicate the dC and 5-mdC are relatively stable against acidic hydrolysis.

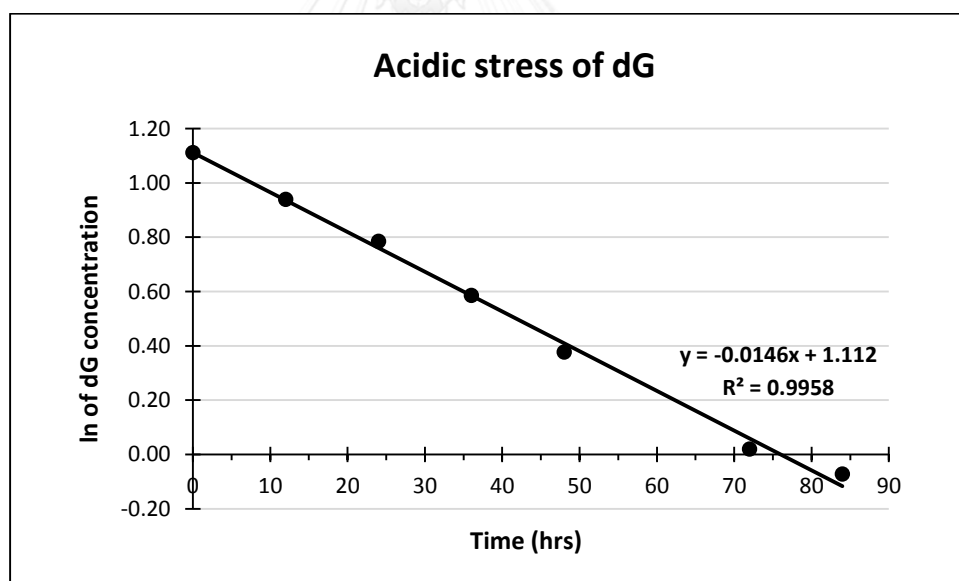


**Figure 4.7** Degradation profile for the first-order kinetics of 2'-deoxyguanosine under acidic stress condition.

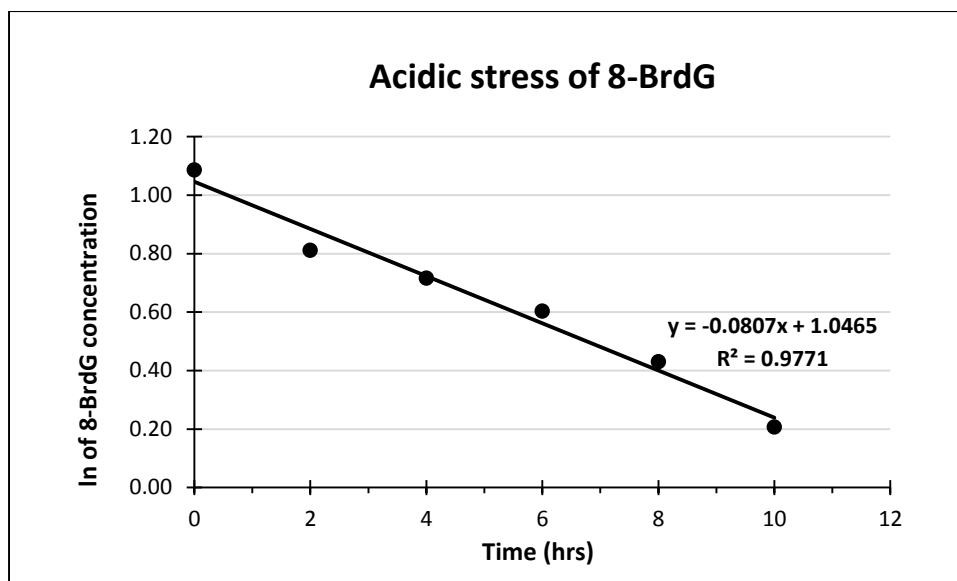


**Figure 4.8** Degradation profile for the first-order kinetics of 8-bromo-2'-deoxyguanosine under acidic stress condition.

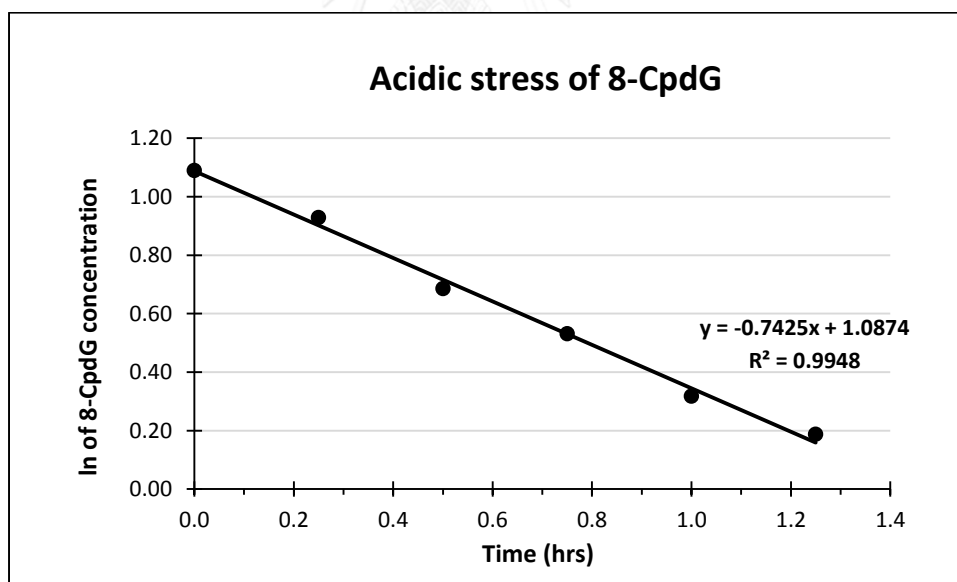


**Figure 4.9** Degradation profile for the first-order kinetics of 8-carboxyphenyl-2'-deoxyguanosine under acidic stress condition.

### 1.3 Alkaline stress of modified nucleosides

In alkaline hydrolysis study, the degradation of all nucleosides could not be observed under alkaline stress condition for 48 hours which indicates the unmodified and modified nucleosides are relatively stable to alkaline hydrolysis.

From all results of stability study, hydrolysis rate of the modified nucleosides were higher than the unmodified nucleosides. Under thermal stress condition, the 8-BrdG and 8-CpdG were hydrolyzed faster than dG at around 23 times and 50 times, respectively, while 5-mdC was quite stable compare to the other modifications. Because the substitution group may increase strain in the structure of nucleosides leading to structural destabilization, the modified nucleosides are more readily hydrolyzed than the unmodified nucleosides to stabilize their structure. In comparison of the modified nucleosides, 5-mdC had the lowest thermal and acidic hydrolysis rate. Hence, 5-mdC has been proved to be the most stable modified nucleosides which is suitable to be used to facilitate Z-DNA conformation in DNA probe.

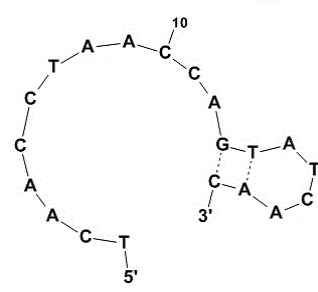
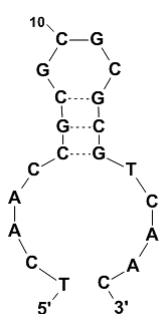
## 2. Z-DNA forming probe design and selection

The oligonucleotide probe used on B/Z-DNA nanobiosensor was designed to have 20 nucleotide bases in length. A thiol-modified linkage with six carbon spacer at 5'-end were chosen for immobilization process. In general, thiol group or sulfhydryl group is unstable so it is supplied with protecting group. Non-self-complementary sequences lay on both ends of an oligonucleotide were designed to help to hybridize completely. Oligo-4 and oligo-5 were specified as Z-DNA forming sequence because of containing a CG decamer track to convert to Z-DNA conformation. In oligo-5, base modification, methylation on the C5 position of all cytosine, on CG decamer track was chosen to enhance B- to Z-DNA conversion. Hybridization potential, self-complementarity and hairpin loop formation were estimated based on  $\Delta G$  value from OligoAnalyzer. All selected oligonucleotides have a calculated  $\Delta G$  value for

fully hybridized duplex much lower than for self-dimerization, hairpin formation or partially hybridized duplex (Table 4.2). Their apparent calculated  $\Delta G$  values showed that the duplexes of oligo-2+3, oligo-4+6, and oligo-5+6 were likely to form fully hybridization.



**Table 4.2** Estimated  $\Delta G$  of dimer and hairpin loops structures of the selected oligonucleotides from OligoAnalyzer software.

Oligo-2	Oligo-4
<p>5'– TCAACCTAACCAGTATCAAC –3'                             3'– AGTTGGATTGGTCATAGTTG –5'</p> <p>Duplex (Oligo-2+3), <math>\Delta G = -32.94</math> kcal/mole</p>	<p>5'– TCAACCGCGCGCGGTCAAC –3'                             3'– AGTTGGCGCGCGCAGTTG –5'</p> <p>Duplex (Oligo-4+6), <math>\Delta G = -48.66</math> kcal/mole</p>
<p>5'– TCAACCTAACCAGTATCAAC –3'                          3'– CAACTATGACCAATCCAAC –5'</p> <p>Self-dimer, <math>\Delta G = -1.6</math> kcal/mole</p>	<p>5'– TCAACCGCGCGCGGTCAAC –3'                          3'– CAACTGCGCGCGGCCAAC –5'</p> <p>Self-dimer, <math>\Delta G = -1.34</math> kcal/mole</p>
<p>5'– TCAACCTAACCAGTATCAAC –3'                          3'– CAACTATGACCAATCCAAC –5'</p> <p>Self-dimer, <math>\Delta G = -1.47</math> kcal/mole</p>	<p>5'– TCAACCGCGCGCGGTCAAC –3'                          3'– CAACTGCGCGCGGCCAAC –5'</p> <p>Self-dimer, <math>\Delta G = -1.34</math> kcal/mole</p>
 <p>Hairpin, <math>\Delta G = 0.77</math> kcal/mole</p>	 <p>Hairpin, <math>\Delta G = 0.77</math> kcal/mole</p>



### 3. Characterization of Z-DNA prone sequences

#### 3.1 Purity determination of the selected oligonucleotides

All the oligonucleotides were purchased from Sigma Aldrich. The major impurities of the synthesized oligonucleotides are incomplete sequences, including other impurities such as residual by-products, protecting group or truncated sequences, which can interfere the experiments thus purity of DNA is needed to be evaluated. The gradient RP-HPLC condition was developed from acetonitrile and 100 mM TEAA, pH 7 by starting gradient from 10% to 40% acetonitrile in 30 minutes. The gradient slope was 1% acetonitrile per minute. From the chromatographic results, the oligo-1 was eluted at 13.86 minutes but the peak of the target oligonucleotides was not completely separated from other impurities, which could be observed from several secondary peaks buried under the shoulder of the main oligonucleotide peak (Figure 4.10). The gradient system was adjusted to improve the separation of the oligo-1 from other impurities. The gradient slope was reduced from 1% acetonitrile/min to 0.5% acetonitrile/min and 0.25% acetonitrile/min.

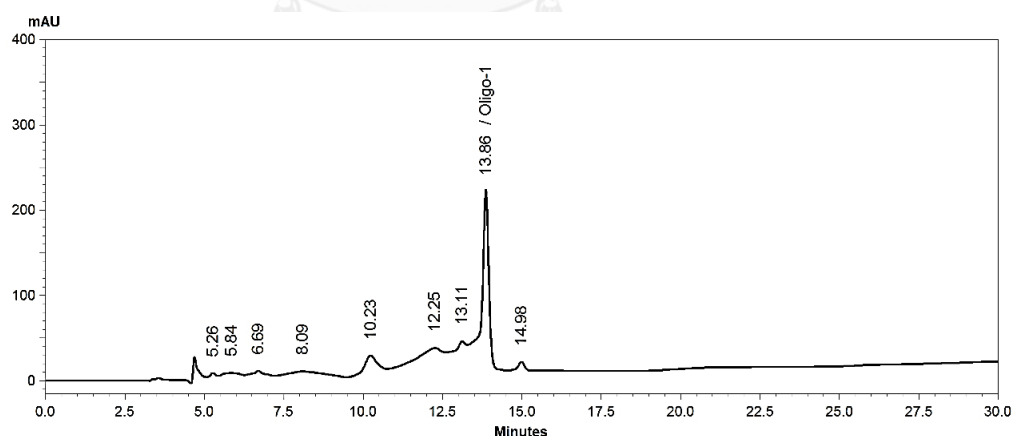


**Figure 4.10** Chromatogram of oligo-1 under gradient method from 10% to 40% ACN in 30 minutes (a gradient slope of 1 %ACN/min). The mobile phase was comprised of acetonitrile and 100 mM TEAA, pH 7. The injection volume was set 10  $\mu$ L. The column temperature was maintained at 40  $^{\circ}$ C and the UV detection monitored at 260 nm.

The reduction of gradient slope from 1% acetonitrile/min to 0.5% acetonitrile/min has improved separation between oligo-1 and impurities. The retention time of oligo-1 was 16.76 minutes with resolution 1.54. The purity of oligo-1 was estimated to be around 70% based on its peak area is not sufficient for further study. The resolution between oligo-1 and impurities can be further improved by reduction of gradient slope to 0.25% acetonitrile/min (Figure 4.11).

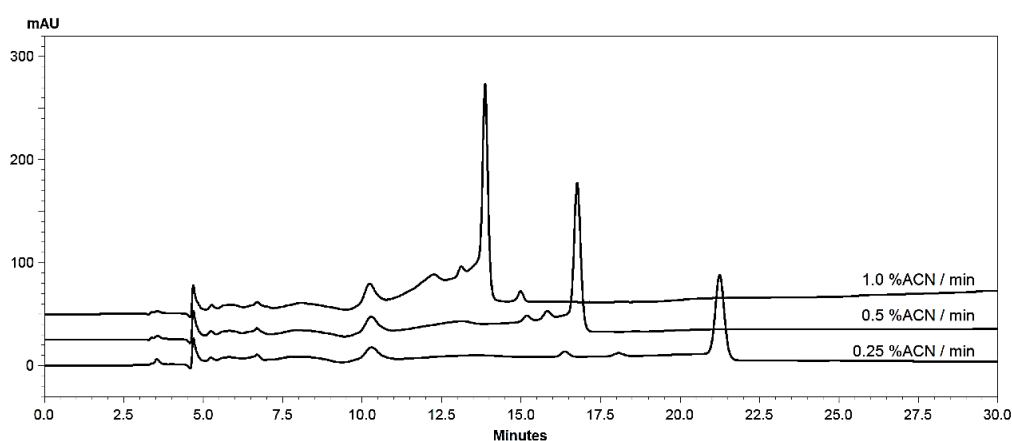


**Figure 4.11** Chromatograms of oligo-1 under various gradient conditions.

The chromatographic condition with a gradient slope of acetonitrile of 0.25 %/min is proper for evaluation of oligonucleotide purity. All chromatographic results indicates the purity of the purchased oligonucleotides, which were supplied in desalting grade purification, is not sufficient. Further purification of the oligonucleotides is necessary to reduce potential problem during the experiments. Due to lacking of suitable DNA purity, RP-HPLC was chosen an additional purification method to separate the synthesized oligonucleotides from several impurities. This method could provide the highly purified oligonucleotides.

Due to DNA purity issue, the oligo-2 was synthesized and purified by RP-HPLC method. The purity of purchased oligonucleotide was verified by previous chromatographic condition. The mobile phase was comprised of acetonitrile and 100 mM TEAA, pH 7. The gradient slope was set of 0.25% acetonitrile per minute as before while the gradient started from 20% to 30% of ACN. The flow rate was 0.5 mL/min. The chromatogram showed isolated peak of the oligo-2 with 99% of purity based on its peak area which indicates the purchased oligonucleotides supplied in RP-HPLC purification have purity enough for characterization and protein-DNA binding study, and immobilization study.

In addition, this HPLC gradient condition was used to determine the purity of oligonucleotides in DNA probe preparation before immobilization step. DTT was eluted at retention time of 5.76 minutes separated from the protected oligonucleotides (at around 11.0 minutes). When oligo-2 mixed with 0.1 M DTT to remove a protecting group, the deprotected oligo-2 must be isolated from other components. From the chromatogram of the mixture of oligo-2 and DTT, the isolated peak of the deprotected oligo-2 could not be observed and defined its elution time which indicates this chromatographic condition is still not suitable for purity evaluation of the deprotected oligonucleotides in DNA probe preparation.

The aim of HPLC method development is to obtain the optimal chromatographic condition can use for purity determination of the purchased oligonucleotides and the deprotected oligonucleotides prior to immobilize on gold surface at the same time. HPLC gradient condition was further optimized by starting the gradient ACN from 10% to 30% in 30 minutes. The gradient slope was 0.67% acetonitrile per minute. The flow rate was increased to 1.0 mL/min. This HPLC method was used to isolate the deprotected oligo-2 from other reaction mixtures in DNA probe preparation, the chromatogram in Figure 4.12 showed all target oligonucleotides were eluted separately which illustrated an improvement of separation power of the chromatographic

system over the previous method. Thus this chromatographic condition is an optimal method to evaluate the purity of oligonucleotides.

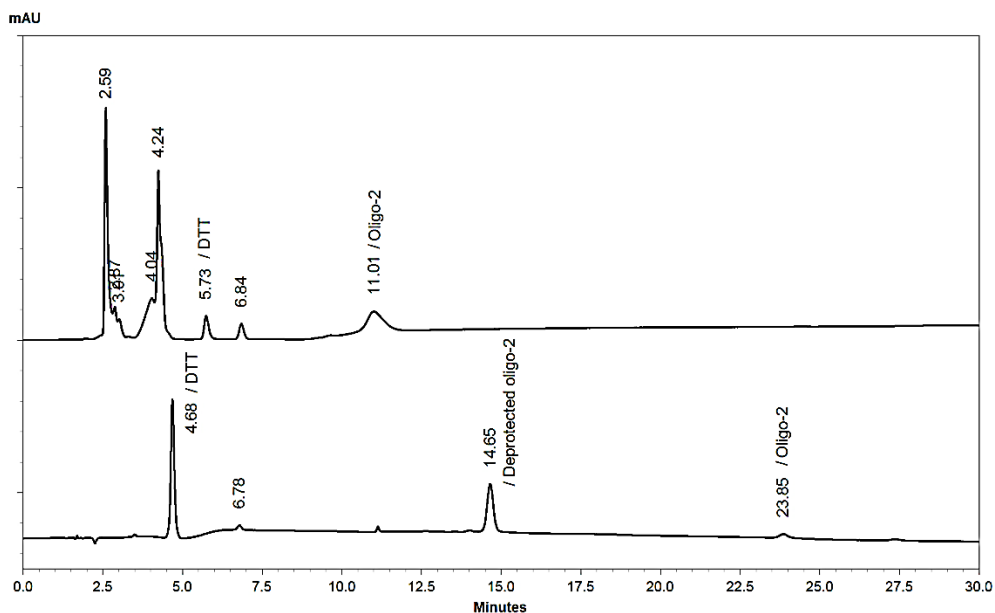


**Figure 4.12** Chromatogram of the reaction mixture of oligo-2 and DTT under gradient method from 10% to 30% ACN in 30 minutes (a gradient slope of 0.67 %ACN/min) (Bottom) compared to chromatogram of the reaction mixture of oligo-2 and DTT under previous HPLC method (Top). The mobile phase was comprised of acetonitrile and 100 mM TEAA, pH 7. The injection volume was set to 10  $\mu$ L. The column temperature was maintained at 40  $^{\circ}$ C and the UV detection monitored at 260 nm.

When the chromatographic condition was used to determine purity of oligo-2, the chromatogram showed isolated peak at retention time of 24.23 minutes with 97% of purity based on its peak area (Figure 4.13) which indicates this optimized chromatographic condition can be used to evaluate the purity of oligonucleotides. Furthermore, all chromatograms of the purchased oligonucleotides showed isolated peak of target oligonucleotide with chromatographic purity more than 95% which indicates the purity of

purchased oligonucleotides is enough for characterization, immobilization step and protein-DNA binding study step.

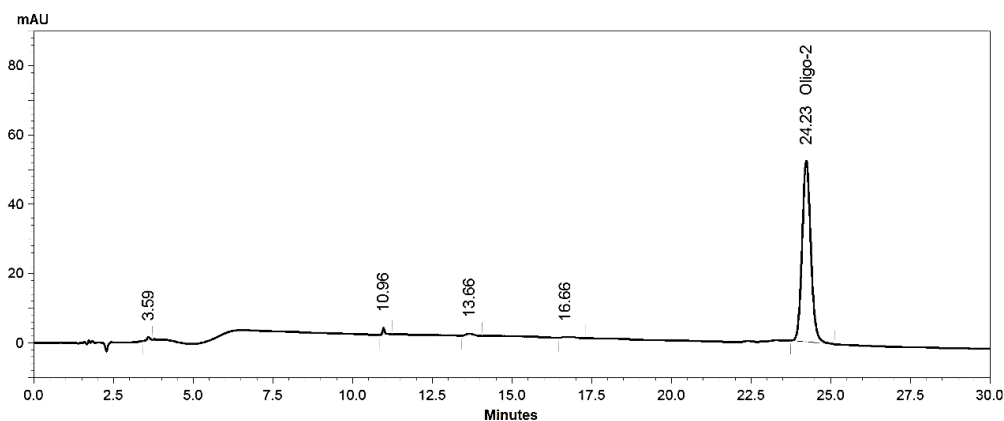


**Figure 4.13** Chromatogram of oligo-2 under gradient method from 10% to 30% ACN in 30 minutes (a gradient slope of 0.67 %ACN/min). The mobile phase was comprised of acetonitrile and 100 mM TEAA, pH 7. The injection volume was set 10  $\mu$ L. The column temperature was maintained at 40  $^{\circ}$ C and the UV detection monitored at 260 nm.

### 3.2 Oligonucleotide quantification

The content of purchased oligonucleotides were quantified by UV spectrometry based on UV absorption. All UV spectra of the oligonucleotides showed positive pattern with  $\lambda_{\max}$  closed to 260 nm resulting from absorption of nitrogenous bases as shown in Appendix C-1-7. The oligonucleotides concentration was calculated from UV absorption at 260 nm by using Beer-Lambert law. All the purchased oligonucleotides contained DNA content approximately as labeled claim, Table 4.3. The calculated DNA concentrations were used to determine appropriate dilution in other experiments.

$$A = \epsilon bc$$

A = UV absorbance at 260 nm

$\epsilon$  = molar absorptivity of each oligonucleotide

b = UV cell path length (cm)

c = concentration of oligonucleotide sample

**Table 4.3** DNA content of the purchased oligonucleotides.

Oligonucleotides	Absorbance at 260 nm	Calculated DNA content (nmole)
Oligo-1	0.199310	587.6
Oligo-2	0.240367	61.4
Oligo-3	0.171586	171.8
Oligo-4	0.267142	74.2
Oligo-5	0.233371	106.3
Oligo-6	0.212785	122.2
Oligo-7	0.182349	70.3

### 3.3 Melting temperature measurement

Thermal analysis was performed to determine melting temperature ( $T_m$ ) of oligonucleotides. The experiments were performed by heating the oligonucleotide duplex solution in the range of 10-90 °C. When temperature is raised, the double-stranded DNA is denatured into single stranded. The denaturation of duplex contributes an increased UV absorption intensity, hyperchromic effect, because of base unstacking. The melting curves of oligonucleotide duplex were constructed from the UV absorbance as a function of temperature. A sharp inflection point of the melting curve oligonucleotide duplex was observed, while it did not occurred in negative control samples which were prepared without the presence of their complementary targets. All melting curves indicate the oligonucleotides can be hybridized to their complementary strands as duplex.

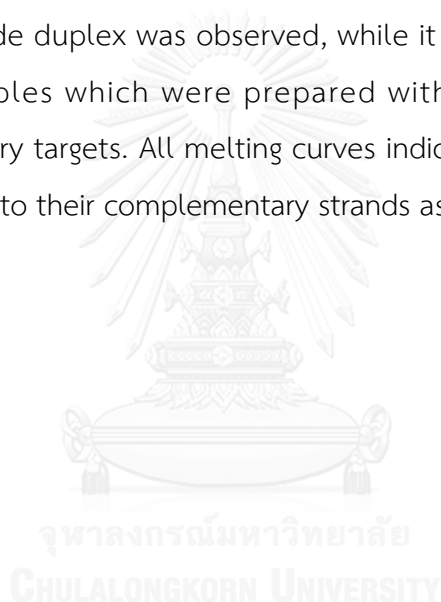


**Table 4.4**  $T_m$  of the oligonucleotide duplexes.

Oligonucleotide duplexes	Structure of duplexes	Observed $T_m$ (°C)
Oligo-2+3	$5'-(CH_2)_6-S-S-(CH_2)_6-TCAACCTAACCAAGTATCAAC-3'$ $3'-AGTTGGATTGGTCATAGTTG-5'$	59
Oligo-4+6	$5'-(CH_2)_6-S-S-(CH_2)_6-TCAACCGCGCGCGCGTCAAC-3'$ $3'-AGTTGGCGCGCGCGCAGTTG-5'$	78
Oligo-5+6	$5'-(CH_2)_6-S-S-(CH_2)_6-TCAAC C^*G C^*G C^*G C^*G TCAAC-3'$ $3'-AGTTG GCGCGCGCGC AGTTG-5'$	79

Note : C\* is 5-methylcytosine

### 3.4 B-Z DNA transition study

#### 3.4.1 Effect of monovalent cations

Due to the differences of CD spectrum between B-DNA and Z-DNA conformation, the Z-DNA forming potential of designed oligonucleotide probes can be determined by CD study. The CD signal of B-DNA shows positive ellipticity at approximately 280 nm and 220 nm and a negative ellipticity at approximately 250 nm. In contrast, the CD spectrum of Z-DNA shows negative ellipticity at approximately 295 nm and a positive ellipticity at approximately 250 nm. Owing to structural feature of Z-conformation, it tends to be an unstable form. The cations can stabilize the Z-DNA structure by shielding the negative charges of phosphate groups to reduce the electrostatic repulsion. Monovalent cation, Na<sup>+</sup> ion, is commonly used in B-Z-DNA conversion study. In general, the alternating CG sequences exist as a B-DNA conformation at low salt condition while a B to Z conformational conversion can be observed



under high salt conditions. Likewise, CD spectra of oligo-1 predominantly appeared as a CD pattern of B-conformation at low salt concentrations (below 2 M NaCl). When the salt concentration was increased to 4 M, CD spectrum of Z-DNA became predominant (Figure 4.14).

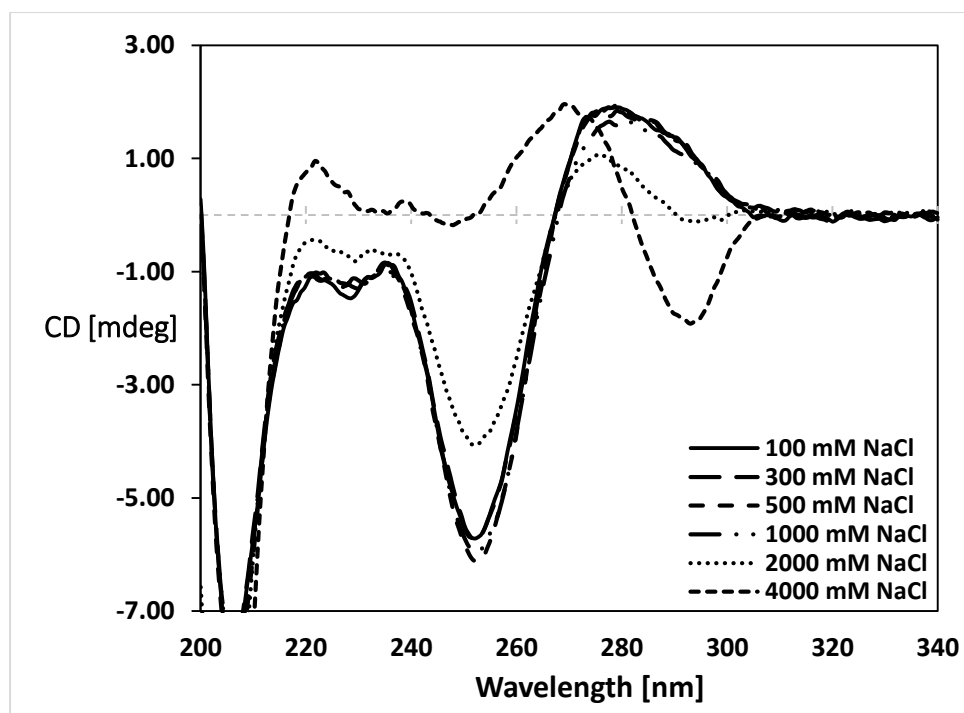


**Figure 4.14** CD spectra of the oligo-1, CG decamer, with various concentrations of NaCl. The oligonucleotide sample, approximately 6  $\mu\text{M}$ , was prepared in 50 mM phosphate buffer pH 7.4. The CD spectra were monitored at 25  $^{\circ}\text{C}$  with a scanning rate of 50 nm/min. Accumulation was set to 5 scans.

Oligo-4 was designed to have CG decamer track in the sequence so that their duplex, oligo-4+6, can convert to Z conformation in the same way as oligo-1. In B-Z transition study, an inversion of CD spectra to Z-DNA pattern was not observed in the CD spectra of the duplex of oligo-4+6 even in high  $\text{Na}^+$  condition as expected (Figure 4.15). The duplex of oligo-4+6 gives all the

same CD results to the negative control duplex, oligo-2+3, which cannot be converted to Z-DNA. The blank controls were made up of 50 mM phosphate buffer with varying NaCl concentration levels, without DNA. Their signals did not interfere to CD pattern of DNA. The CD results suggest that the neighboring sequences on both sides of CG track, which are the non-Z-DNA prone sequences, may perturb DNA conformational change. When the oligo-5+6 was under various salt concentrations, the CD signals have been found to shift into CD pattern of Z-DNA after addition of NaCl (Figure 4.16) which indicates 5-methylcytosine in CG track of oligo-5 facilitated their duplex to form a left-handed DNA.

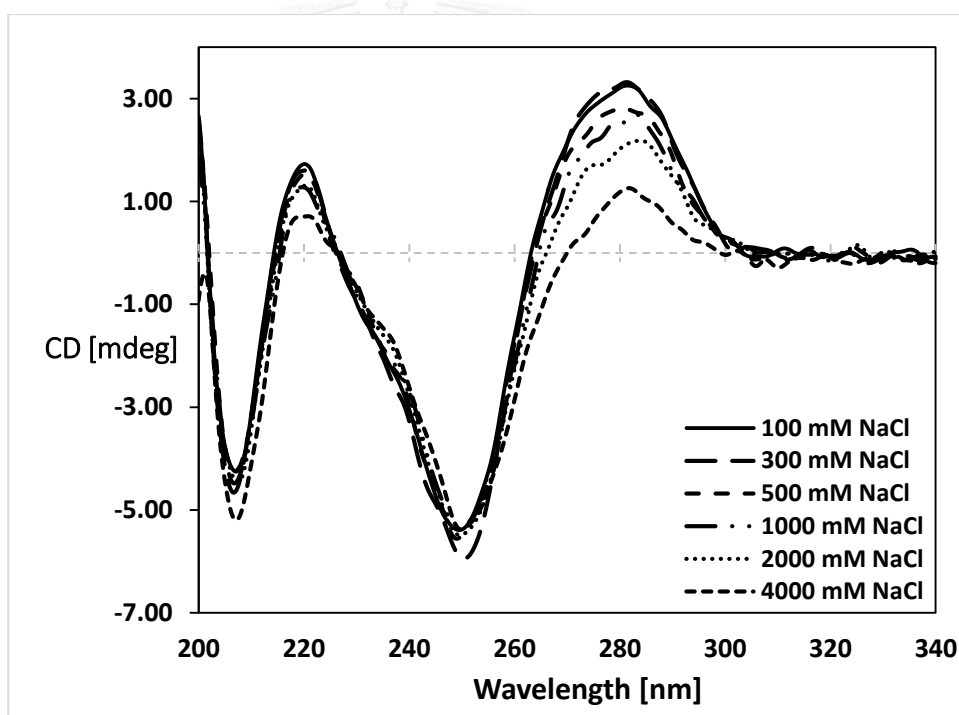


**Figure 4.15** CD spectra of the duplex of oligo-4+6 with NaCl range from 100 mM to 4000 mM. The oligonucleotide duplex, approximately 6  $\mu$ M, was prepared in 50 mM phosphate buffer pH 7.4. The CD spectra were monitored at 25  $^{\circ}$ C with a scanning rate of 50 nm/min. Accumulation was set to 5 scans.

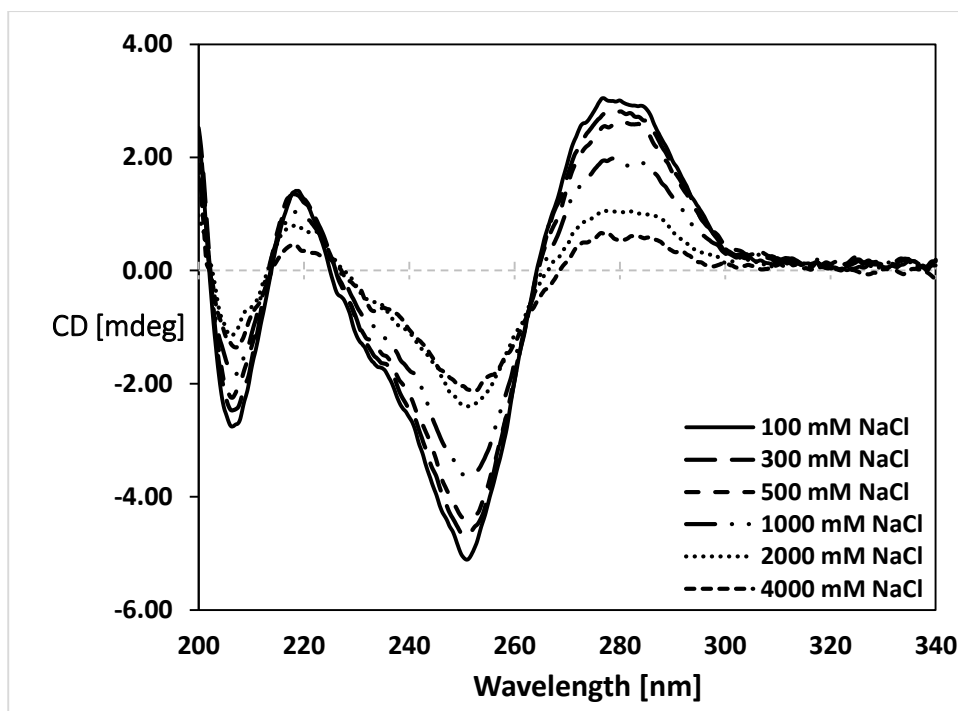


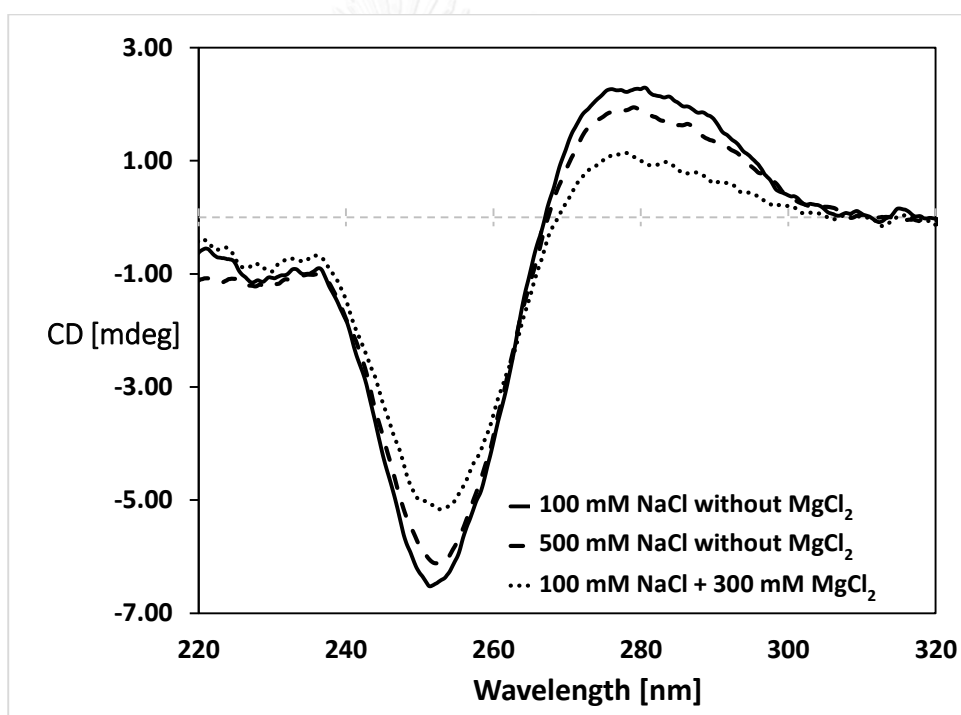
**Figure 4.16** CD spectra of the duplex of oligo-5+6 with NaCl range from 100 mM to 4000 mM. The oligonucleotide duplex, approximately 6  $\mu$ M, was prepared in 50 mM phosphate buffer pH 7.4. The CD spectra were monitored at 25  $^{\circ}$ C with a scanning rate of 50 nm/min. Accumulation was set to 5 scans.

### 3.4.2 Effect of divalent cations

In addition to monovalent cation, the effect of divalent cation,  $Mg^{2+}$ , was also investigated in transition of B to Z-helice of Z-DNA forming oligonucleotides.  $Mg^{2+}$  ion which can strongly diminish electrostatic repulsion from narrow phosphate backbone of Z-DNA was used to enhance the stability of left-handed Z-DNA. From CD spectra of oligo-1 in Figure 4.17, the duplex of oligo-1 primarily existed in B-form in low salt concentration (100 mM NaCl). The CD signal of the duplex shifted into CD pattern of Z-DNA after addition of  $MgCl_2$  at 300 mM while there was no significantly change in CD signal was observed in the presence of 500 mM of NaCl. The CD results show  $Mg^{2+}$  ion has more potential to stabilize Z-DNA structure than  $Na^+$  ion.

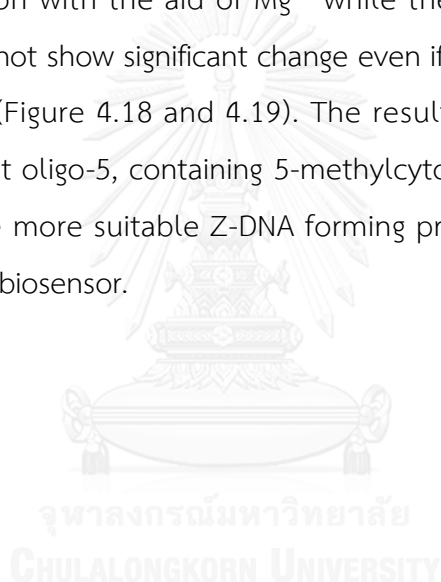
However, the precipitate has occurred at higher magnesium concentration than 300 mM because magnesium ions can react to phosphate to form an insoluble salt.

When the duplex of oligo-4+6 was investigated under 300 mM of  $\text{MgCl}_2$ , the CD signal showed a significant change into CD pattern of Z-DNA compared to the CD signal of the duplex under 500 mM of NaCl. The CD results indicate  $\text{Mg}^{2+}$  ion can stabilize the duplex of oligo-4+6 to form Z-DNA more than  $\text{Na}^+$  ion.



**Figure 4.17** CD spectra of the duplex of oligo-1 in the presence of  $\text{MgCl}_2$  300 mM compared to the duplex of oligo-1 in the presence of NaCl 500 mM. The oligonucleotide duplex, approximately 6  $\mu\text{M}$ , was prepared in 50 mM phosphate buffer pH 7.4. The CD spectra were monitored at 25  $^\circ\text{C}$  with a scanning rate of 50 nm/min. Accumulation was set to 5 scans.

From all CD results of the B-Z transition study, the utilization of a divalent cation cooperating with a high level of monovalent cation would facilitate Z-DNA forming oligonucleotides to convert into Z-conformation. Sodium salt was used in a high concentration level, nevertheless, the use of magnesium salt was limited to only 100 mM since the previous study of the divalent cation effect has shown precipitation when the higher concentration of magnesium salt were used. The B-Z transition capability of oligo-4+6 and oligo-5+6 were studied by adding  $\text{MgCl}_2$  to DNA sample with 4 M NaCl. According to CD spectra, only the duplex of oligo-5+6 was able to convert to Z conformation with the aid of  $\text{Mg}^{2+}$  while the CD signal of the duplex of oligo-4+6 did not show significant change even if  $\text{MgCl}_2$  concentration is raised up to 50 mM (Figure 4.18 and 4.19). The result of B-Z transition study has confirmed that oligo-5, containing 5-methylcytosine residues in CG-decamer track, was the more suitable Z-DNA forming probe for development of the B/Z-DNA nanobiosensor.



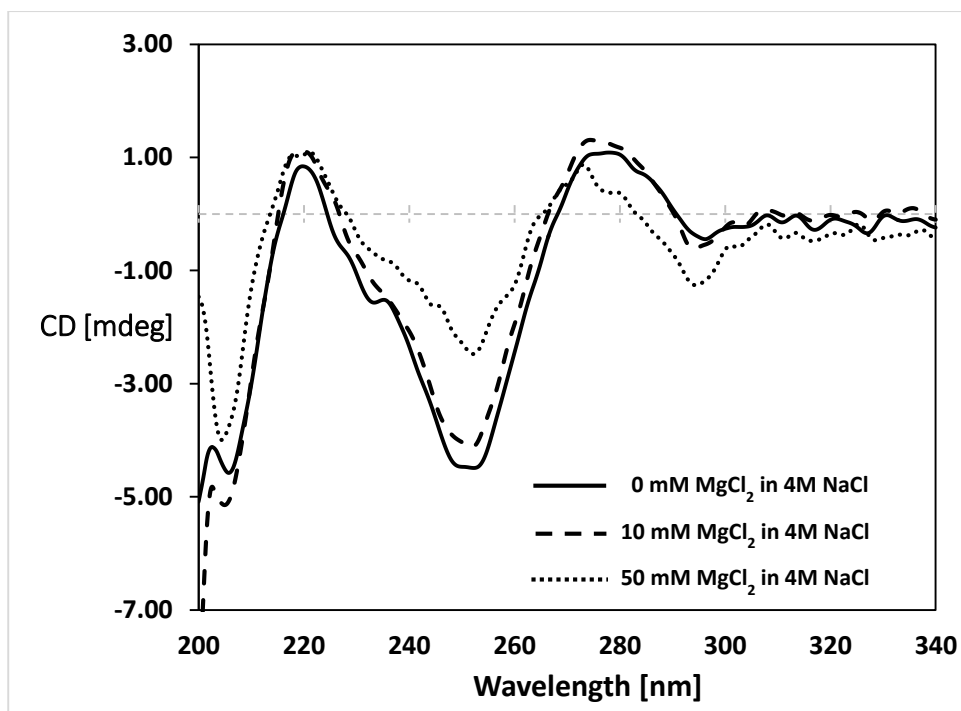


**Figure 4.18** CD spectra of oligo-5+6 in 4 M of NaCl without adding MgCl<sub>2</sub> and with MgCl<sub>2</sub> in range from 10-50 mM. The oligonucleotide duplex, approximately 6  $\mu$ M, was prepared in 50 mM phosphate buffer pH 7.4 and 4 M NaCl. The CD spectra were monitored at 25  $^{\circ}$ C with a scanning rate of 50 nm/min. Accumulation was set to 5 scans.

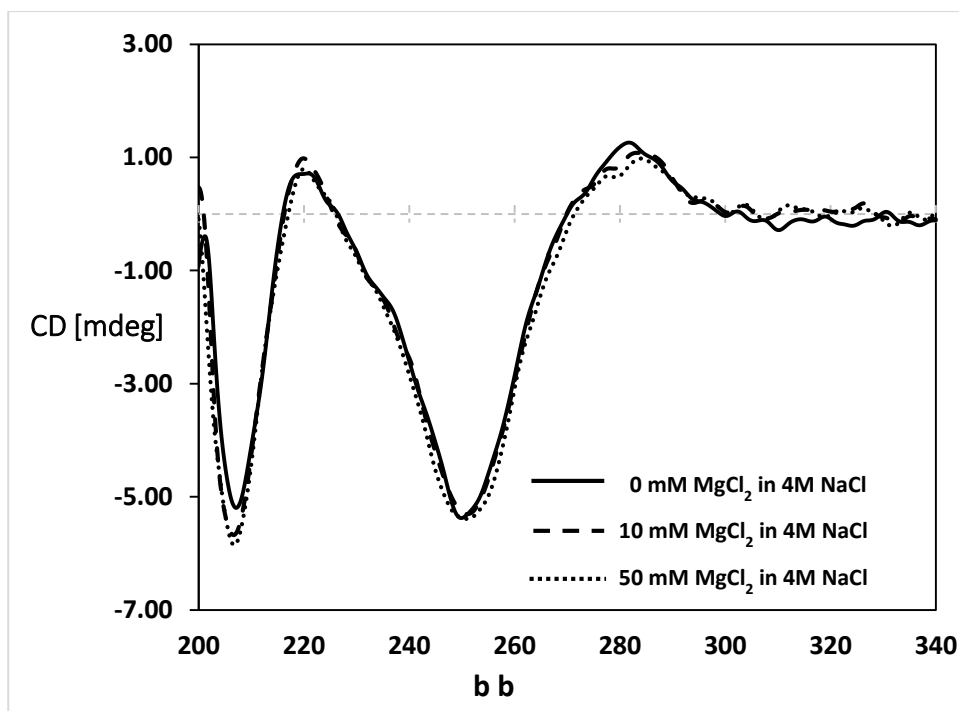


**Figure 4.19** CD spectra of oligo-4+6 in 4 M of NaCl without adding MgCl<sub>2</sub> and with MgCl<sub>2</sub> in range from 10-50 mM. The oligonucleotide duplex, approximately 6  $\mu$ M, was prepared in 50 mM phosphate buffer pH 7.4 and 4 M NaCl. The CD spectra were monitored at 25 °C with a scanning rate of 50 nm/min. Accumulation was set to 5 scans.

#### 4. Determination of the interaction between Z-DNA prone sequence and specific Z-DNA binding protein in solution condition

From B-Z DNA transition study, the duplex of oligo-5+6 is a suitable oligonucleotide which can convert to left-handed conformation. So the study of DNA-binding capability to specific Z-DNA binding protein was performed on this oligonucleotide. Z-ab is a Z-DNA specific protein acted as a model for Z-DNA binding protein. At a high salt (4 M NaCl) condition, the duplex of oligo-5+6 has partially formed Z-conformation and was readily bound to Z-ab. The CD spectra of binding study between the duplex of oligo-5+6 and Z-ab showed the unchanged CD bands at about 250 nm and 280 nm. This experiment was limited at a Z-ab : DNA ratio of 0.16 because of the precipitation of denatured Z-ab. Therefore, the study of DNA-protein binding was investigated only at low salt condition. The CD spectra of the duplex of oligo-5+6 interacting with Z-ab showed the positive band at around 280 nm and the negative band at approximately 250 nm gradually change into CD spectral pattern of Z-DNA when a ratio of Z-ab : oligo-5+6 was increased (Figure 4.20). The alteration in the ellipticity bands was actually occurred from binding between the oligo-5+6 duplex and Z-ab because Z-ab does not give CD signal in this region presented in CD spectra of blank control (without DNA).



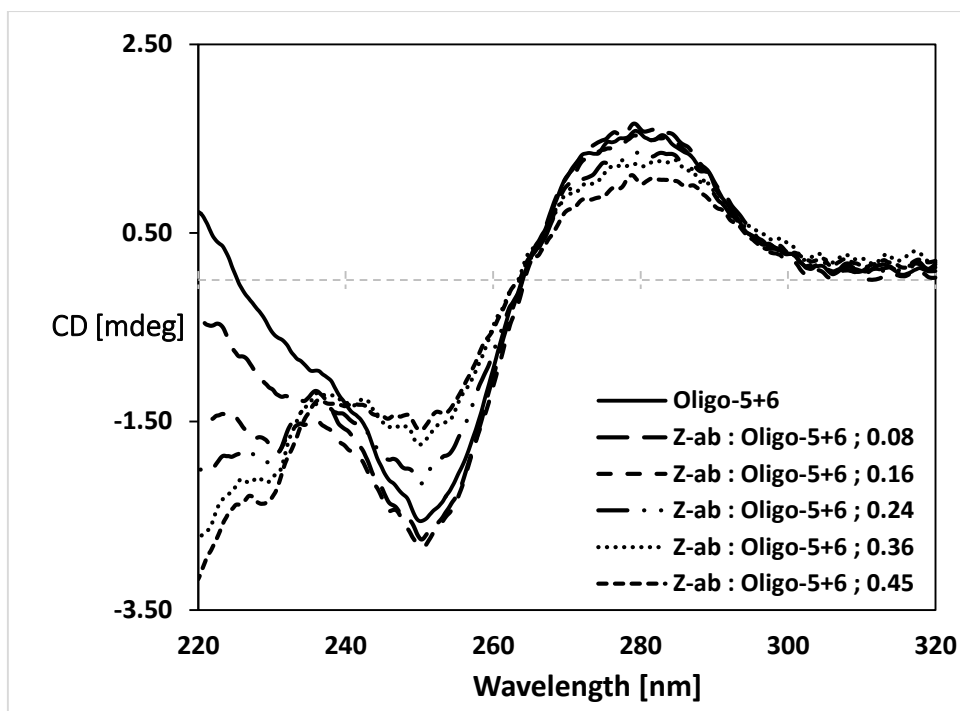


**Figure 4.20** CD spectra of oligo-5+6 in 50 mM  $\text{Na}_2\text{HPO}_4$  buffer, pH 7.0 with varied molar ratio of Z-ab. The oligonucleotide concentration was at 3.2  $\mu\text{M}$ . The CD spectra were monitored at 25 °C with a scanning rate of 20 nm/min. Accumulation was set to 10 scans.

As well as the blank control, the dilution effect from adding Z-ab stock solution was proved by the addition of 50 mM  $\text{Na}_2\text{HPO}_4$  buffer at the same volume of Z-ab to confirm CD alteration did not result from diluting DNA. The CD spectra of the duplex of oligo-5+6 were slightly changed when 50 mM  $\text{Na}_2\text{HPO}_4$  buffer was added upon 1.5 times the maximum volume of Z-ab used at a Z-ab : DNA ratio of 0.45 in previous experiment of binding study between the duplex of oligo-5+6 and Z-ab.

Additionally, the oligo-2+3 was used as a negative control DNA. Due to non Z-DNA prone sequence, a significant change in the intensity of CD bands was not observed in the CD spectra which shows oligo-2+3 cannot bind to Z-ab. All CD results confirm the duplex of oligo-5+6 has been bound to Z-ab to form

Z-DNA-Z-ab complex. The possibility for a complex of oligo-5+6 duplex and Z-ab formation were proposed in 2 mechanisms (Figure 4.21). In the first proposed mechanism, the oligo-5+6 duplex exists in an equilibrium between B-form and Z-form. Z-ab could directly bind to Z-DNA to form Z-DNA-Z-ab complex when Z-ab was added. While the second mechanism was proposed that Z-ab could bind to B-DNA and induced conformational change from B-DNA to Z-DNA, Z-DNA-Z-ab complex was observed.

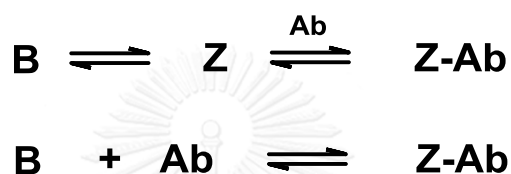


**Figure 4.21** The proposed mechanisms for a complex of oligo-5+6 duplex and Z-ab.

Besides a negative control DNA, the Z-DNA forming probe-protein binding study was conducted by using BSA, a negative control protein. As expected, the CD spectra did not indicate the binding between the Z-DNA forming probe and BSA does not occur. Overall CD results of DNA probe-protein interaction study revealed the duplex of oligo-5+6 is selective to Z-DNA binding protein.

## 5. Immobilization study of the Z-DNA prone sequence on gold surface

Prior to the immobilization process, the 5'-thiol modified oligonucleotide was supplied in the protected form as disulfide linkages to prevent oxidation reaction of free SH group. The disulfide bonds must be cleaved by incubating with 0.1 M DTT, as a reducing agent, to give reactive thiol group (reduced form) before immobilized on gold chip (Figure 4.22). In principle, the DTT solution must be prepared fresh to provide a reactive form because DTT prefers to form a stable six-membered ring in solution under atmosphere and only a reduced DTT is a reactive form to oxidize disulfide bond. The DTT obtained with oligo-2 from Sigma Aldrich was evaluated, its chromatogram showed 2 major peaks at retention time of 5.74 and 6.83 minutes which indicates DTT solution have two species, reduced form and oxidized form, while the chromatogram of freshly prepared DTT solution showed a main peak at 5.76 minutes which is a reduced DTT and a small peak of oxidized DTT at 6.87 minutes (Figure 4.23). This experiment illustrates only in the freshly prepared solution gives DTT suitable for deprotection step.

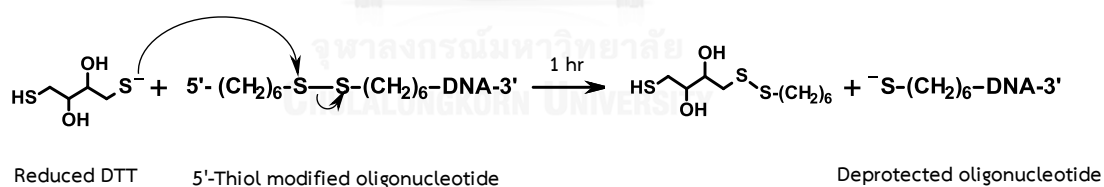


**Figure 4.22** Thiol-modified oligonucleotide reduction reaction in deprotection step.

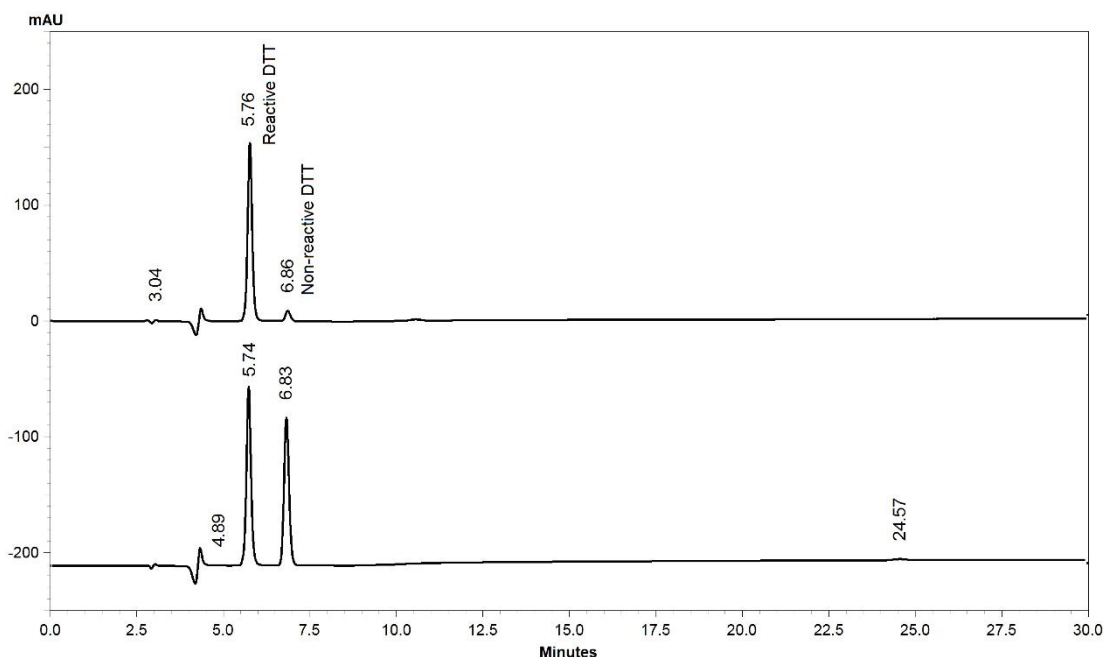


**Figure 4.23** Chromatograms of DTT solution supplied from Sigma Aldrich (Bottom) and DTT solution prepared in 50 mM phosphate buffer, pH 8.4 (freshly prepared) (Top) under gradient method from 10% to 25% ACN in 30 minutes (a gradient slope of 0.25 %ACN/min). The mobile phase was comprised of acetonitrile and 100 mM TEAA, pH 7. The injection volume was set 10  $\mu$ L. The column temperature was maintained at 40  $^{\circ}$ C and the UV detection monitored at 260 nm.

After the deprotection step, the deprotected oligonucleotide was isolated from protecting groups and excess DTT by passing through illustra NAP<sup>TM</sup> 10 column based on size exclusion chromatography. The purity of the deprotected oligonucleotide is an important factor of DNA immobilization since the impurities, such as excess DTT or other reaction by products, can interfere self-assembly process. Therefore the purity of the deprotected probe needed to be evaluated. HPLC gradient method can be used to determine the purity of the deprotected oligonucleotide.

The chromatogram of a reaction mixture in cleavage step indicates a good separation of the deprotected oligo-5 from other compounds (Figure 4.24). From chromatographic result, the cleaved oligo-5 showed a single major peak at 15.42 minutes with chromatographic purity greater than 95% that indicates the purity of the cleaved oligonucleotides is enough for immobilization step.

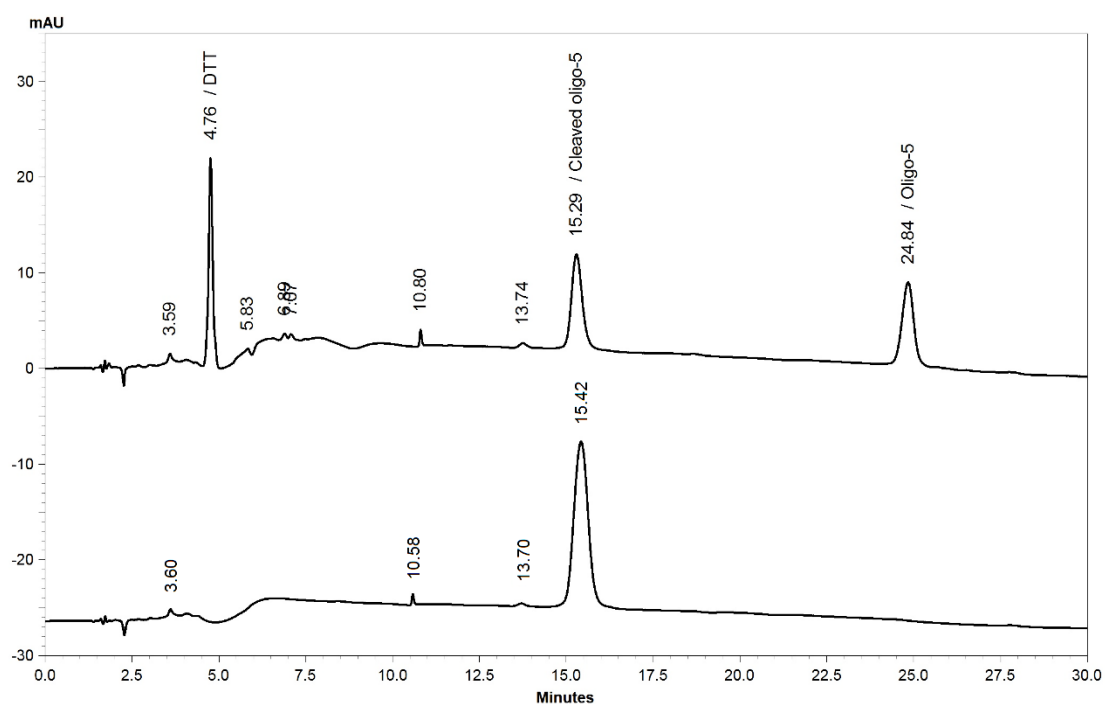
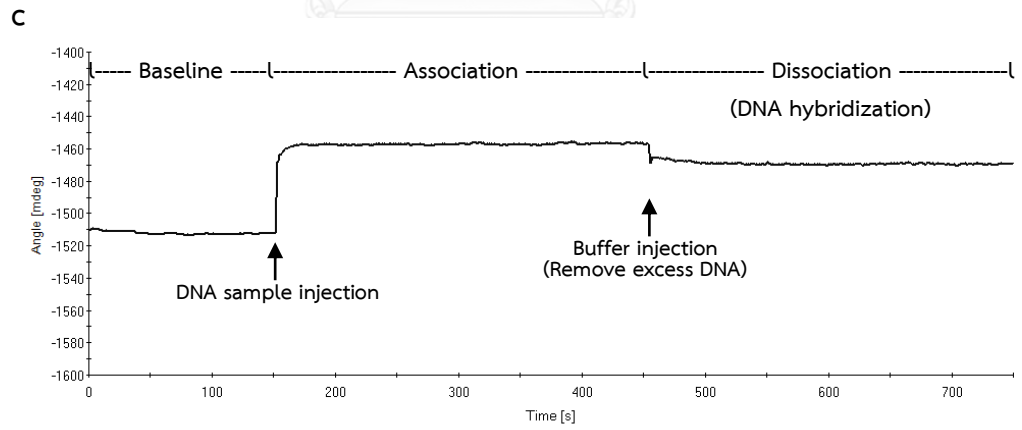
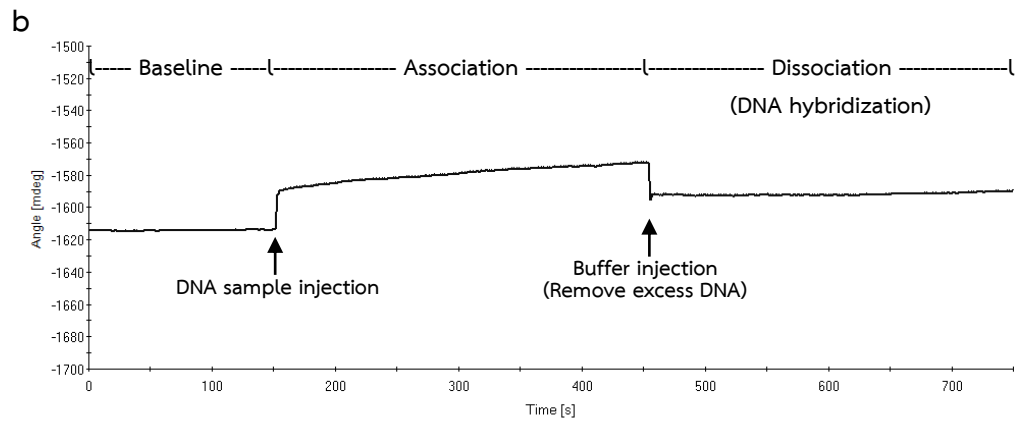
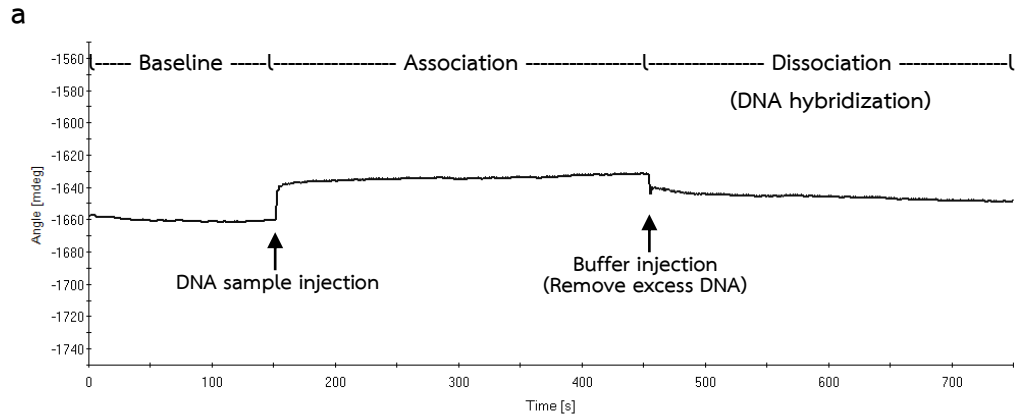


**Figure 4.24** Chromatograms of the reaction mixture of oligo-5 and DTT (Top) and the deprotected oligo-5 (Bottom) under gradient method from 10% to 30% ACN in 30 minutes (a gradient slope of 0.67 %ACN/min). The mobile phase was comprised of acetonitrile and 100 mM TEAA, pH 7. The injection volume was set 10  $\mu$ L. The column temperature was maintained at 40  $^{\circ}$ C and the UV detection monitored at 260 nm.

The DNA immobilized chip was exposed to mercaptohexanol, used as a blocking agent, in order to eliminate nonspecifically adsorbed oligonucleotide and prevent molecular crowding. After immobilization process, the completion of the immobilization was proved by hybridization to complementary strand. The duplex formation of DNA probe attached on a gold surface could confirm the result of immobilization study.

#### **6. Detection of DNA hybridization on biosensor surface**

The positive SPR response occurs upon binding events between the surface-immobilized DNA probe and its complementary strand or DNA binding proteins. On the other side, when the non-complementary strand is incubated to the probe, there is no response from SPR. At the beginning of the hybridization study, the ionic strength is a factor that effects on the hybridization efficiency therefore an optimized SPR condition was found out by varying salt concentration of running buffer solution. The running buffer was comprised of 50 mM phosphate buffer solution, pH 7.4, and a various NaCl concentration, 0-300 mM. The SPR sensograms of hybridization process for determination an optimized ionic strength condition were demonstrated in Figure 4.25. The SPR signal of duplex formation of oligo-2+3 under running buffer with containing 0 mM, 50 mM, 100 mM and 300 mM NaCl were 11.6 mdeg, 23.8 mdeg, 43.1 mdeg, and 23.3 mdeg, respectively. Accordingly, the optimal hybridization condition was under using running buffer that contained 100 mM NaCl due to the consistently maximum SPR response while the duplex hybridization at higher salt concentration gave a lower SPR response which may result from the high salt can stabilize DNA probe to other conformations such as hairpin contributing to lower amount of DNA available for hybridization. The regeneration solution was using deionized water for ion removal and dehybridization step.



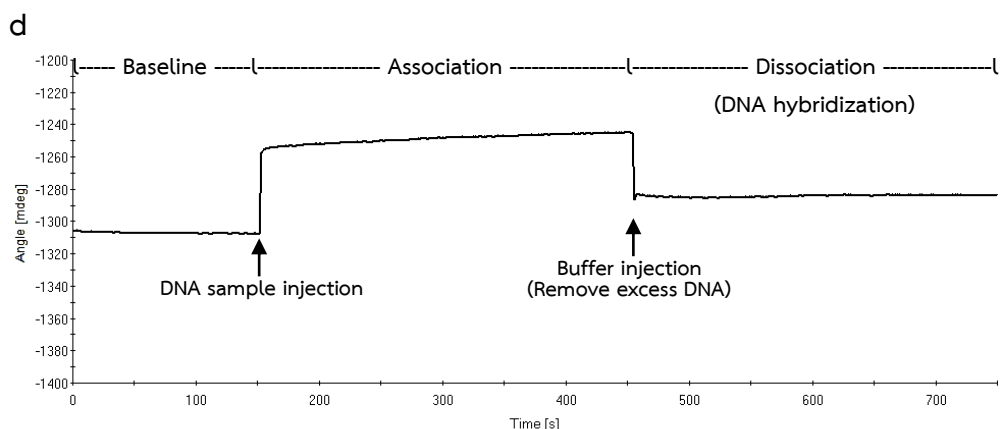


**Figure 4.25** SPR sensograms of hybridization process of immobilized oligo-2 and oligo-3 under running buffer contained only 50 mM  $\text{Na}_2\text{HPO}_4$  buffer, without adding NaCl (a), with adding 50 mM NaCl (b), with adding 100 mM NaCl (c) and with adding 300 mM NaCl (d). The SPR signal of duplex formation of oligo-2+3 were 11.6 mdeg, 23.8 mdeg, 43.1 mdeg, and 23.3 mdeg respectively. The concentration of oligo-3 was prepared of 2  $\mu\text{M}$  in running buffer. The association time and dissociation time were 300 seconds with five-cycle surface regeneration at 25  $^\circ\text{C}$ .

In the DNA hybridization study of immobilized oligo-5 probe, the SPR sensogram of the duplex of oligo-5+6 showed the positive SPR response which imply oligo-5 probe can hybridize to oligo-6 to form duplex (Figure 4.26a). While a non-complementary sequence strand, oligo-7, was used incubated to the surface-bound oligonucleotides to confirm the DNA hybridization. The SPR sensogram of oligo-5 probe treated with a negative control DNA showed no change in SPR signal (Figure 4.26b) which was similar to the result of a blank control (Figure 4.26c). The SPR results indicate hybridization between oligo-5 probe and oligo-7 cannot occur. All SPR results of hybridization study indicate that there are oligo-5 exist on gold surface and the DNA hybridization process is highly specific.



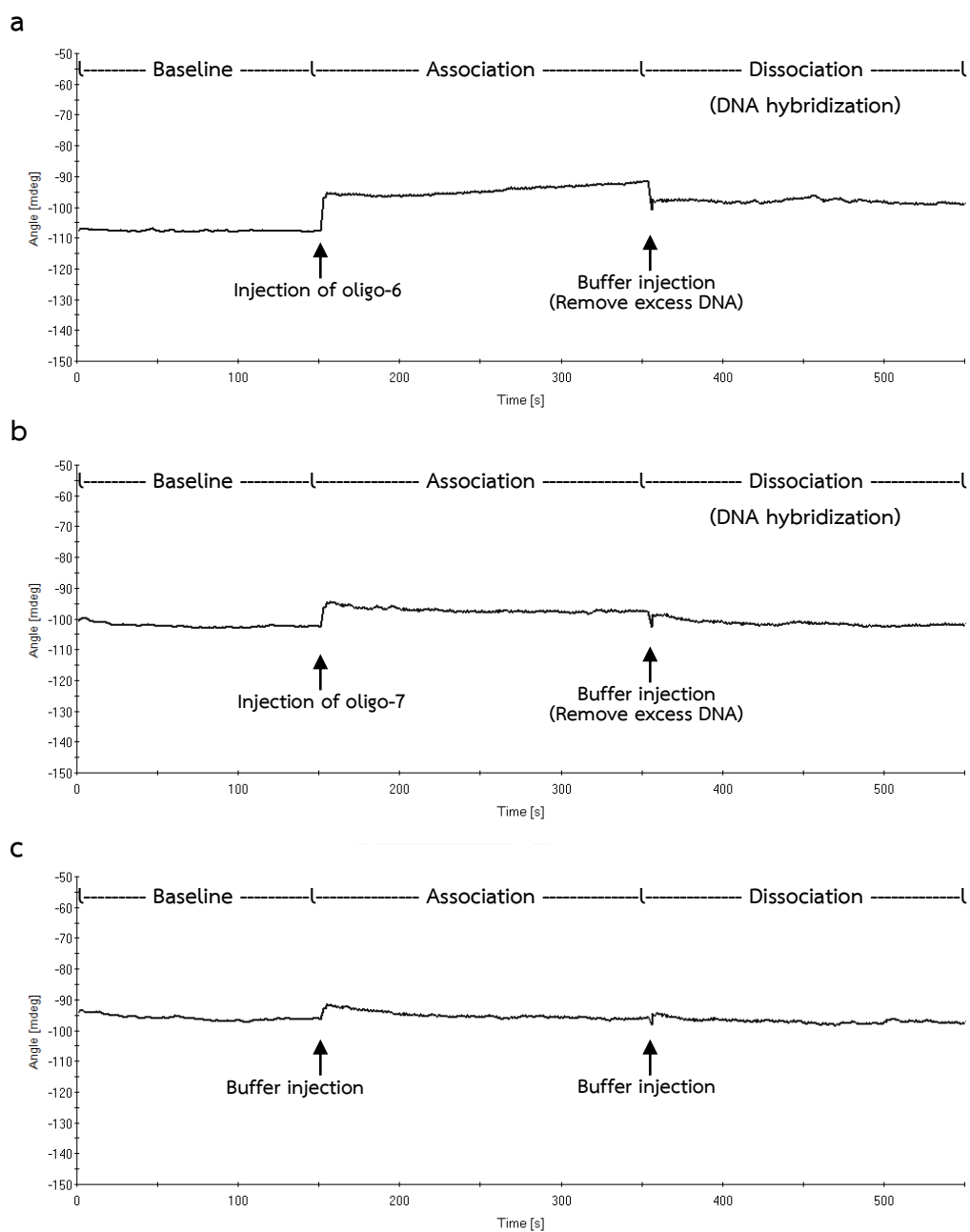


**Figure 4.26** SPR sensograms of hybridization study of immobilized oligo-5 with a complementary strand, oligo-6 (a), a non-complementary sequence, oligo-7 (b), and a blank control, 50 mM phosphate buffer solution under running buffer comprising phosphate buffer solution (pH 7.4, 50 mM) and 100 mM NaCl. The oligo-6 gave a relative response of 8.8 mdeg while the oligo-7 and blank control gave only relative response of 0.3 mdeg and -1.4 mdeg, respectively. The association time and dissociation time were 200 seconds with five-cycle surface regeneration at 25 °C.

## 7. Study of Z-DNA forming probe and specific Z-DNA binding protein interaction on biosensor surface

After the hybridization study, the immobilized duplex DNA-protein interaction was investigated by using a specific Z-DNA binding protein, Z-ab. When the antibodies were applied for binding to the hybridized oligo-2+3, which was favorable to B-form, on the gold chip, the SPR signal occurred highly in dissociation phase (Figure 4.27). The unexpected response might be from non-specific binding between DNA and the Z-ab. Additionally, the SPR signal still remained around 82.5 mdeg after regeneration phase which indicates deionized water is not suitable regeneration solution to regenerate the sensor surface. As a result, the regeneration condition needs to be optimized for removal of non-specific Z-ab binding.

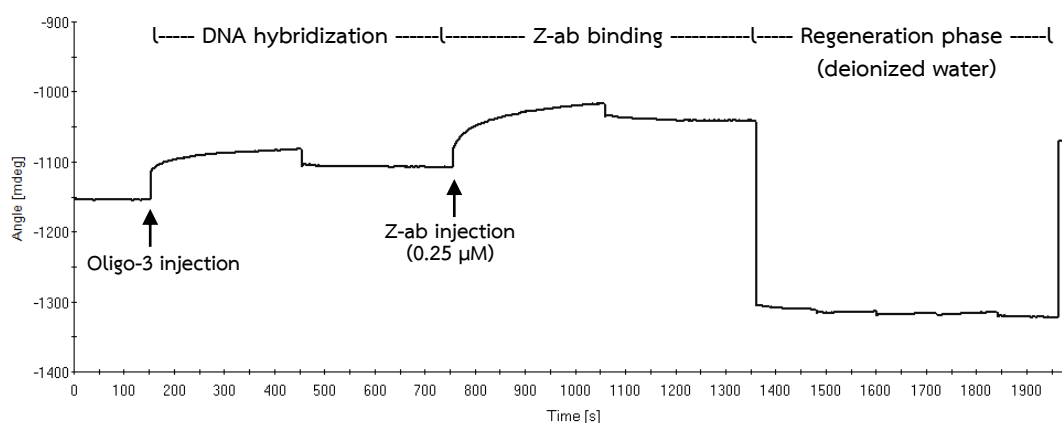


**Figure 4.27** SPR sensogram of the interaction between immobilized oligo-2 and Z-ab under running buffer comprising phosphate buffer solution (pH 7.4, 50 mM) and 100 mM NaCl. The DNA hybridization step gave a relative response of 46.0 mdeg and the DNA-Z-ab binding step gave a relative response of 112.7 mdeg while the relative response of the post-regeneration phase was 82.5 mdeg. The concentration of oligo-3 solution was 2  $\mu\text{M}$  in running buffer. The concentration of Z-ab solution was 0.250  $\mu\text{M}$  in running buffer. The association time and dissociation time were 300 seconds with five-cycle surface regeneration at 25  $^{\circ}\text{C}$ .

To optimize the regeneration condition started from mild condition to harsh condition. The efficiency of regeneration reagent was evaluated from the post-regeneration SPR signal which was lower than baseline signal. The high salt concentrations at neutral pH, 1 M and 2 M NaCl, were selected for the mild condition to remove Z-ab. The SPR sensogram, as in Figure 4.28, showed no significantly change of the post-regeneration SPR signal which indicates the neutral solution could not remove Z-ab on the chip surface even in 2 M NaCl.

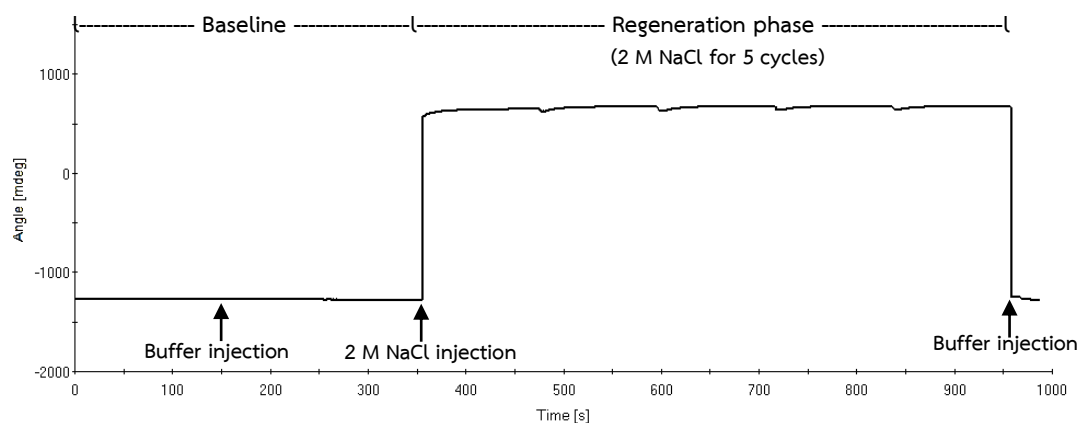


**Figure 4.28** SPR sensogram of surface regeneration with 2 M NaCl. The relative response of the post-regeneration phase was 0.2 mdeg. The regeneration time was set to 120 seconds with five repeated cycles at 25 °C.

The harsher conditions used to eliminate the Z-ab binding were the solutions at basic pH, 10-100 mM NaOH. The high pH of regeneration reagents causes denaturation of proteins which disturbs DNA-protein interaction. The SPR sensograms of surface regeneration with 10 mM NaOH showed the post-regeneration SPR signal was lower than baseline about 14.4 mdeg (Figure 4.29a) which indicates Z-ab was slightly removed from the chip surface. The ionic strength of regeneration reagents was increased to enhance the efficiency of regeneration, however, Z-ab could not be further removed even in 100 mM NaOH as seen in Figure 4.29b. From the SPR results of surface regeneration, 10 mM NaOH has efficiency to regenerate the surface

thus it can be an initial choice for optimizing the regeneration reagents for DNA-protein interaction study.

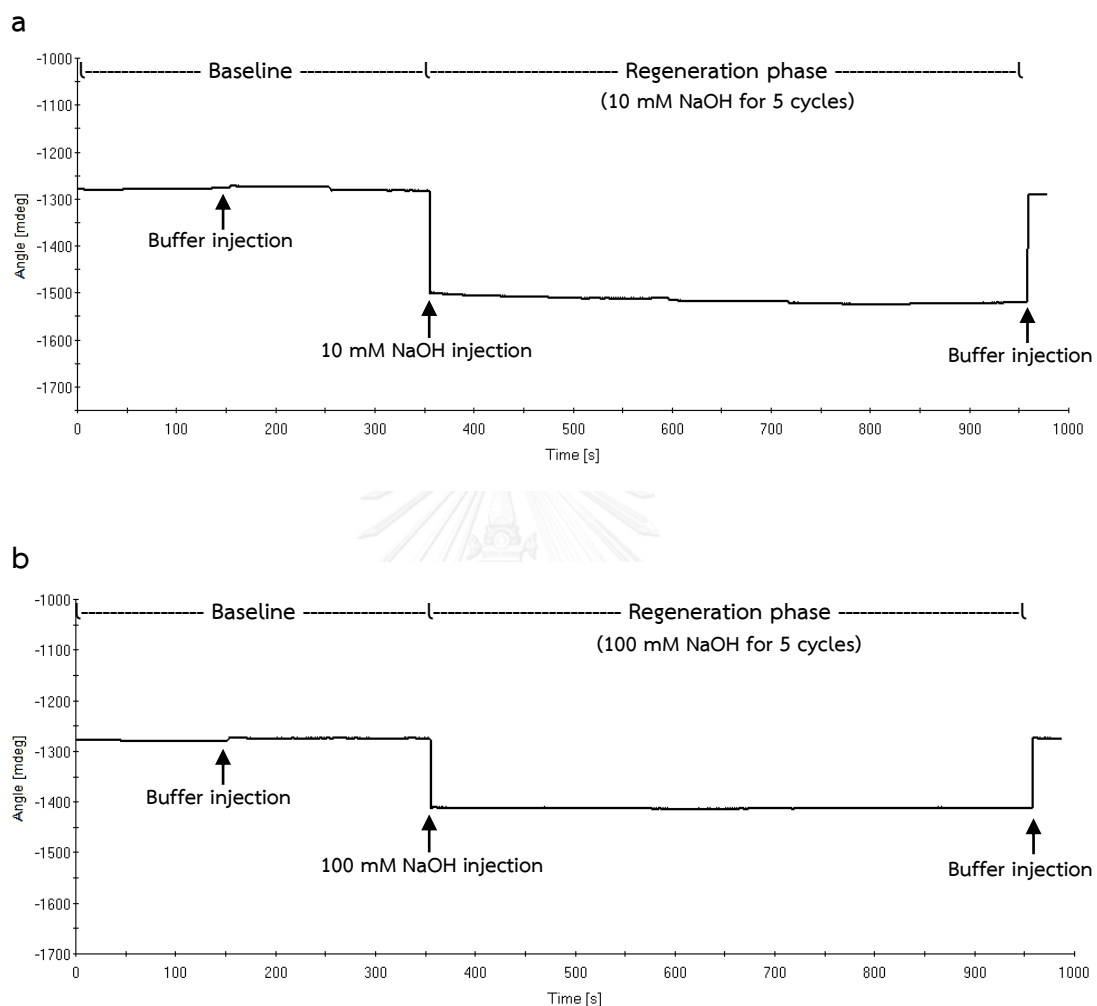


**Figure 4.29** SPR sensogram of surface regeneration with 10 mM NaOH (a) and 100 mM NaOH (b). The relative responses of the post-regeneration phase were -14.4 mdeg and 4.3 mdeg, respectively. The regeneration time was set to 120 seconds with five repeated cycles at 25 °C.

From the SPR sensogram of the interaction between the hybridized oligo-2+3 and Z-ab, the undesired response in dissociation phase presumed to be from non-specific binding between DNA and proteins was proved by injection of Z-ab to the immobilized oligo-2 without duplex hybridization. The non-specific binding of Z-ab to single-stranded DNA should not occur so the SPR signal of the interaction of Z-ab with immobilized oligo-2 was not observed. Despite decreasing the concentration of Z-ab ( $0.125 \mu\text{M}$ ), the high SPR signal obviously showed in dissociation phase which indicates the binding has occurred (Figure 4.30). The non-specific binding of Z-ab to DNA was confirmed with injection of Z-ab on the free gold surface. The SPR sensogram in Figure 4.31 showed the SPR signal occurred apparently even with no immobilized DNA on surface which implies the Z-ab can deposit on gold surface.

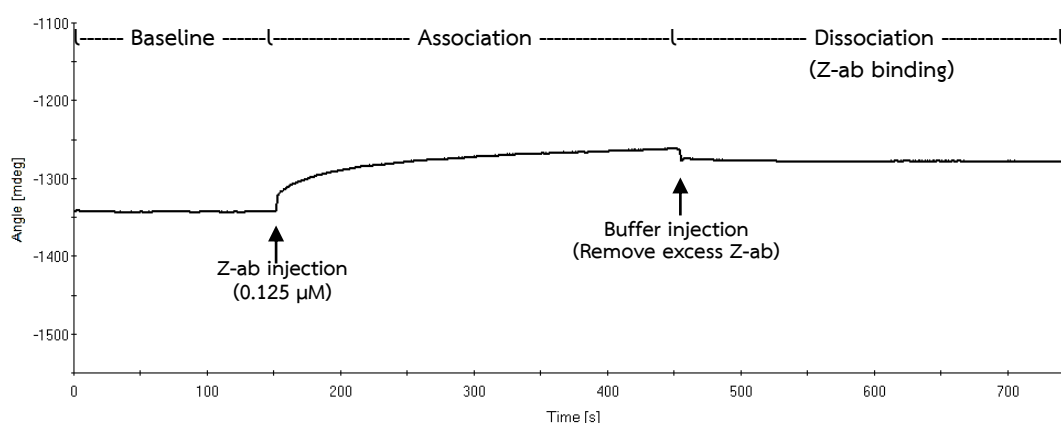


**Figure 4.30** SPR sensogram of the interaction between only immobilized oligo-2 and Z-ab under running buffer comprising phosphate buffer solution (pH 7.4, 50 mM) and 100 mM NaCl. The immobilized DNA-Z-ab binding step gave a relative response of 64.1 mdeg. The concentration of Z-ab solution was  $0.125 \mu\text{M}$  in running buffer. The association time and dissociation time were 300 seconds at  $25^\circ\text{C}$ .

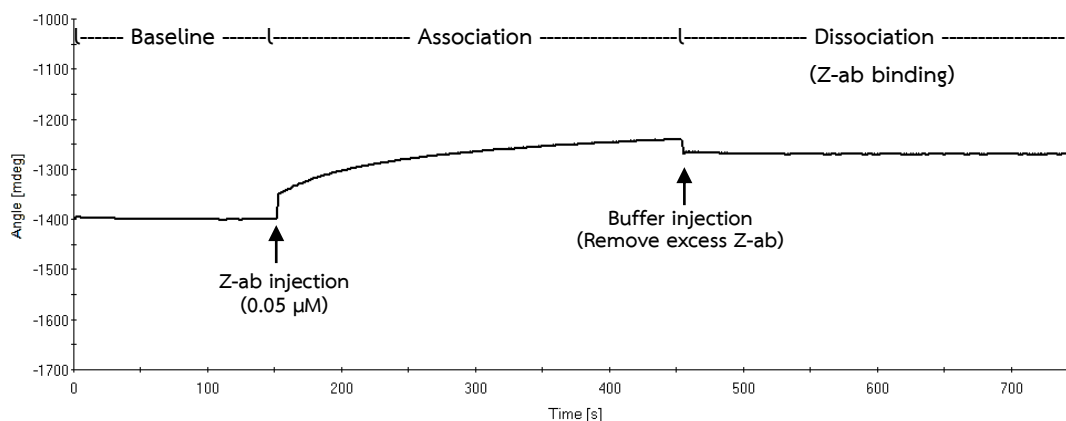


**Figure 4.31** SPR sensogram of the interaction between Z-ab and free gold surface under running buffer comprising phosphate buffer solution (pH 7.4, 50 mM) and 100 mM NaCl. The Z-ab binding on surface gave a relative response of 129.5 mdeg. The concentration of Z-ab solution was 0.05  $\mu\text{M}$  in running buffer. The association time and dissociation time were 300 seconds at 25  $^{\circ}\text{C}$ .

All SPR results reveal Z-ab does not bind specifically to DNA on surface unlike in solution study. Instead, Z-ab can be adsorbed on the chip surface. The occurrence of protein adsorption on gold surface might due to the fact that the concentration of Z-ab used in the study of DNA-protein interaction is too high. The Z-ab samples contained high concentration that the non-specific adsorption of proteins has found from protein overload and the surface regeneration cannot remove protein completely. In according to assumption, the experiments of the interaction between Z-DNA forming probe and Z-DNA binding protein were performed by starting the concentration of Z-ab at 0.5 nM. The duplex of the immobilized oligo-5+6 on gold surface was supposed to bind to Z-ab as shown in B-Z transition study. From the SPR sensogram in Figure 4.32 and 4.33, when the Z-ab was applied to bind to the hybridized Z-DNA forming probe, no significant difference in the SPR response between the DNA-protein binding step and hybridization step.

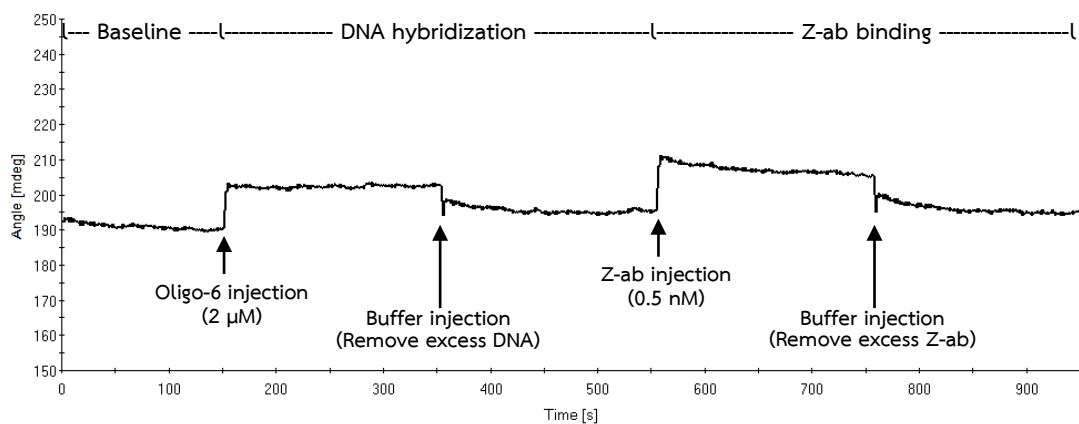


**Figure 4.32** SPR sensograms of the interaction between immobilized oligo-5 and Z-ab. under running buffer comprising phosphate buffer solution (pH 7.4, 50 mM) and 100 mM NaCl. The DNA hybridization step gave a relative response of 4.3 mdeg and the DNA-Z-ab binding step gave a relative response of 5.6 mdeg. The concentration of oligo-6 solution was 2  $\mu\text{M}$  in running buffer. The concentration of Z-ab solution was 0.5 nM in running buffer. The association time and dissociation time were 200 seconds with five-cycle surface regeneration at 25  $^{\circ}\text{C}$ .

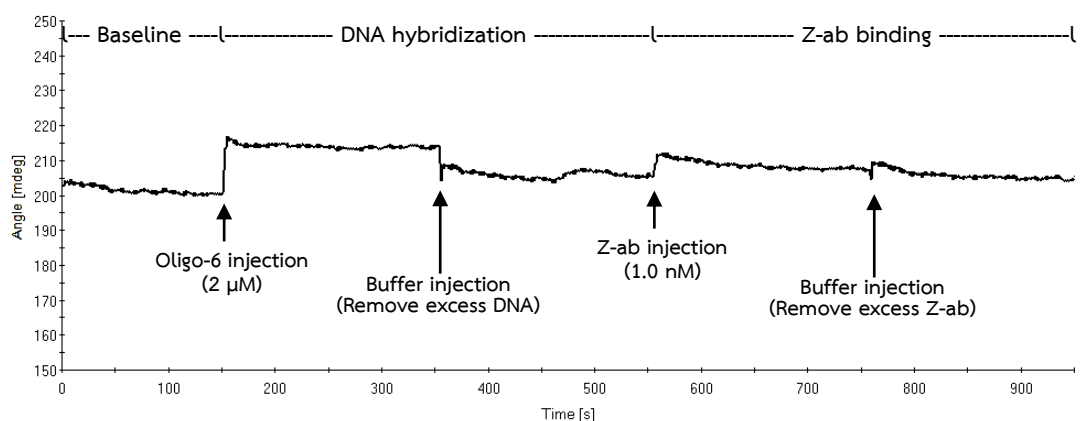


**Figure 4.33** SPR sensograms of the interaction between immobilized oligo-5 and Z-ab. under running buffer comprising phosphate buffer solution (pH 7.4, 50 mM) and 100 mM NaCl. The DNA hybridization step gave a relative response of 4.3 mdeg and the DNA-Z-ab binding step gave a relative response of 4.5 mdeg. The concentration of oligo-6 solution was 2  $\mu$ M in running buffer. The concentration of Z-ab solution was 1.0 nM in running buffer. The association time and dissociation time were 200 seconds with five-cycle surface regeneration at 25  $^{\circ}$ C.

All SPR experiments indicate the interaction between immobilized Z-DNA forming probe on gold chip and Z-DNA binding protein cannot occur. Attachment of Z-DNA forming sequence probe on the gold surface has been suspected to effect on B to Z transition potential of oligonucleotide. The 5'-end terminal is fixed which contributes to minimizing of the flexibility of Z-DNA forming probe therefore their capability to form Z-DNA is limited. In addition, these unexpected results might result from using a polyclonal antibody of Z-ab which gives multiple epitope recognition. Many epitopes are not specific to structure of the 5-methylcytosine containing oligonucleotide and can interfere DNA-protein binding reaction. The difference of production batches of polyclonal antibody causes a varying in amount of each epitope. The production batch of Z-ab used in DNA probe-protein binding study on the surface was different from the binding study in solution condition. To prove this hypothesis, the binding between the duplex of oligo-5+6 and polyclonal Z-ab was



evaluated in solution condition by CD study. The CD spectra of the duplex of oligo-5+6 interacting with Z-ab showed the CD signals were scarcely changed at a ratio Z-ab : oligo-5+6 of 0.5 while the previous study has presented an apparent change of CD signal (Figure 4.34). The alteration of CD pattern of oligo-5+6 duplex to Z-DNA conformation could be observed when the mole of Z-ab was added as much as 1.5 times of mole of DNA duplex, Figure 4.35. The CD results have confirmed there is a variation of production batch of Z-ab affecting to the interaction between Z-DNA forming probe and Z-ab.

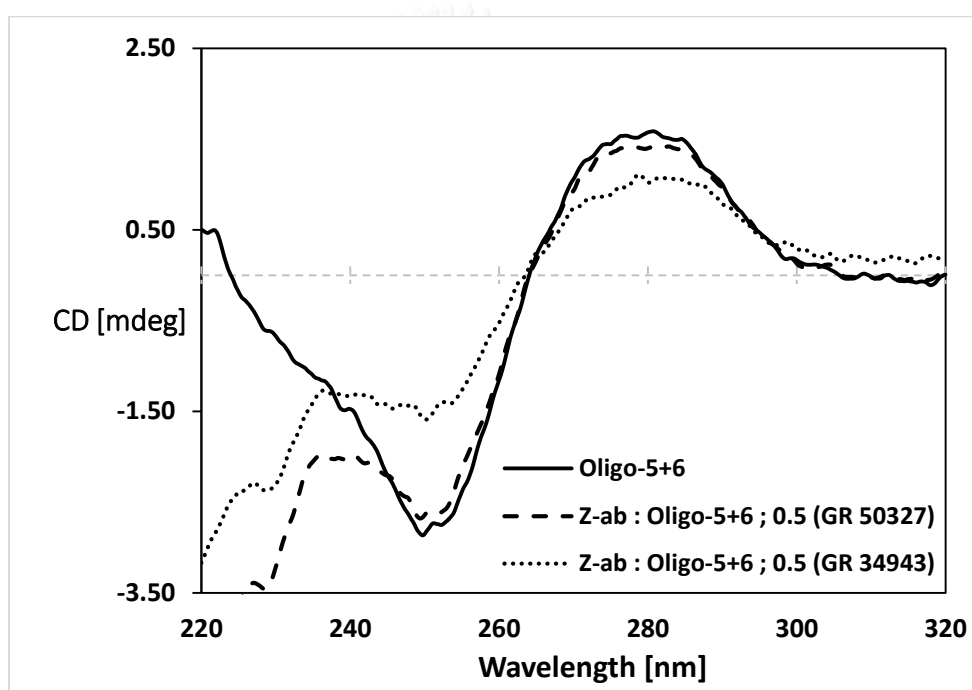


**Figure 4.34** CD spectra of oligo-5+6 in 50 mM  $\text{Na}_2\text{HPO}_4$  buffer, pH 7.0 with different production batches of Z-ab at a ratio Z-ab : oligo-5+6 of 0.5. GR 50327 was a new production batches of Z-ab and GR 34943 was a production batches of Z-ab used in the study of DNA-specific Z-DNA binding protein in solution condition.

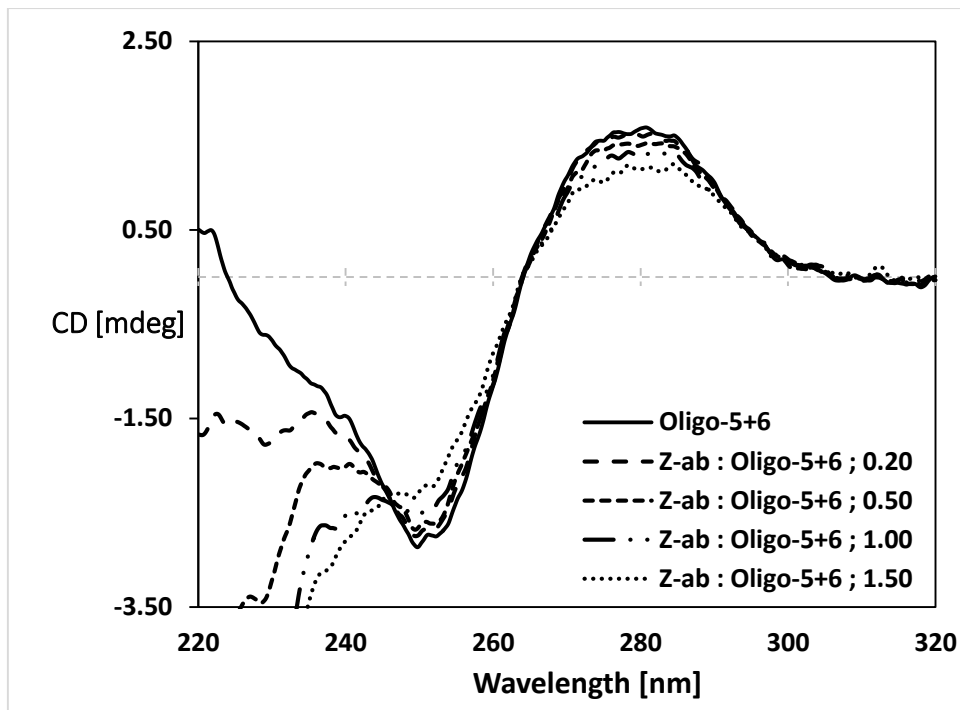


**Figure 4.35** CD spectra of oligo-5+6 in 50 mM  $\text{Na}_2\text{HPO}_4$  buffer, pH 7.0 with varied molar ratio of the new production batch of Z-ab (GR 50327). The oligonucleotide concentration was at 3.2  $\mu\text{M}$ . The CD spectra were monitored at 25  $^\circ\text{C}$  with a scanning rate of 20 nm/min. Accumulation was set to 10 scans.

## CHAPTER V

### CONCLUSIONS

The DNA-based biosensor was successfully developed for detection Z-DNA binding protein. The designed oligonucleotide comprise 5'-thiol terminal for immobilization, Z-DNA prone CG track, and non-self complimentary track. The Z-DNA forming probe can convert to Z-DNA and selectively bind to Z-ab. All SPR results have shown the complete of DNA immobilization process and obtained the optimal SPR condition for hybridization. The B/Z-DNA biosensor can specifically hybridized to complementary sequence, however, the optimal SPR condition for DNA-protein binding on surface needs to be further optimized.

## REFERENCES

1. Watson JD, Crick FH. Molecular structure of nucleic acids; a structure for deoxyribose nucleic acid. *Nature*. 1953;171(4356):737-8.
2. Wang AH, Quigley GJ, Kolpak FJ, Crawford JL, van Boom JH, van der Marel G, et al. Molecular structure of a left-handed double helical DNA fragment at atomic resolution. *Nature*. 1979;282(5740):680-6.
3. Herbert A, Rich A. Left-handed Z-DNA: structure and function. *Genetica*. 1999;106(1-2):37-47.
4. Rich A, Nordheim A, Wang AH. The chemistry and biology of left-handed Z-DNA. *Annual review of biochemistry*. 1984;53:791-846.
5. Wang G, Vasquez KM. Z-DNA, an active element in the genome. *Frontiers in bioscience : a journal and virtual library*. 2007;12:4424-38.
6. Lafer EM, Valle RP, Moller A, Nordheim A, Schur PH, Rich A, et al. Z-DNA-specific antibodies in human systemic lupus erythematosus. *The Journal of clinical investigation*. 1983;71(2):314-21.
7. Allinquant B, Malfoy B, Schuller E, Leng M. Presence of Z-DNA specific antibodies in Crohn's disease, polyradiculoneuritis and amyotrophic lateral sclerosis. *Clinical and experimental immunology*. 1984;58(1):29-36.
8. Sibley JT, Lee JS, Decoteau WE. Left-handed "Z" DNA antibodies in rheumatoid arthritis and systemic lupus erythematosus. *The Journal of rheumatology*. 1984;11(5):633-7.
9. Lafer EM, Moller A, Nordheim A, Stollar BD, Rich A. Antibodies specific for left-handed Z-DNA. *Proceedings of the National Academy of Sciences of the United States of America*. 1981;78(6):3546-50.
10. Vasudevaraju P, Bharathi, Garruto RM, Sambamurti K, Rao KS. Role of DNA dynamics in Alzheimer's disease. *Brain research reviews*. 2008;58(1):136-48.
11. Herbert A, Alfken J, Kim YG, Mian IS, Nishikura K, Rich A. A Z-DNA binding domain present in the human editing enzyme, double-stranded RNA adenosine deaminase.

Proceedings of the National Academy of Sciences of the United States of America. 1997;94(16):8421-6.

12. Barraud P, Allain FH. ADAR proteins: double-stranded RNA and Z-DNA binding domains. *Current topics in microbiology and immunology*. 2012;353:35-60.

13. Hedgpeth J, Goodman HM, Boyer HW. DNA Nucleotide Sequence Restricted by the RI Endonuclease. *Proceedings of the National Academy of Sciences of the United States of America*. 1972;69(11):3448-52.

14. Boyer HW. DNA Restriction and Modification Mechanisms in Bacteria. *Annual Review of Microbiology*. 1971;25(1):153-76.

15. Jerome SS, Richard FT. Taylor & Francis; 1996.

16. Kerman K, Morita Y, Takamura Y, Tamiya E. Escherichia coli single-strand binding protein-DNA interactions on carbon nanotube-modified electrodes from a label-free electrochemical hybridization sensor. *Anal Bioanal Chem*. 2005;381(6):1114-21.

17. Xu K, Huang J, Ye Z, Ying Y, Li Y. Recent Development of Nano-Materials Used in DNA Biosensors. *Sensors (Basel, Switzerland)*. 2009;9(7):5534-57.

18. Wang J. SURVEY AND SUMMARY: From DNA biosensors to gene chips. *Nucleic Acids Research*. 2000;28(16):3011-6.

19. Monošík R, Stredánský M, Šturdík E. Biosensors - classification, characterization and new trends. *Acta Chimica Slovaca* 2012. p. 109.

20. Disruption of the SCL gene by a t(1;3) translocation in a patient with T cell acute lymphoblastic leukemia. *The Journal of Experimental Medicine*. 1992;176(5):1303-10.

21. Pohl FM, Jovin TM. Salt-induced co-operative conformational change of a synthetic DNA: equilibrium and kinetic studies with poly (dG-dC). *J Mol Biol*. 1972;67(3):375-96.

22. Behe M, Felsenfeld G. Effects of methylation on a synthetic polynucleotide: the B-Z transition in poly(dG-m5dC).poly(dG-m5dC). *Proceedings of the National Academy of Sciences of the United States of America*. 1981;78(3):1619-23.

23. Fujii S, Wang AH, van der Marel G, van Boom JH, Rich A. Molecular structure of (m<sup>5</sup> dC-dG)<sub>3</sub>: the role of the methyl group on 5-methyl cytosine in stabilizing Z-DNA. *Nucleic Acids Res.* 1982;10(23):7879-92.
24. Sugiyama H, Kawai K, Matsunaga A, Fujimoto K, Saito I, Robinson H, et al. Synthesis, structure and thermodynamic properties of 8-methylguanine-containing oligonucleotides: Z-DNA under physiological salt conditions. *Nucleic Acids Research.* 1996;24(7):1272-8.
25. Xu Y, Ikeda R, Sugiyama H. 8-Methylguanosine: A Powerful Z-DNA Stabilizer. *Journal of the American Chemical Society.* 2003;125(44):13519-24.
26. Möller A, Nordheim A, Nichols SR, Rich A. 7-Methylguanine in poly(dG-dC).poly(dG-dC) facilitates z-DNA formation. *Proceedings of the National Academy of Sciences of the United States of America.* 1981;78(8):4777-81.
27. Moller A, Nordheim A, Kozłowski SA, Patel D, Rich A. Bromination stabilizes poly(dG-dC) in the Z-DNA form under low-salt conditions. *Biochemistry.* 1984;23(1):54-62.
28. Vongsutilers V, Phillips DJ, Train BC, McKelvey GR, Thomsen NM, Shaughnessy KH, et al. The conformational effect of para-substituted C8-arylguanine adducts on the B/Z-DNA equilibrium. *Biophys Chem.* 2011;154(1):41-8.
29. Boehm T, Mengle-Gaw L, Kees UR, Spurr N, Lavenir I, Forster A, et al. Alternating purine-pyrimidine tracts may promote chromosomal translocations seen in a variety of human lymphoid tumours. *The EMBO Journal.* 1989;8(9):2621-31.
30. Adachi M, Tsujimoto Y. Potential Z-DNA elements surround the breakpoints of chromosome translocation within the 5' flanking region of bcl-2 gene. *Oncogene.* 1990;5(11):1653-7.
31. Seite P, Leroux D, Hillion J, Monteil M, Berger R, Mathieu-Mahul D, et al. Molecular analysis of a variant 18;22 translocation in a case of lymphocytic lymphoma. *Genes, chromosomes & cancer.* 1993;6(1):39-44.

32. Wölfl S, Wittig B, Rich A. Identification of transcriptionally induced Z-DNA segments in the human c-myc gene. *Biochimica et Biophysica Acta (BBA) - Gene Structure and Expression*. 1995;1264(3):294-302.
33. Rimokh R, Rouault JP, Wahbi K, Gadoux M, Lafage M, Archimbaud E, et al. A chromosome 12 coding region is juxtaposed to the MYC protooncogene locus in a t(8;12)(q24;q22) translocation in a case of B-cell chronic lymphocytic leukemia. *Genes, chromosomes & cancer*. 1991;3(1):24-36.
34. Oh DB, Kim YG, Rich A. Z-DNA-binding proteins can act as potent effectors of gene expression in vivo. *Proceedings of the National Academy of Sciences of the United States of America*. 2002;99(26):16666-71.
35. Wang G, Christensen LA, Vasquez KM. Z-DNA-forming sequences generate large-scale deletions in mammalian cells. *Proceedings of the National Academy of Sciences of the United States of America*. 2006;103(8):2677-82.
36. Suram A, Rao KS, Latha KS, Viswamitra MA. First evidence to show the topological change of DNA from B-DNA to Z-DNA conformation in the hippocampus of Alzheimer's brain. *Neuromolecular medicine*. 2002;2(3):289-97.
37. Latha KS, Anitha S, Rao KS, Viswamitra MA. Molecular understanding of aluminum-induced topological changes in (CCG)<sub>12</sub> triplet repeats: relevance to neurological disorders. *Biochimica et biophysica acta*. 2002;1588(1):56-64.
38. Hegde ML, Anitha S, Latha KS, Mustak MS, Stein R, Ravid R, et al. First evidence for helical transitions in supercoiled DNA by amyloid Beta Peptide (1-42) and aluminum: a new insight in understanding Alzheimer's disease. *Journal of molecular neuroscience : MN*. 2004;22(1-2):19-31.
39. Thomas TJ, Messner RP. A left-handed (Z) conformation of poly(dA-dC).poly(dG-dT) induced by polyamines. *Nucleic Acids Research*. 1986;14(16):6721-33.
40. Schwartz T, Behlke J, Lowenhaupt K, Heinemann U, Rich A. Structure of the DLM-1-Z-DNA complex reveals a conserved family of Z-DNA-binding proteins. *Nat Struct Biol*. 2001;8(9):761-5.

41. Kim Y-G, Muralinath M, Brandt T, Percy M, Hauns K, Lowenhaupt K, et al. A role for Z-DNA binding in vaccinia virus pathogenesis. *Proceedings of the National Academy of Sciences*. 2003;100(12):6974-9.
42. Long L, TLLZ, HJ. DNA and RNA sensor. *SCIENCE CHINA Chemistry*. 2005;48(1):1-10.
43. Zhang S, Wright G, Yang Y. Materials and techniques for electrochemical biosensor design and construction. *Biosensors and Bioelectronics*. 2000;15(5-6):273-82.
44. Zhou Y, Chiu CW, Liang H. Interfacial structures and properties of organic materials for biosensors: an overview. *Sensors (Basel, Switzerland)*. 2012;12(11):15036-62.
45. Byfield MP, Abuknesha RA. Biochemical aspects of biosensors. *Biosensors & bioelectronics*. 1994;9(4-5):373-400.
46. Gedig ET. Chapter 6 Surface Chemistry in SPR Technology. *Handbook of Surface Plasmon Resonance: The Royal Society of Chemistry*; 2008. p. 173-220.
47. Guiseppi-Elie A, Lingerfelt L. Impedimetric Detection of DNA Hybridization: Towards Near-Patient DNA Diagnostics. In: Wittmann C, editor. *Immobilisation of DNA on Chips I. Topics in Current Chemistry*. 260: Springer Berlin Heidelberg; 2005. p. 161-86.
48. Sassolas A, Leca-Bouvier BD, Blum LJ. DNA biosensors and microarrays. *Chemical reviews*. 2008;108(1):109-39.
49. Wilchek M, Bayer EA. The avidin-biotin complex in bioanalytical applications. *Analytical Biochemistry*. 1988;171(1):1-32.
50. Nimse SB, Song K, Sonawane MD, Sayyed DR, Kim T. Immobilization techniques for microarray: challenges and applications. *Sensors (Basel, Switzerland)*. 2014;14(12):22208-29.
51. Dupont-Filliard A, Roget A, Livache T, Billon M. Reversible oligonucleotide immobilisation based on biotinylated polypyrrole film. *Analytica Chimica Acta*. 2001;449(1-2):45-50.



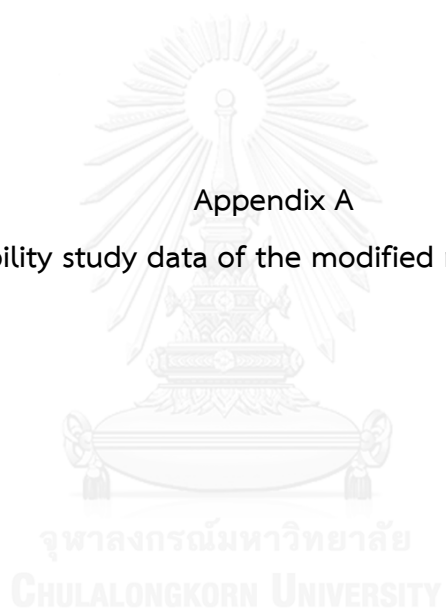
52. Johnson WC. CD of Nucleic Acids. In: Berova N, Nakanishi K, R.W. W, editors. Circular Dichroism: Principles and Applications. 2 ed. New York: John Wiley & Sons, Inc.; 2000. p. 703-18.
53. Homola J, Yee SS, Gauglitz G. Surface plasmon resonance sensors: review. *Sensors and Actuators B: Chemical*. 1999;54(1-2):3-15.
54. Salamon Z, Macleod HA, Tollin G. Surface plasmon resonance spectroscopy as a tool for investigating the biochemical and biophysical properties of membrane protein systems. I: Theoretical principles. *Biochimica et biophysica acta*. 1997;1331(2):117-29.
55. Kretschmann E, Raether H. Radiative decay of nonradiative surface plasmons excited by light. *Z Naturforsch A*. 1968;23:2135.
56. Kibbe WA. OligoCalc: an online oligonucleotide properties calculator. *Nucleic Acids Research*. 2007;35(suppl 2):W43-W6.
57. Vongsutilers V, Daft JR, Shaughnessy KH, Gannett PM. A general synthesis of C8-aryl-purine phosphoramidites. *Molecules*. 2009;14(9):3339-52.
58. Kochetkov NK, Budovskii EI. Hydrolysis of N-glycosidic Bonds in Nucleosides, Nucleotides, and their Derivatives. In: Kochetkov NK, Budovskii EI, editors. *Organic Chemistry of Nucleic Acids*: Springer US; 1972. p. 425-48.



APPENDICES

จุฬาลงกรณ์มหาวิทยาลัย  
CHULALONGKORN UNIVERSITY

Appendix A  
Stability study data of the modified nucleosides



จุฬาลงกรณ์มหาวิทยาลัย

CHULALONGKORN UNIVERSITY

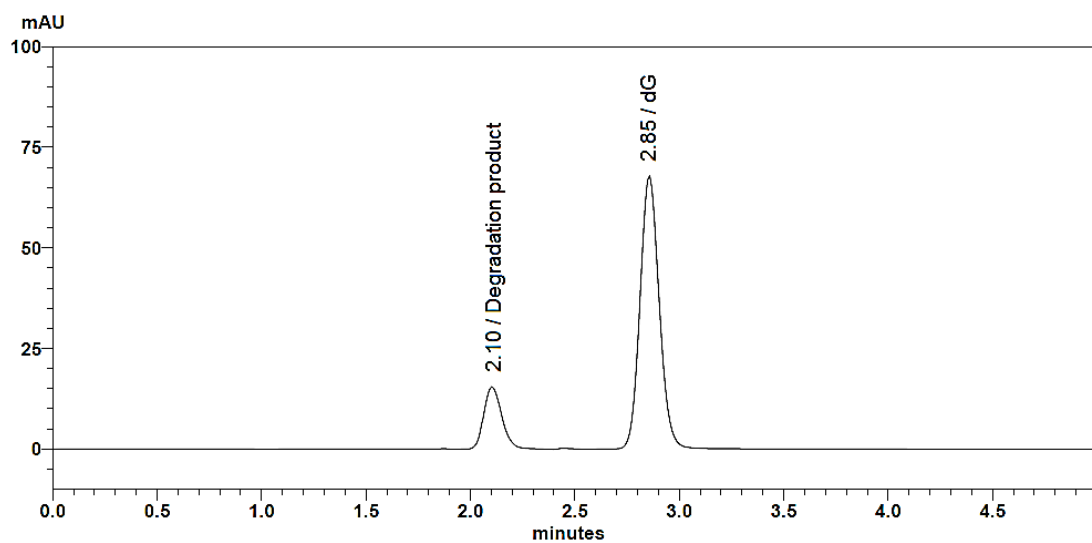


**Figure A-1** Chromatogram of 2'-deoxyguanosine and its degradation product under thermal stress condition. The mobile phase was comprised of 90 mM ammonium acetate buffer pH 6.0 and acetonitrile in the ratio of 92:8, %v/v. The injection volume was set 20  $\mu$ L. The column temperature was maintained at 30  $^{\circ}$ C and the UV detection monitored at 253 nm.

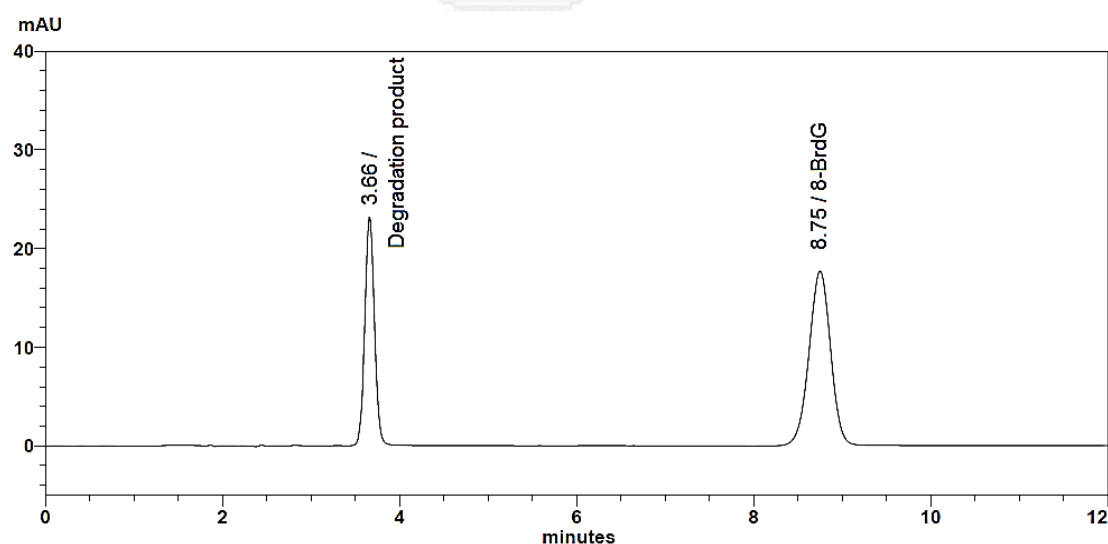


**Figure A-2** Chromatogram of 8-bromo-2'-deoxyguanosine and its degradation product under thermal stress condition. The mobile phase was comprised of 90 mM ammonium acetate buffer pH 6.0 and acetonitrile in the ratio of 92:8, %v/v. The injection volume was set 20  $\mu$ L. The column temperature was maintained at 30  $^{\circ}$ C and the UV detection monitored at 253 nm.

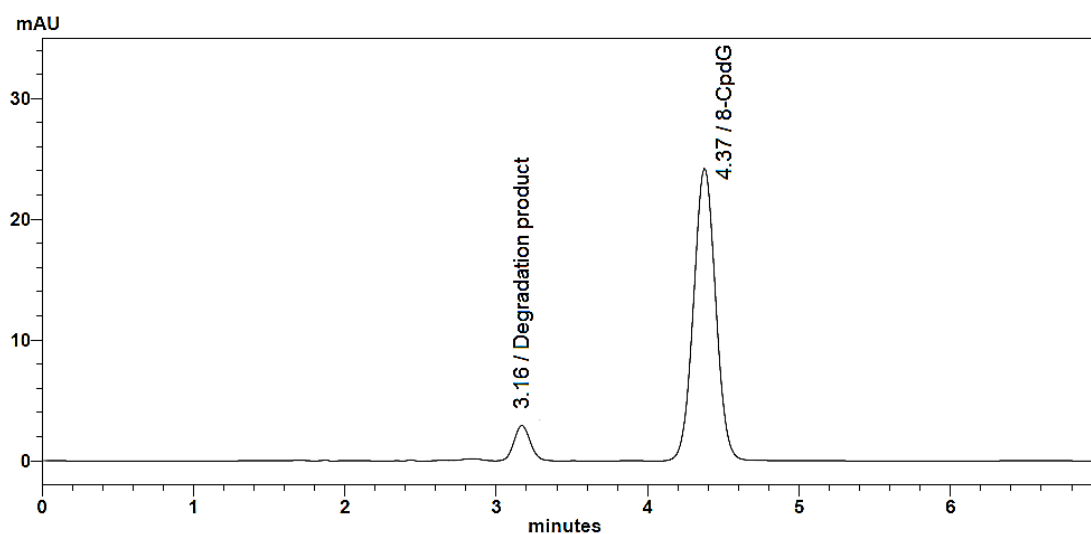


**Figure A-3** Chromatogram of 8-carboxyphenyl-2'-deoxyguanosine and its degradation product under thermal stress condition. The mobile phase was comprised of 90 mM ammonium acetate buffer pH 6.0 and acetonitrile in the ratio of 92:8, %v/v. The injection volume was set 20  $\mu$ L. The column temperature was maintained at 30  $^{\circ}$ C and the UV detection monitored at 253 nm.

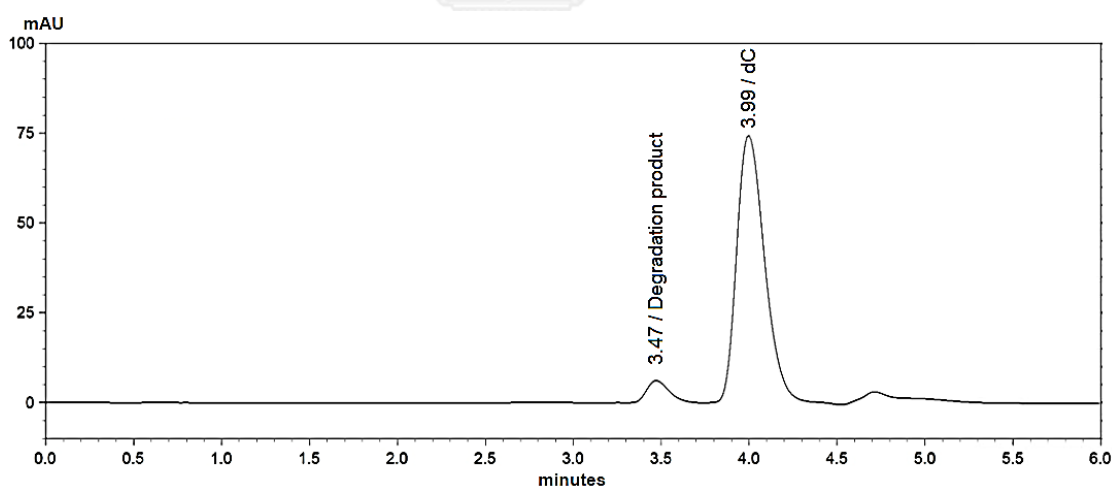


**Figure A-4** Chromatogram of 2'-deoxycytidine and its degradation product under thermal stress condition. The mobile phase was comprised of 90 mM ammonium acetate buffer pH 6.0 and acetonitrile in the ratio of 92:8, %v/v. The injection volume was set 20  $\mu$ L. The column temperature was maintained at 30  $^{\circ}$ C and the UV detection monitored at 270 nm.

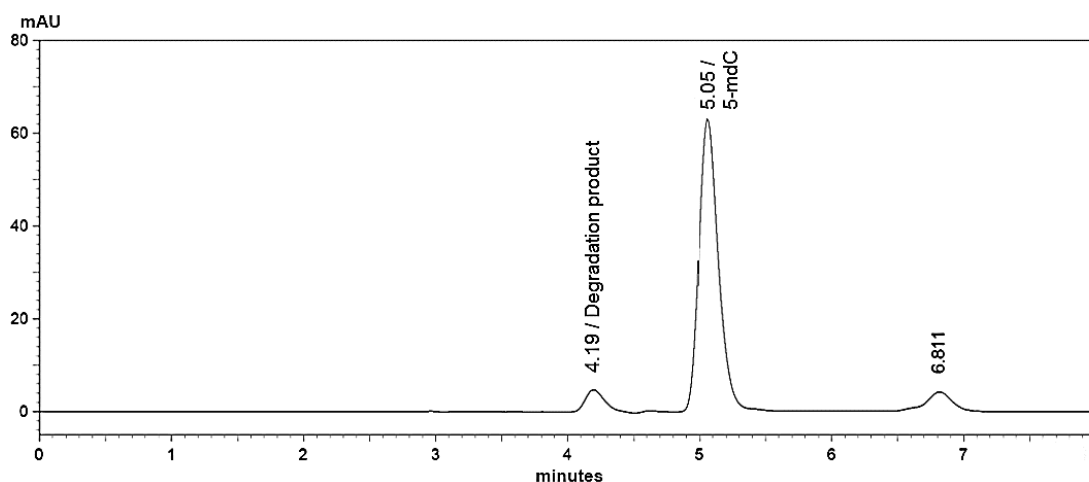


**Figure A-5** Chromatogram of 5-Methyl-2'-deoxycytidine and its degradation product under thermal stress condition. The mobile phase was comprised of 90 mM ammonium acetate buffer pH 6.0 and acetonitrile in the ratio of 92:8, %v/v. The injection volume was set 20  $\mu$ L. The column temperature was maintained at 30  $^{\circ}$ C and the UV detection monitored at 270 nm.

**Table A-6** Stability data of 2'-deoxyguanosine under thermal stress condition at 80  $^{\circ}$ C.

Incubation time (hours)	Concentration of dG ( $\mu$ g/mL)	ln [dG]
0 hour	10.1378	2.3163
12 hours	8.8254	2.1776
24 hours	7.7529	2.0481
48 hours	5.8995	1.7749
60 hours	5.0065	1.6107
72 hours	4.5035	1.5049

Note ln [dG] represents the natural logarithm of 2'-deoxyguanosine concentration.

**Table A-7** Stability data of 8-bromo-2'-deoxyguanosine under thermal stress condition at 80 °C.

Incubation time (hours)	Concentration of 8-BrdG (µg/mL)	ln [8-BrdG]
0 hour	9.9325	2.2958
2 hours	6.0363	1.7978
4 hours	3.5550	1.2684
6 hours	2.1107	0.7470
8 hours	1.2090	0.1898
10 hours	0.6807	-0.3847

Note ln [8-BrdG] represents the natural logarithm of 8-bromo-2'-deoxyguanosine concentration

**Table A-8** Stability data of 8-carboxyphenyl-2'-deoxyguanosine under thermal stress condition at 80 °C.

Incubation time (hours)	Concentration of 8-CpdG (µg/mL)	ln [8-CpdG]
0 hour	9.6745	2.2695
2 hours	3.2859	1.1896
4 hours	1.0626	0.0608
6 hours	0.3448	-1.0647
8 hours	0.1023	-2.2802

Note ln [8-CpdG] represents the natural logarithm of 8-carboxyphenyl-2'-deoxyguanosine concentration.

**Table A-9** Stability data of 2'-deoxycytidine under thermal stress condition at 80 °C.

Incubation time (hours)	Concentration of 8-CpdG ( $\mu\text{g/mL}$ )	ln [8-CpdG]
0 hour	10.161	2.3186
5 hours	10.047	2.3073
20 hours	9.820	2.2844
46 hours	9.377	2.2383
69 hours	9.150	2.2138
92 hours	8.978	2.1948
117 hours	8.612	2.1531

Note ln [dC] represents the natural logarithm of 2'-deoxycytidine concentration.

**Table A-10** Stability data of 5-Methyl-2'-deoxycytidine under thermal stress condition at 80 °C.

Incubation time (hours)	Concentration of 5-mdC ( $\mu\text{g/mL}$ )	ln [5-mdC]
0 hour	10.472	2.3487
4 hours	10.378	2.3397
20 hours	10.201	2.3225
45 hours	9.864	2.2889
68 hours	9.493	2.2506
92 hours	9.364	2.2369
116 hours	8.993	2.1964

Note ln [5-mdC] represents the natural logarithm of 5-methyl-2'-deoxycytidine concentration.



**Table A-11** Stability data of 2'-deoxyguanosine under acidic stress condition.

Incubation time (hours)	Concentration of dG ( $\mu\text{g/mL}$ )	ln [dG]
0 hour	3.0395	1.1117
12 hours	2.5590	0.9396
24 hours	2.1918	0.7847
48 hours	1.7959	0.5855
60 hours	1.4582	0.3772
72 hours	1.0200	0.0198
84 hours	0.9305	-0.0721

Note ln [dG] represents the natural logarithm of 2'-deoxyguanosine concentration.

**Table A-12** Stability data of 8-bromo-2'-deoxyguanosine under acidic stress condition.

Incubation time (hours)	Concentration of 8-BrdG ( $\mu\text{g/mL}$ )	ln [8-BrdG]
0 hour	2.9631	1.0862
2 hours	2.2522	0.8119
4 hours	2.0480	0.7169
6 hours	1.8297	0.6042
8 hours	1.5389	0.4310
10 hours	1.2304	0.2074

Note ln [8-BrdG] represents the natural logarithm of 8-bromo-2'-deoxyguanosine concentration

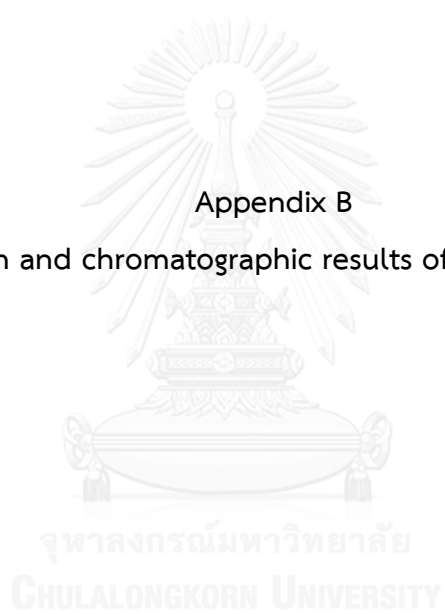
**Table A-13** Stability data of 8-carboxyphenyl-2'-deoxyguanosine under acidic stress condition.

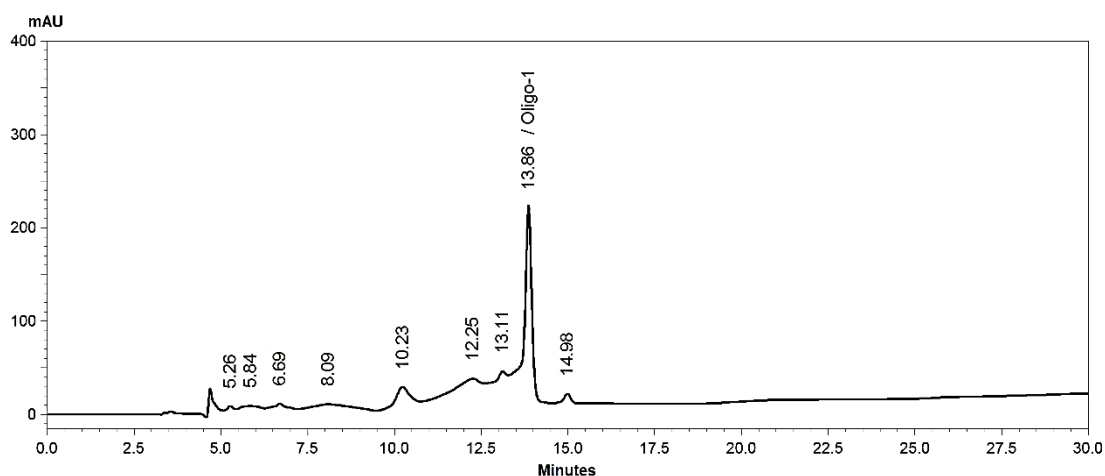
Incubation time (hours)	Concentration of 8-CpdG ( $\mu\text{g/mL}$ )	$\ln$ [8-CpdG]
0 hour	2.9726	1.0894
0.25 hours	2.5304	0.9284
0.5 hours	1.9854	0.6858
0.75 hours	1.7011	0.5313
1 hours	1.3738	0.3175
1.25 hours	1.2061	0.1874

Note  $\ln$  [8-CpdG] represents the natural logarithm of 8-carboxyphenyl-2'-deoxyguanosine concentration.

Appendix B

Chromatogram and chromatographic results of the oligonucleotides

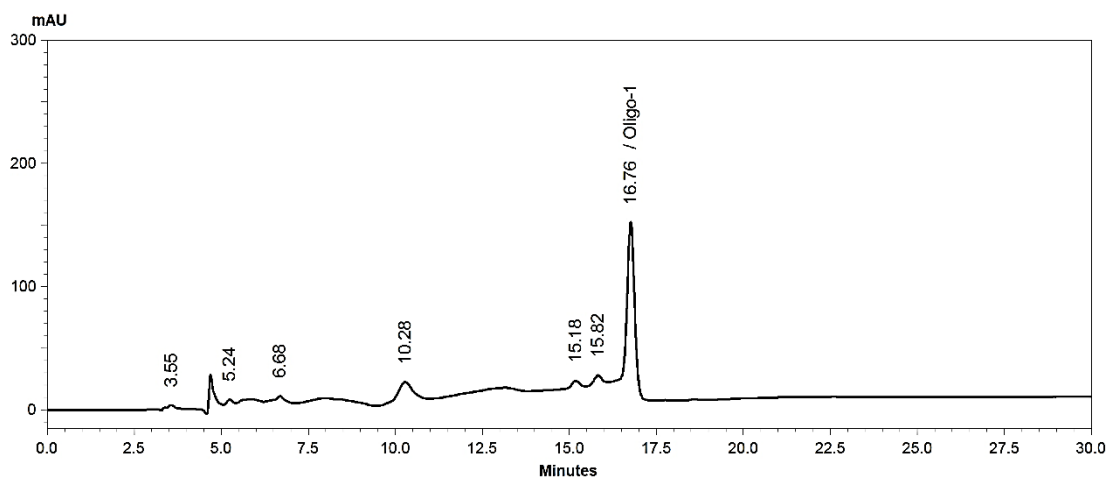




Detector A Ch1 260 nm

Peak #	Retention Time (min)	Area	Area %	Resolution	Theoretical Plates	Tailing Factor
1	5.26	51366	0.57	0.00	4524	0.00
2	5.84	182336	2.04	0.82	451	0.00
3	6.69	217400	2.43	1.05	2754	0.00
4	8.09	513586	5.74	0.96	181	0.00
5	10.23	789617	8.83	1.34	2653	0.00
6	12.25	2128720	23.81	1.22	374	0.00
7	13.11	1217149	13.61	0.44	1506	0.00
8	13.86	3675397	41.11	0.89	27303	0.00
9	14.98	16482	1.84	3.21	27518	0.00
Total		8940452	100.00			

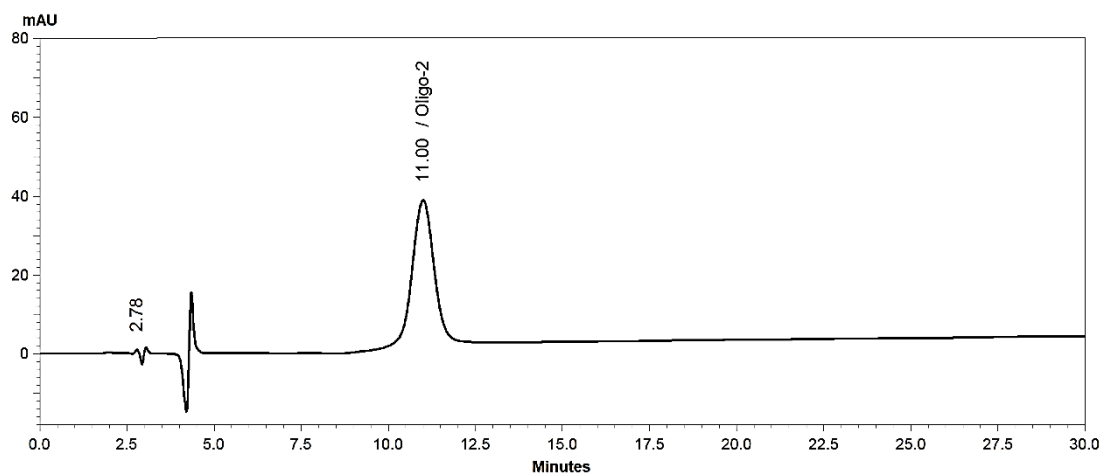
**Figure B-1** Chromatogram and chromatographic result of oligo-1 under gradient method from 10% to 40% ACN in 30 minutes (a gradient slope of 1 %ACN/min). The mobile phase was comprised of acetonitrile and 100 mM TEAA, pH 7. The injection volume was set 10  $\mu$ L. The column temperature was maintained at 40  $^{\circ}$ C and the UV detection monitored at 260 nm.



Detector A Ch1 260 nm

Peak #	Retention Time (min)	Area	Area %	Resolution	Theoretical Plates	Tailing Factor
1	3.55	47842	1.29	0.00	1624	0.00
2	5.24	33558	0.90	5.45	6198	1.07
3	6.69	92018	2.48	4.49	5042	0.86
4	10.28	489882	13.21	6.32	2909	1.00
5	15.18	173766	4.68	7.21	10383	0.00
6	15.82	392284	10.58	0.91	5973	0.00
7	16.76	2479650	66.85	1.54	27810	0.84
Total		3709001	100.00			

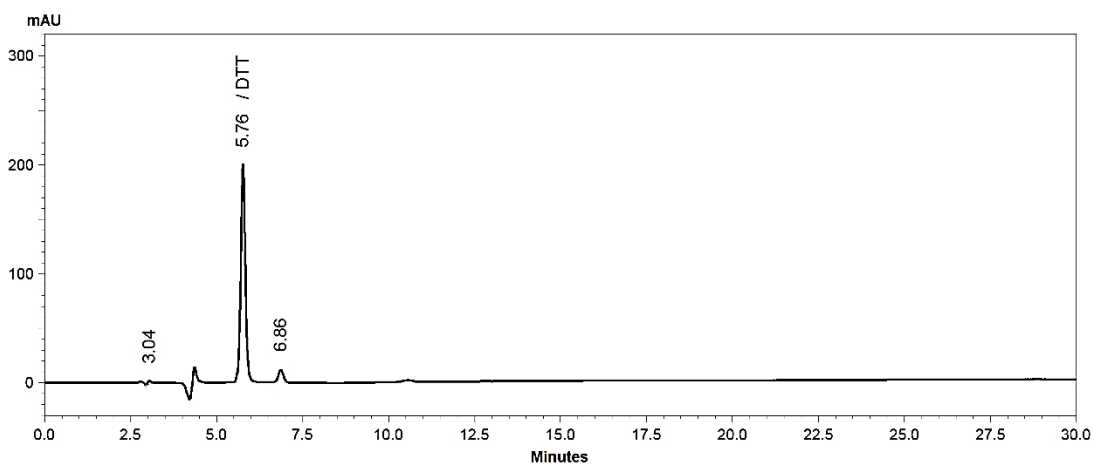
**Figure B-2** Chromatogram and chromatographic result of oligo-1 under gradient method from 10% to 25% ACN in 30 minutes (a gradient slope of 0.5 %ACN/min). The mobile phase was comprised of acetonitrile and 100 mM TEAA, pH 7. The injection volume was set 10  $\mu$ L. The column temperature was maintained at 40  $^{\circ}$ C and the UV detection monitored at 260 nm.



Detector A Ch1 260 nm

Peak #	Retention Time (min)	Area	Area %	Resolution	Theoretical Plates	Tailing Factor
1	2.78	20742	1.24	0.00	2056	1.10
2	11.00	1646021	98.76	11.96	1519.38	1.01
Total		1666763	100.00			

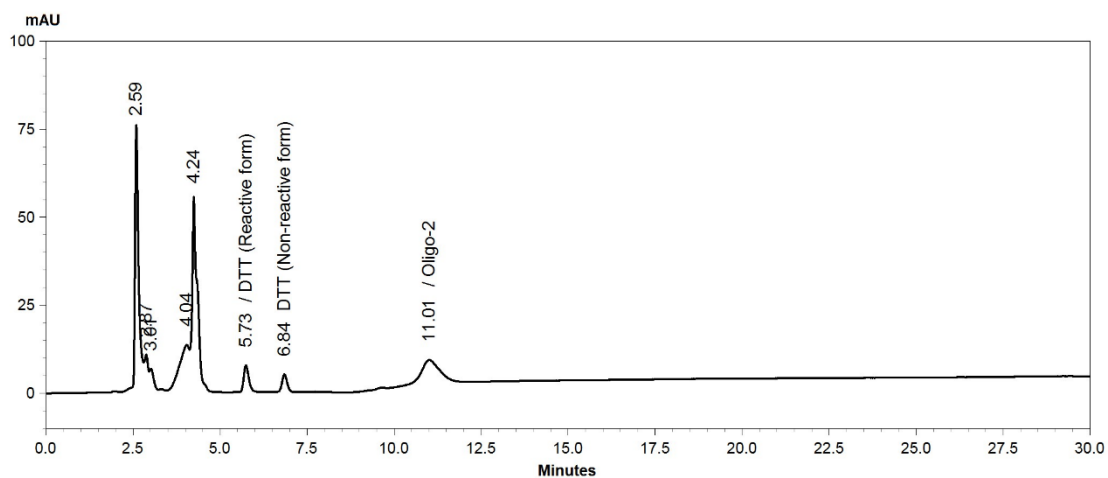
**Figure B-3** Chromatogram and chromatographic result of oligo-2 under gradient method from 20% to 30% ACN in 40 minutes (a gradient slope of 0.25 %ACN/min). The mobile phase was comprised of acetonitrile and 100 mM TEAA, pH 7. The injection volume was set 10  $\mu$ L. The column temperature was maintained at 40  $^{\circ}$ C and the UV detection monitored at 260 nm.



Detector A Ch1 260 nm

Peak #	Retention Time (min)	Area	Area %	Resolution	Theoretical Plates	Tailing Factor
1	3.04	22596	1.13	0.00	3222	1.31
2	5.76	1865349	93.00	11.97	9215	1.07
3	6.86	117743	5.87	4.29	10216	1.12
Total		2005688	100.00			

**Figure B-4** Chromatogram and chromatographic result of DTT prepared in 50 mM phosphate buffer, pH 8.4 under gradient method from 20% to 30% ACN in 40 minutes (a gradient slope of 0.25 %ACN/min). The mobile phase was comprised of acetonitrile and 100 mM TEAA, pH 7. The injection volume was set 10  $\mu$ L. The column temperature was maintained at 40  $^{\circ}$ C and the UV detection monitored at 260 nm.

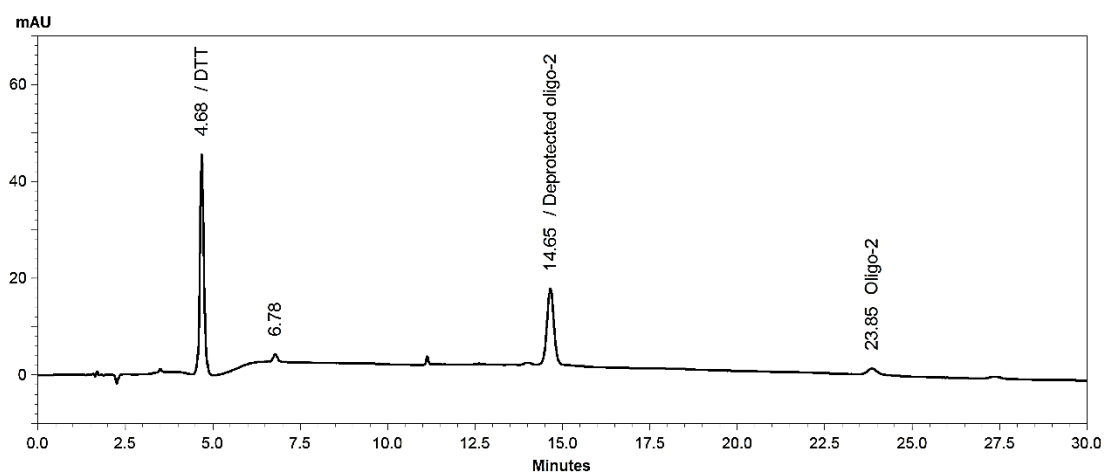


Detector A Ch1 260 nm

Peak #	Retention Time (min)	Area	Area %	Resolution	Theoretical Plates	Tailing Factor
1	2.59	558068	29.29	0.00	3491	0.00
2	2.87	77913	4.09	1.03	904	0.00
3	3.01	45526	2.39	0.00	0.00	0.00
4	4.04	258061	13.54	0.00	268	0.00
5	4.24	566755	29.74	0.34	6493	0.00
6	5.73	76748	4.03	6.29	7458	1.42
7	6.84	51662	2.71	4.12	10116	1.13
8	11.01	270664	14.21	6.40	1830	1.04
Total		1905397	100.00			

**Figure B-5** Chromatogram and chromatographic result of the mixture of oligo-2 and DTT under gradient method from 20% to 30% ACN in 40 minutes (a gradient slope of 0.25 %ACN/min). The mobile phase was comprised of acetonitrile and 100 mM TEAA, pH 7. The injection volume was set 10  $\mu$ L. The column temperature was maintained at 40  $^{\circ}$ C and the UV detection monitored at 260 nm.

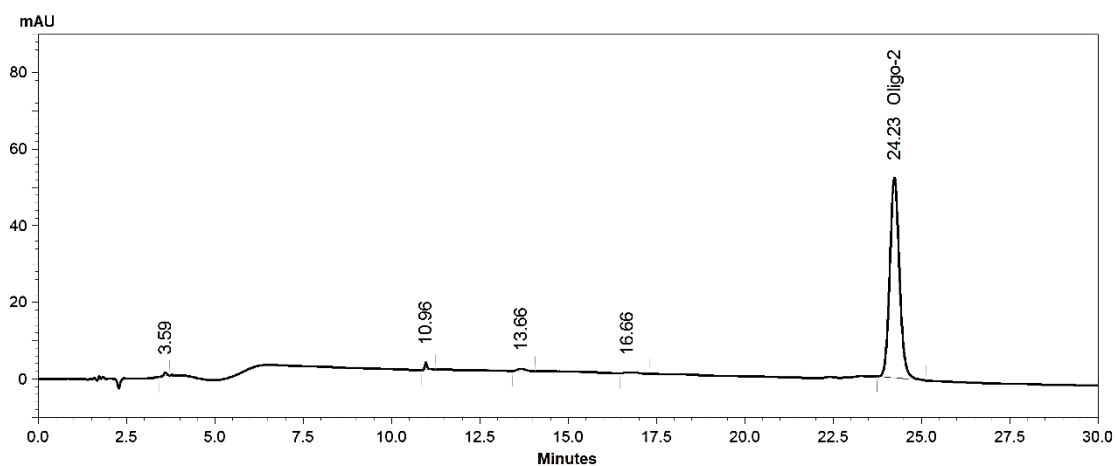




Detector A Ch1 260 nm

Peak #	Retention Time (min)	Area	Area %	Resolution	Theoretical Plates	Tailing Factor
1	4.68	355592	57.29	0.00	8620	1.14
2	6.78	13583	2.19	9.52	12730	1.14
3	14.65	226314	36.46	25.88	25392	1.06
4	23.85	25149	4.05	21.17	36185	1.18
Total		620637	100.00			

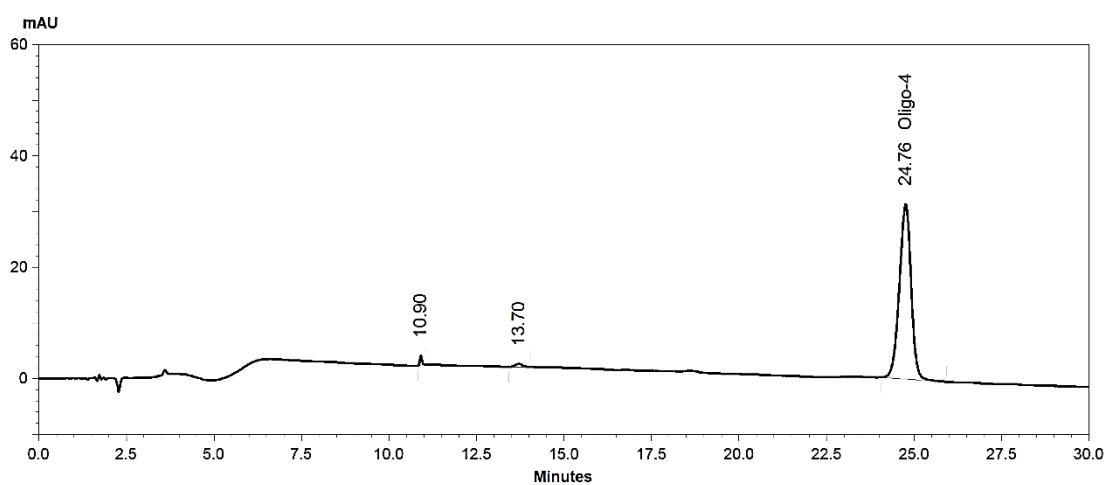
**Figure B-6** Chromatogram and chromatographic result of the reaction mixture of oligo-2 and DTT under gradient method from 10% to 30% ACN in 30 minutes (a gradient slope of 0.67 %ACN/min). The mobile phase was comprised of acetonitrile and 100 mM TEAA, pH 7. The injection volume was set 10  $\mu$ L. The column temperature was maintained at 40  $^{\circ}$ C and the UV detection monitored at 260 nm.



Detector A Ch1 260 nm

Peak #	Retention Time (min)	Area	Area %	Resolution	Theoretical Plates	Tailing Factor
1	3.59	5259	0.52	0.00	8150	1.03
2	10.96	9541	0.94	51.97	124094	1.82
3	13.66	9240	0.91	10.38	19100	1.22
4	16.66	5751	0.56	5.64	9904	2.09
5	24.23	989843	97.07	12.99	38427	1.13
Total		1019671	100.00			

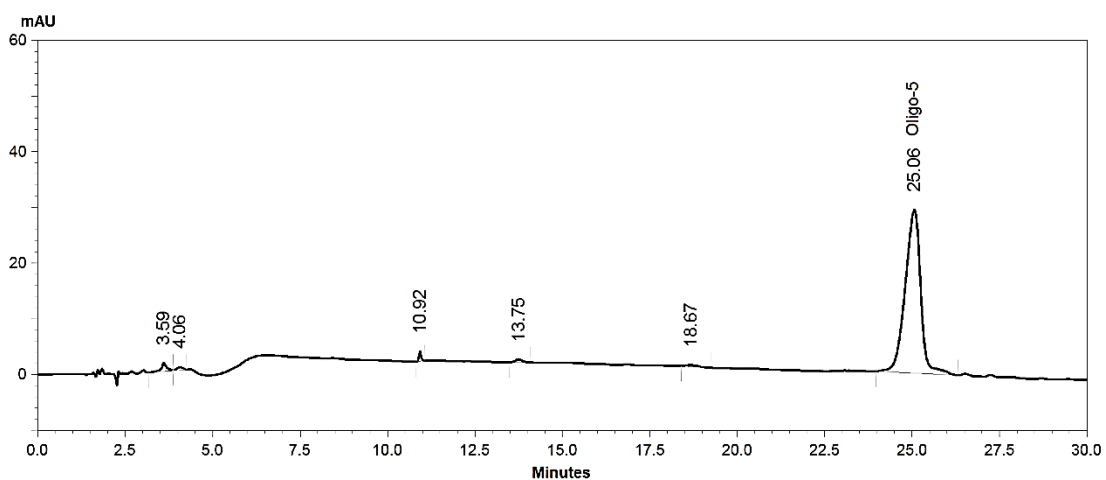
**Figure B-7** Chromatogram and chromatographic result of oligo-2 under gradient method from 10% to 30% ACN in 30 minutes (a gradient slope of 0.67 %ACN/min). The mobile phase was comprised of acetonitrile and 100 mM TEAA, pH 7. The injection volume was set 10  $\mu$ L. The column temperature was maintained at 40  $^{\circ}$ C and the UV detection monitored at 260 nm.



Detector A Ch1 260 nm

Peak #	Retention Time (min)	Area	Area %	Resolution	Theoretical Plates	Tailing Factor
1	10.90	7798	1.04	0.00	130871	1.31
2	13.70	8226	1.10	10.84	19188	1.13
3	24.76	734195	97.86	21.89	25976	0.95
Total		750219	100.00			

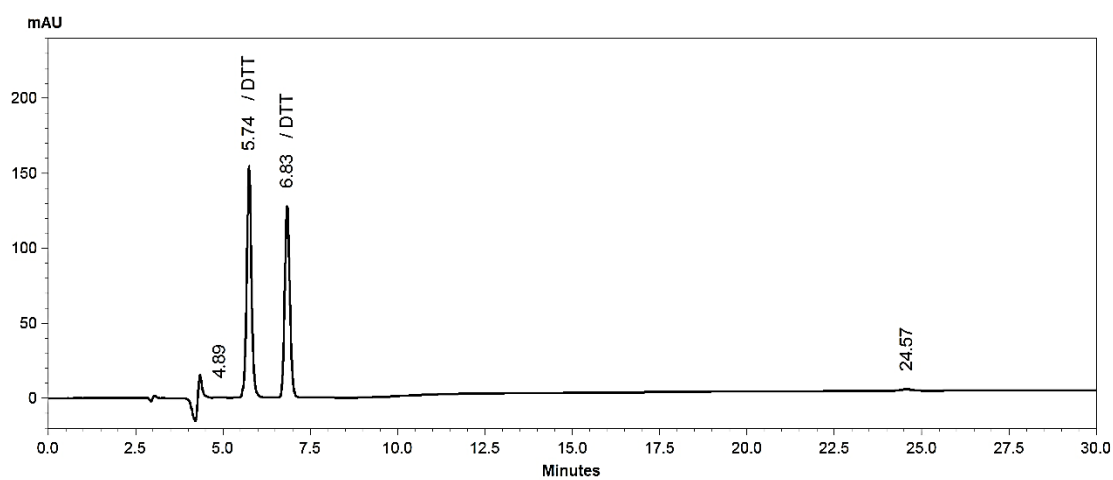
**Figure B-8** Chromatogram and chromatographic result of oligo-4 under gradient method from 10% to 30% ACN in 30 minutes (a gradient slope of 0.67 %ACN/min). The mobile phase was comprised of acetonitrile and 100 mM TEAA, pH 7. The injection volume was set 10  $\mu$ L. The column temperature was maintained at 40  $^{\circ}$ C and the UV detection monitored at 260 nm



Detector A Ch1 260 nm

Peak #	Retention Time (min)	Area	Area %	Resolution	Theoretical Plates	Tailing Factor
1	3.59	17112	1.80	0.00	3718	0.76
2	4.06	7292	0.77	1.57	2093	0.53
3	10.92	7575	0.80	28.92	133190	1.30
4	13.75	8092	0.85	11.13	20056	1.04
5	18.67	6435	0.68	10.26	17151	1.36
6	25.06	903418	95.10	9.33	15768	0.87
Total		949924	100.00			

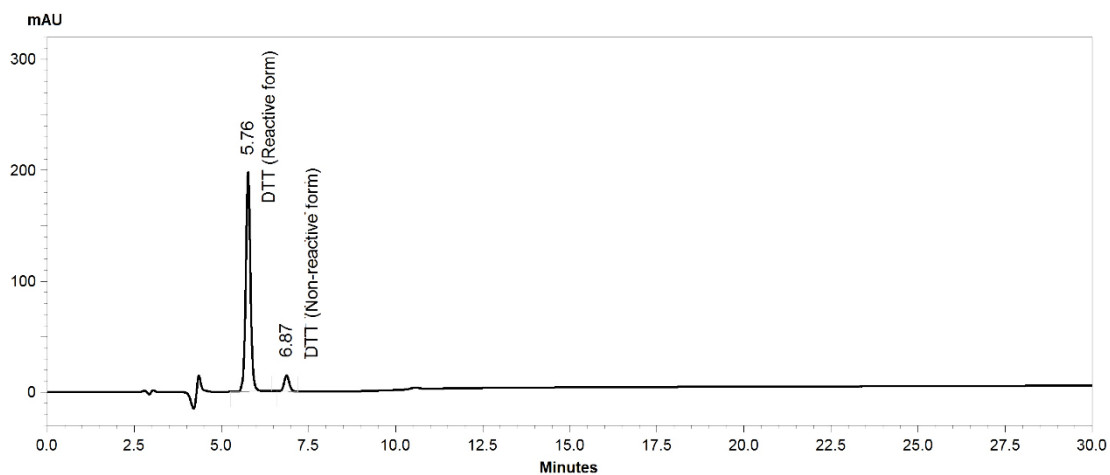
**Figure B-9** Chromatogram and chromatographic result of oligo-5 under gradient method from 10% to 30% ACN in 30 minutes (a gradient slope of 0.67 %ACN/min). The mobile phase was comprised of acetonitrile and 100 mM TEAA, pH 7. The injection volume was set 10  $\mu$ L. The column temperature was maintained at 40  $^{\circ}$ C and the UV detection monitored at 260 nm.



Detector A Ch1 260 nm

Peak #	Retention Time (min)	Area	Area %	Resolution	Theoretical Plates	Tailing Factor
1	4.89	4700	0.17	0.00	2104	1.17
2	5.74	1457723	52.27	2.54	8775	1.08
3	6.83	1302543	46.71	4.21	10050	1.14
4	24.57	23779	0.85	37.75	21717	1.00
Total		2788746	100.00			

**Figure B-10** Chromatogram and chromatographic result of DTT supplied from Sigma Aldrich under gradient method from 10% to 25% ACN in 30 minutes (a gradient slope of 0.25 %ACN/min). The mobile phase was comprised of acetonitrile and 100 mM TEAA, pH 7. The injection volume was set 10  $\mu$ L. The column temperature was maintained at 40  $^{\circ}$ C and the UV detection monitored at 260 nm.



Detector A Ch1 260 nm

Peak #	Retention Time (min)	Area	Area %	Resolution	Theoretical Plates	Tailing Factor
1	5.76	1847105	91.24	0.00	9189	1.08
2	6.87	147756	7.30	4.30	10068	1.14
3	10.57	29575	1.46	9.55	7093	0.86
Total		2024436	100.00			

**Figure B-11** Chromatogram and chromatographic result of DTT prepared in 50 mM phosphate buffer, pH 8.4 (freshly prepared) under gradient method from 10% to 25% ACN in 30 minutes (a gradient slope of 0.25 %ACN/min). The mobile phase was comprised of acetonitrile and 100 mM TEAA, pH 7. The injection volume was set 10  $\mu$ L. The column temperature was maintained at 40  $^{\circ}$ C and the UV detection monitored at 260 nm.

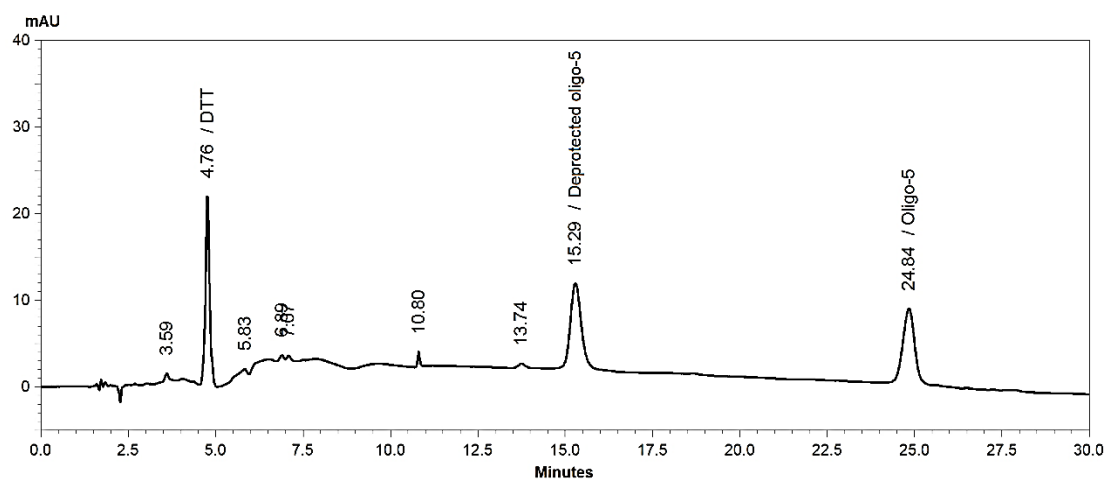
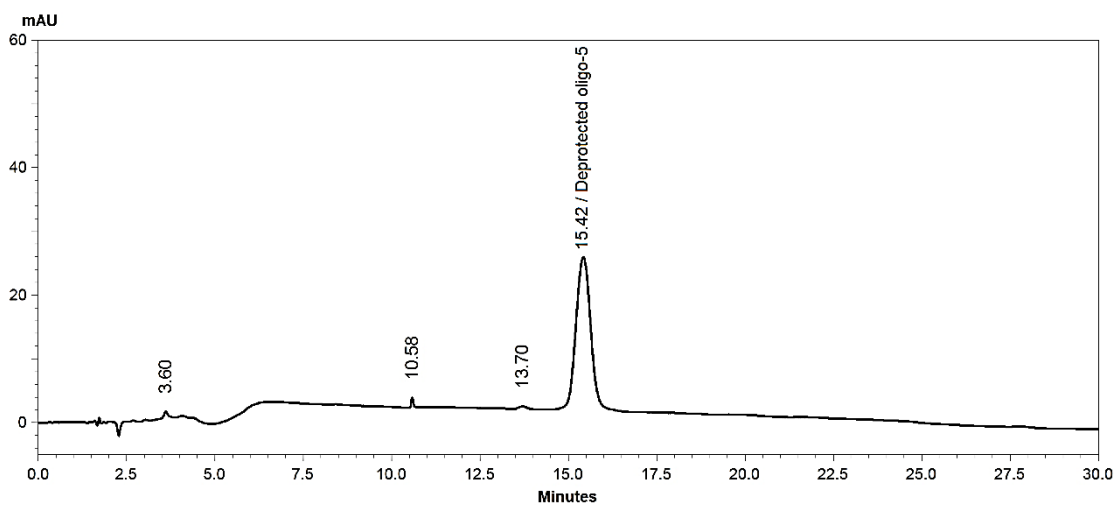


**Figure B-12** Chromatogram of the reaction mixture of oligo-5 and DTT under gradient method from 10% to 30% ACN in 30 minutes (a gradient slope of 0.67 %ACN/min). The mobile phase was comprised of acetonitrile and 100 mM TEAA, pH 7. The injection volume was set 10  $\mu$ L. The column temperature was maintained at 40  $^{\circ}$ C and the UV detection monitored at 260 nm.



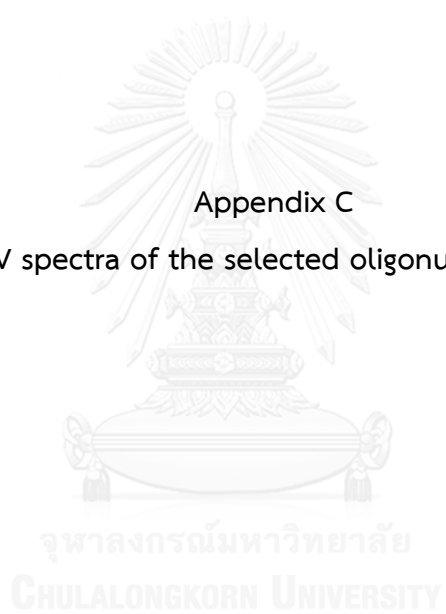
Detector A Ch1 260 nm

Peak #	Retention Time (min)	Area	Area %	Resolution	Theoretical Plates	Tailing Factor
1	3.60	8740	1.22	0.00	1308747431	1.48
2	10.58	6321	0.88	43.73	149005	1.39
3	13.70	6303	0.88	12.25	18721	1.17
4	15.42	696827	97.03	2.97	6667	1.07
Total		718190	100.00			

**Figure B-13** Chromatogram and chromatographic result of the deprotected oligo-5 under gradient method from 10% to 30% ACN in 30 minutes (a gradient slope of 0.67 %ACN/min). The mobile phase was comprised of acetonitrile and 100 mM TEAA, pH 7. The injection volume was set 10  $\mu$ L. The column temperature was maintained at 40  $^{\circ}$ C and the UV detection monitored at 260 nm.



Appendix C  
UV spectra of the selected oligonucleotides



จุฬาลงกรณ์มหาวิทยาลัย

CHULALONGKORN UNIVERSITY

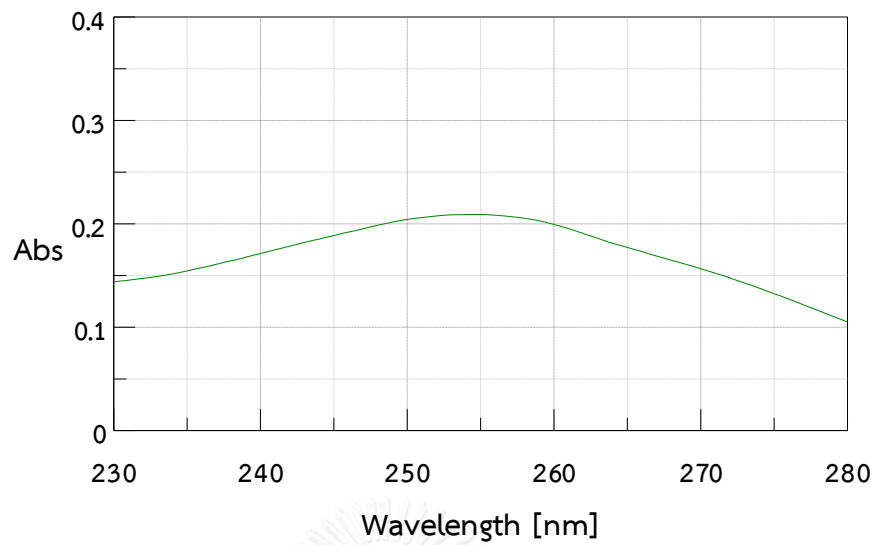


**Figure C-1** UV spectra of oligo-1. The oligonucleotide samples were prepared in 50 mM  $\text{Na}_2\text{HPO}_4$  buffer, pH 7.0.

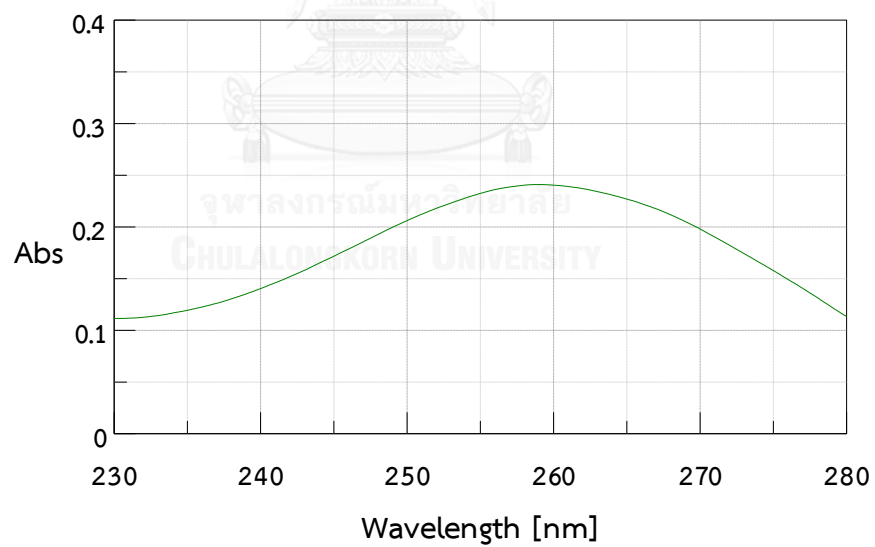


**Figure C-2** UV spectra of oligo-2. The oligonucleotide samples were prepared in 50 mM  $\text{Na}_2\text{HPO}_4$  buffer, pH 7.0.

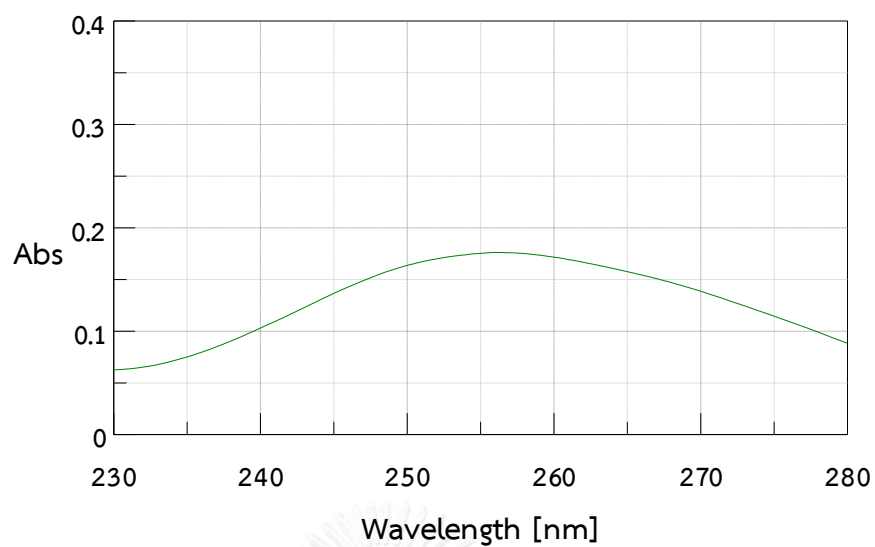


**Figure C-3** UV spectra of oligo-3. The oligonucleotide samples were prepared in 50 mM  $\text{Na}_2\text{HPO}_4$  buffer, pH 7.0.

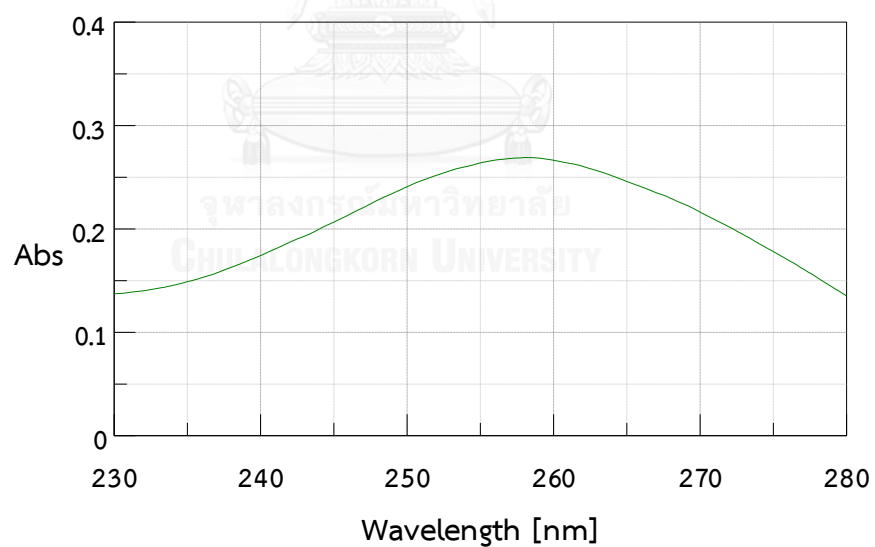


**Figure C-4** UV spectra of oligo-4. The oligonucleotide samples were prepared in 50 mM  $\text{Na}_2\text{HPO}_4$  buffer, pH 7.0.

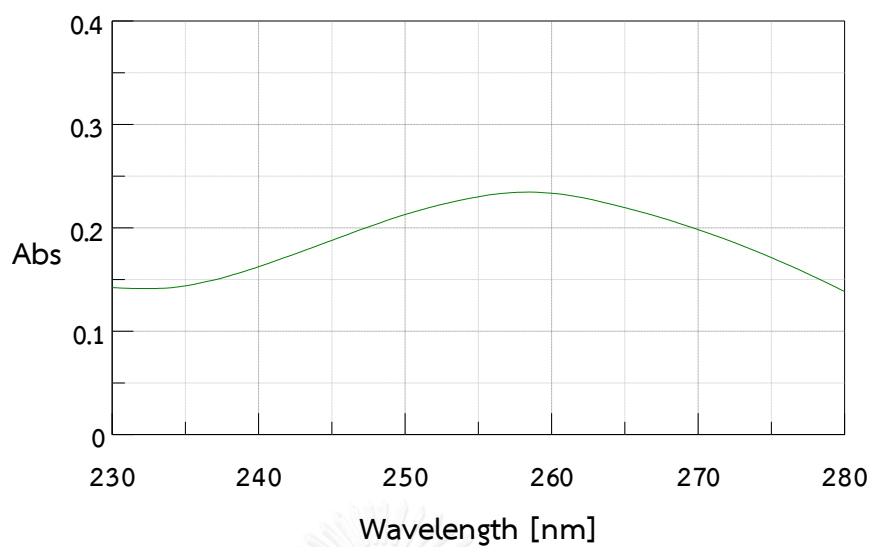


**Figure C-5** UV spectra of oligo-5. The oligonucleotide samples were prepared in 50 mM  $\text{Na}_2\text{HPO}_4$  buffer, pH 7.0.

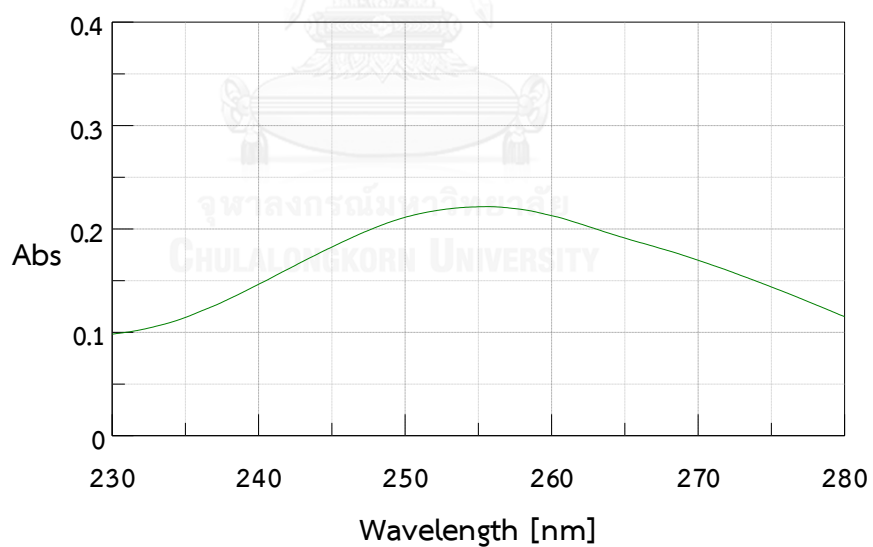


**Figure C-6** UV spectra of oligo-6. The oligonucleotide samples were prepared in 50 mM  $\text{Na}_2\text{HPO}_4$  buffer, pH 7.0.

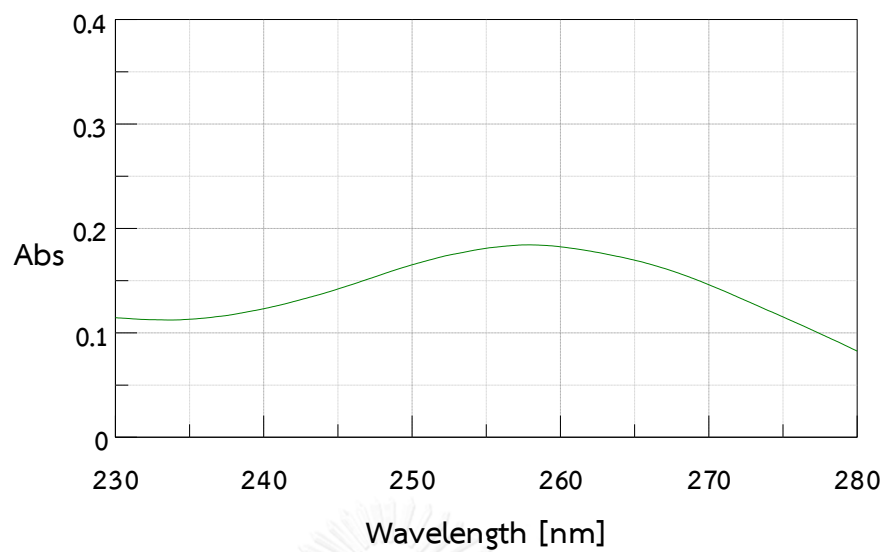
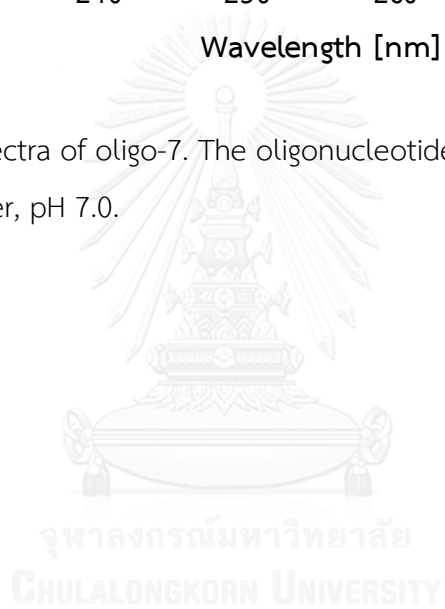


**Figure C-7** UV spectra of oligo-7. The oligonucleotide samples were prepared in 50 mM  $\text{Na}_2\text{HPO}_4$  buffer, pH 7.0.



Appendix D

CD spectra of B-Z transition study and DNA-protein binding study

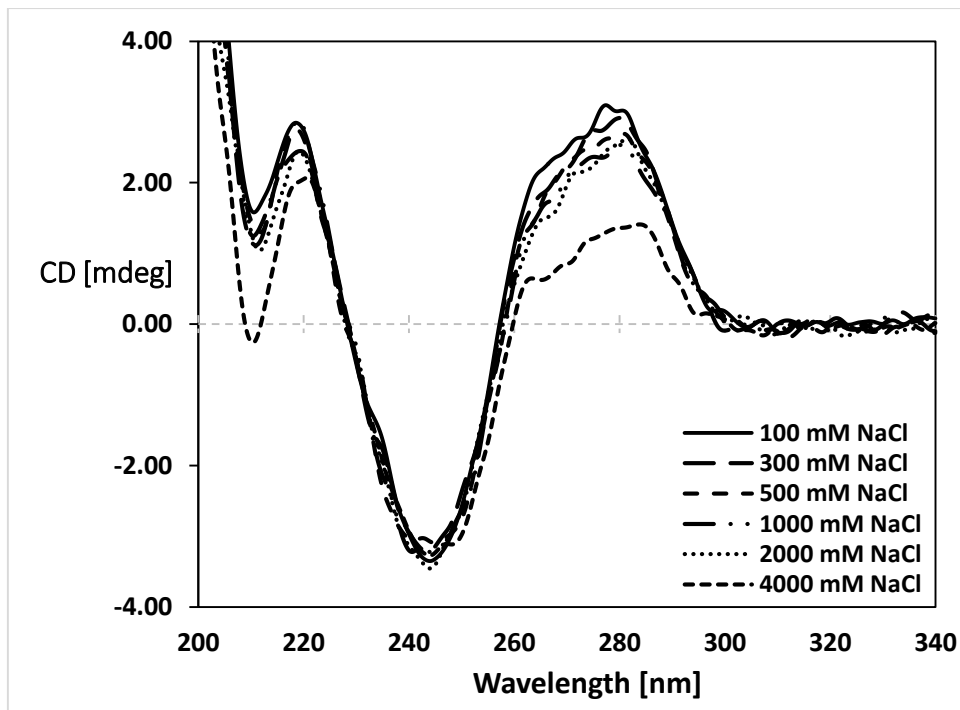


**Figure D-1** CD spectra of the duplex of oligo-2+3 with NaCl range from 100 mM to 4000 mM. The oligonucleotide duplex, approximately 6  $\mu$ M, was prepared in 50 mM phosphate buffer pH 7.4. The CD spectra were monitored at 25  $^{\circ}$ C with a scanning rate of 50 nm/min. Accumulation was set to 5 scans.

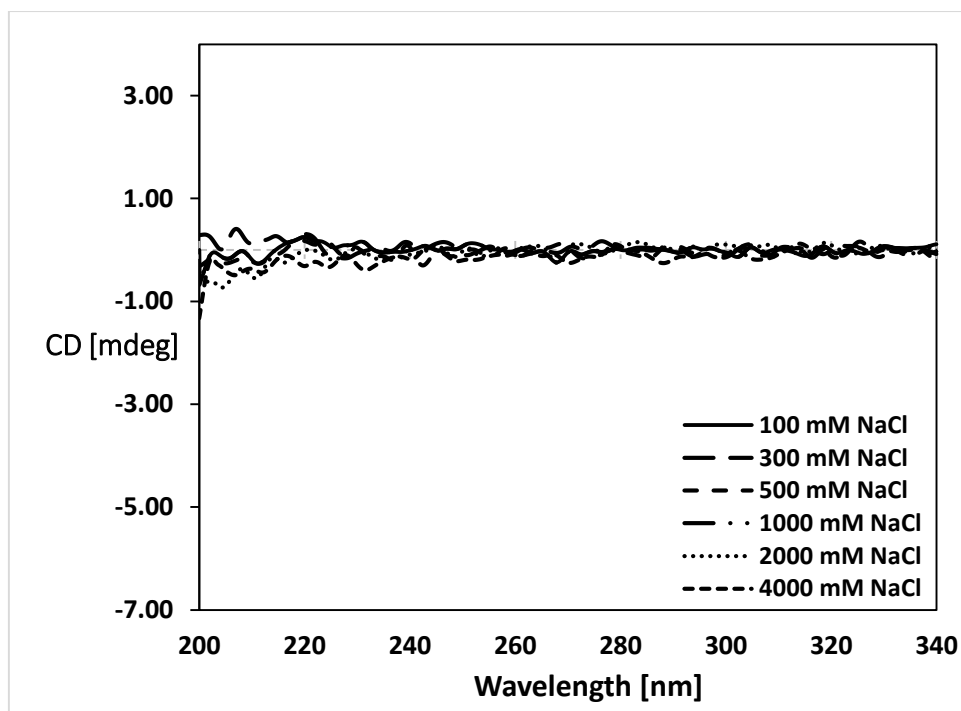


**Figure D-2** CD spectra of the duplex of blank control with NaCl range from 100 mM to 4000 mM. The CD spectra were monitored at 25 °C with a scanning rate of 50 nm/min. Accumulation was set to 5 scans.



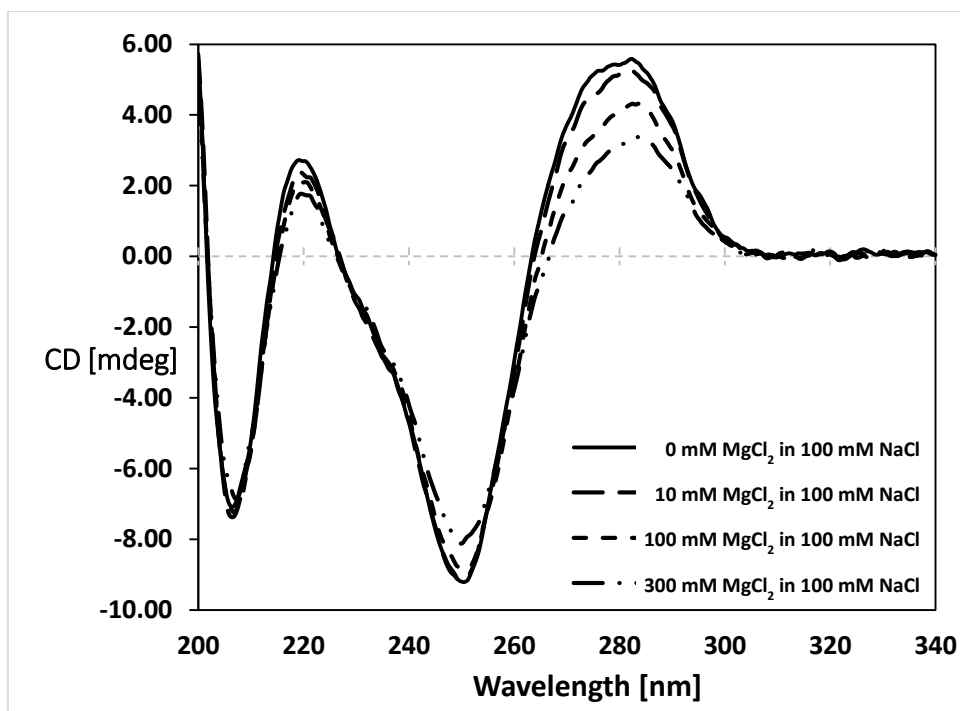


**Figure D-3** CD spectra of the duplex of oligo-4+6 with MgCl<sub>2</sub> range from 0 mM to 300 mM. The oligonucleotide duplex, approximately 6  $\mu$ M, was prepared in 50 mM phosphate buffer pH 7.4. The CD spectra were monitored at 25 °C with a scanning rate of 50 nm/min. Accumulation was set to 5 scans.

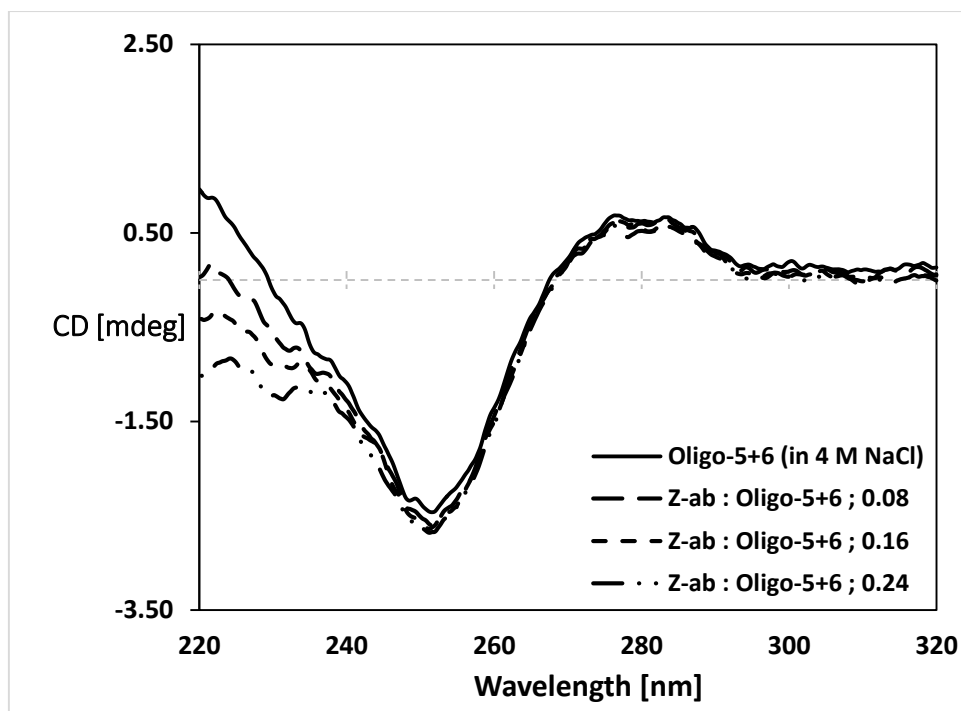


**Figure D-4** CD spectra of oligo-5+6 in high salt 4 M NaCl with varied molar ratio of Z-ab. The oligonucleotide concentration was prepared in 50 mM  $\text{Na}_2\text{HPO}_4$  buffer, pH 7.0 at 3.2  $\mu\text{M}$ . The CD spectra were monitored at 25 °C with a scanning rate of 20 nm/min. Accumulation was set to 10 scans.

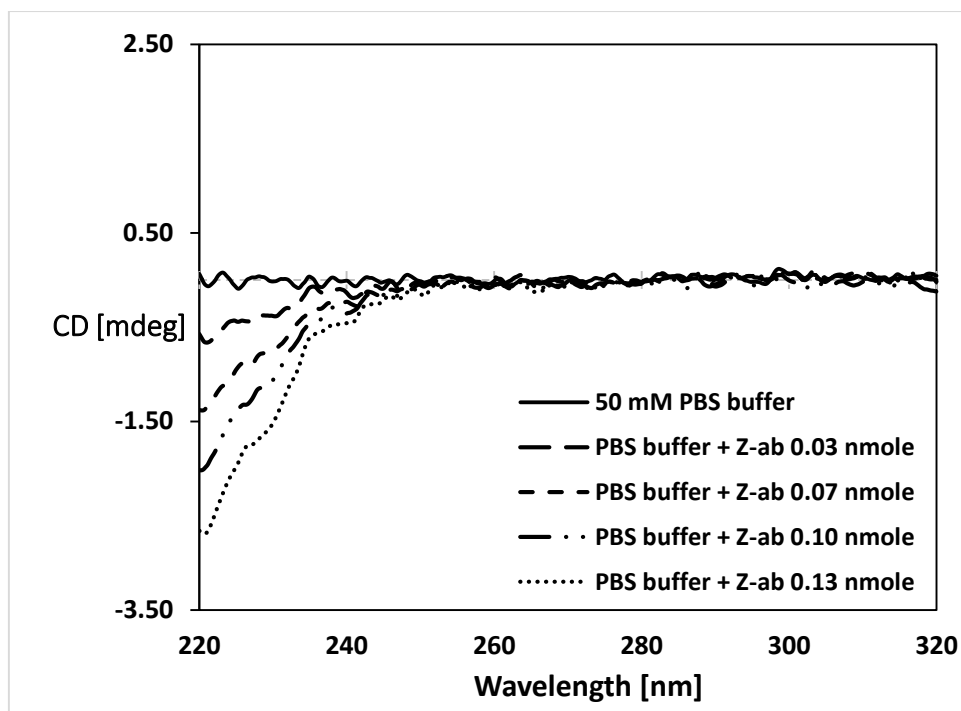


**Figure D-5** CD spectra of blank control which was 50 mM  $\text{Na}_2\text{HPO}_4$  buffer, pH 7.0 with various mole of Z-ab. The Z-ab concentration was approximately at 16  $\mu\text{M}$ . The CD spectra were monitored at 25 °C with a scanning rate of 20 nm/min. Accumulation was set to 10 scans.

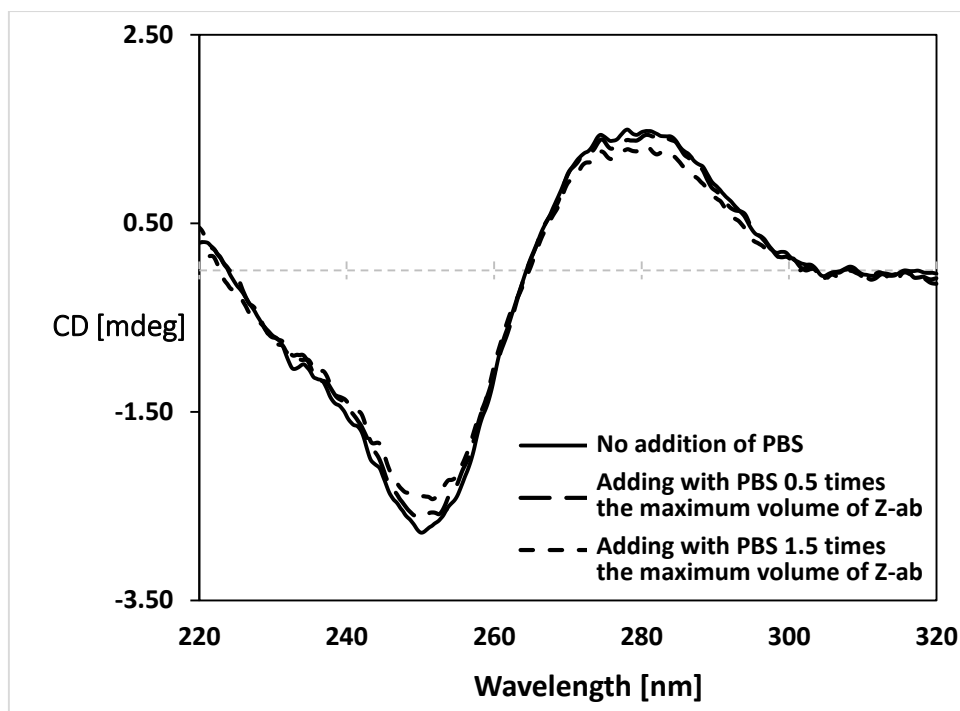


**Figure D-6** CD spectra of the duplex of oligo-5+6 in 50 mM  $\text{Na}_2\text{HPO}_4$  buffer, pH 7.0 without the addition of phosphate buffer and with the addition of phosphate buffer at 0.5 and 1.5 times the maximum volume of Z-ab added at a Z-ab : DNA ratio of 0.45 in previous experiment of binding study between the duplex of oligo-5+6 and Z-ab. The oligonucleotide concentration was at 3.2  $\mu\text{M}$ . The CD spectra were monitored at 25  $^\circ\text{C}$  with a scanning rate of 20 nm/min. Accumulation was set to 10 scans.

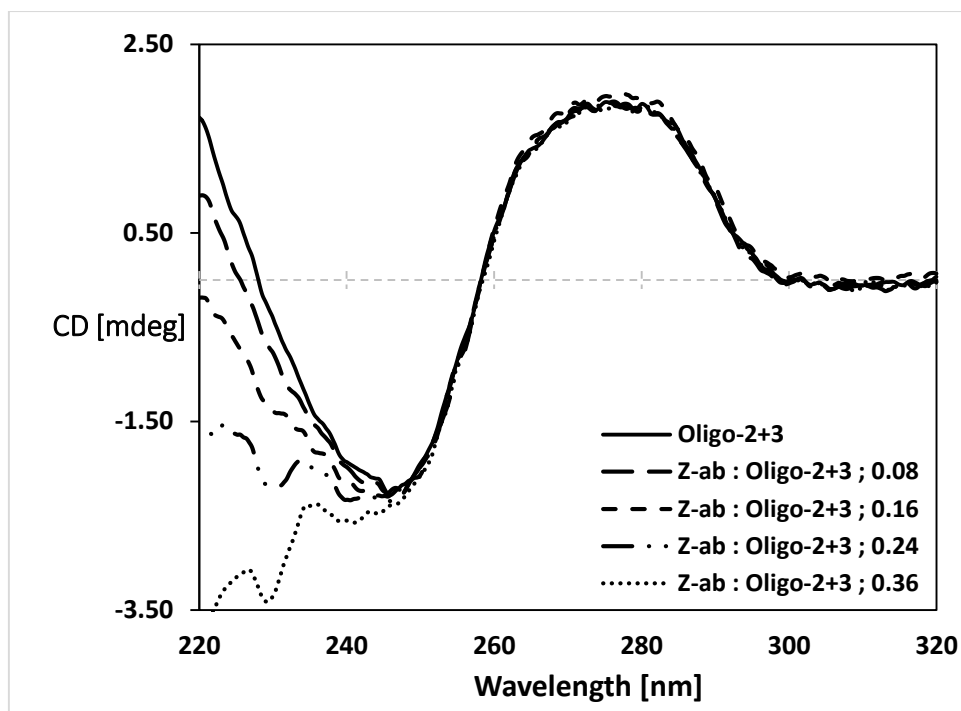


**Figure D-7** CD spectra of oligo-2+3 in 50 mM Na<sub>2</sub>HPO<sub>4</sub> buffer, pH 7.0 with varied molar ratio of Z-ab. The oligonucleotide concentration was at 3.2  $\mu$ M. The CD spectra were monitored at 25  $^{\circ}$ C with a scanning rate of 20 nm/min. Accumulation was set to 10 scans.

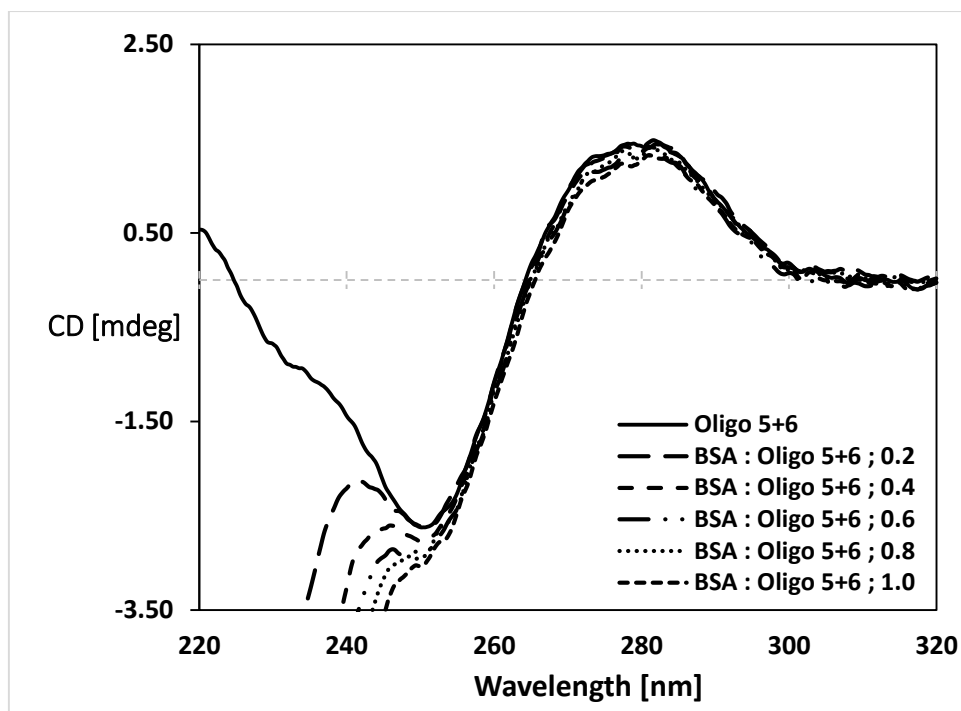


**Figure D-8** CD spectra of oligo-5+6 in 50 mM Na<sub>2</sub>HPO<sub>4</sub> buffer, pH 7.0 with varied molar ratio of BSA. The oligonucleotide concentration was at 3.2 μM. The CD spectra were monitored at 25 °C with a scanning rate of 20 nm/min. Accumulation was set to 10 scans.

**VITA**

NAME OF AUTHOR: Kulwadee Sawatpaiboontawee

DATE AND PLACE OF BIRTH: January 25, 1986, Bangkok, Thailand

EDUCATION: B.S. in Pharmacy, Silpakorn University (Summa cum laude),  
2009

HONORS AND AWARDS:

First Class Honor Certificate, Silpakorn University, 2009

Honorary Pin with Certificate for Academic Excellent Score from King  
Bhumibol Scholarship, 2008

Outstanding Academic Record Certificate, Silpakorn University, 2005–2008

PROFESSIONAL EXPERIENCE:

Teaching Assistant, Department of Food and Pharmaceutical Chemistry,  
Chulalongkorn University, 2012

Regulatory Affairs Pharmacist, The Medicpharma Co., Ltd., Thailand, 2009–  
2011

EXPERTISE/INTERESTS: Pharmaceutical Quality Control, Nucleic Acid  
Research, Nanobiosensor

PUBLICATIONS:

Sawatpaiboontawee, K.; Sermthaveesub, P.; Sangsirimongkolying, P.;  
Kunakorntham, P.; Thongborriboon, S.; Tuesuwan, B.; Vongsutilers, V. Development  
and validation of RP-HPLC method for analysis and stability study of 8-  
carboxyphenyl-2'- deoxyguanosine and 8-bromo-2'-deoxyguanosine. The Thai  
Journal of Pharmaceutical Sciences 2014; 38(4):176-181.